Measuring volumetric flow rate of grains through a crop harvester to improve crop yield estimation accuracy

by

Jason Nicholas Schuster

A thesis submitted to the graduate faculty

in partial fulfillment of the requirements for the degree of

MASTER OF SCIENCE

Major: Agricultural and Biosystems Engineering

Program of Study Committee:
Matthew Darr, Major Professor
Stuart Birrell
Steven Hoff

Iowa State University
Ames, Iowa
2016

TABLE OF CONTENTS

LIST OF FIGURES vi

LIST OF TABLES ix

LIST OF EQUATIONS xi

ACKNOWLEDGEMENTS xii

ABSTRACT xiii

CHAPTER 1. INTRODUCTION 1

1.1. Project Description 1

CHAPTER 2. LITERATURE REVIEW 3

2.1. Combine Operation 3

2.2. Components of Yield Monitoring 6

2.2.1. Grain Flow Sensors 7

2.2.2. Grain Moisture Sensors 13

2.3. Factors Influencing Yield Monitoring Performance 14

2.3.1. Yield Monitor Calibration Procedure 14

2.3.2. Time Delay of Crop 18

2.3.3. Harvester Properties 19

2.3.4. Operator Errors 20

2.3.5. Environmental Properties 21

2.3.6. Crop Test Weight Properties 23

2.4. Conclusion 24

CHAPTER 3. OVERVIEW OF RESEARCH OBJECTIVES 25

3.1. Research Objectives 25

CHAPTER 4. YIELD MONITORING TECHNOLOGY BENCHMARK 26

4.1. Introduction 26

4.2. Materials and Methods 27

4.2.1. Combine Test Stand 27

4.2.2. Yield Monitors 28

4.2.3. Mass Flow Rate of Grain 31

4.2.4. Clean Grain Elevator Paddle Type 32

4.2.5. Machine Orientation 36

4.2.6. Methodology for Yield Monitor Evaluation 38

4.3. Results and Discussion 41

4.3.1. Grain Deterioration 41

4.3.2. Performance Impact of Paddle Configuration 43

4.3.3. Performance Impact of Machine Orientation 50

4.3.4. Performance of Non-Calibrated Flow Rates 54

4.4. Conclusions 56

CHAPTER 5. PARTICLE FLOW YIELD MONITORING 59

5.1. Introduction 59

5.2. Materials and Methods 61

5.2.1. Mechanical Requirements 61

5.2.2. Camera Flow Measurement 65

5.2.3. Imaging Frequency 72

5.2.4. Combine, Sump, and Fountain Auger 73

5.2.5. Development of a Predictive Volumetric Yield Algorithm 76

5.2.6. Description of Data Sets 79

5.2.7. Model Assessment 83

5.3. Results and Discussion 84

5.3.1. Performance with Controlled Data 84

5.3.2. Performance with Uncontrolled Data 90

5.3.3. Model Assessment and Root Cause 99

5.4. Conclusions 102

CHAPTER 6. CONCLUSIONS 103

6.1. Suggestions for Future Testing 103

6.2. Suggestions for Future Development 103

REFERENCES 105

APPENDIX A. YIELD MONITORING PATENT REVIEW 110

APPENDIX B. MASS FLOW YIELD MONITORING UNCERTAINTY ANALYSIS 115

B.1. Combined Standard Uncertainty for Grain Yield 115

B.2. Calibration Impact on Yield Estimation Performance 119

APPENDIX C. PARTICLE FLOW YIELD MONITORING UNCERTAINTY ANALYSIS.....122

C.1. Combined Standard Uncertainty for Grain Yield 122

LIST OF FIGURES

Figure 2.1 : Modern combine with 12-row corn head 3

Figure 2.2: Diagram of the cleaning shoe assembly in a combine 4

Figure 2.3: Functional process of combine harvesting 6

Figure 2.4: Impact-based mass flow sensor after clean grain elevator 8

Figure 2.5: Radiation-based mass flow sensor after clean grain elevator..... 10

Figure 2.6: Volumetric metering of grain using paddle wheel after clean grain elevator 11

Figure 2.7: Beam volumetric sensor pair installed inside of the clean grain elevator 12

Figure 2.8: Moisture sensor 14

Figure 2.9: Single point calibration vs. multi-point calibration for a yield monitoring system 15

Figure 2.10: Reflection of different field properties and soil types into production yield map.....22

Figure 4.1: Combine test stand 27

Figure 4.2: SmartYield Pro yield monitor beam-based volumetric flow sensor and display, respectively..... 29

Figure 4.3: Cumulative distribution of mass flow rate sensor data for different crops 31

Figure 4.4: Paddle set configurations and respective ID numbers..... 33

Figure 4.5: Combine pitch and roll orientation..... 36

Figure 4.6: Distribution of combine pitch and roll angle during harvest..... 37

Figure 4.7: Yield estimation error at observed mass flow rates within the calibrated range.. 40

Figure 4.8: Corn deterioration during test stand repetitions 41

Figure 4.9: Yield monitor accuracy as corn deteriorates during test stand repetitions..... 42

Figure 4.10: Grain pile loading on paddle ID no. 1 and 3 for 5 kg s^{-1} mass flow rate, respectively 46

Figure 4.11: Standard deviation of yield monitor estimation error across all flow rates..... 47

Figure 4.12: Machine orientation impact on grain pile in clean grain elevator..... 51

Figure 4.13: Yield monitor accuracy for flow rates outside of calibration range..... 55

Figure 5.1: Filled cavity area and volumetric flow rate impact on grain velocity..... 61

Figure 5.2 : Auger test stand for determination of cavity power requirement..... 63

Figure 5.3: Power requirement to push grain cavity for range of grain mass flow rates..... 64

Figure 5.4: Camera used to record images of grain 66

Figure 5.5: Camera face and image dimensions 68

Figure 5.6: Example of image tracking algorithm for corn 69

Figure 5.7: Conveyance regions of accumulated grain flow in combine harvester..... 70

Figure 5.8: Particle flow yield monitor topology diagram 72

Figure 5.9: Number of images of a grain particle before parting the camera face for flow rate ranges and imaging frequencies..... 73

Figure 5.10: Fountain auger modifications of baffles, sump, and tapered auger to deliver grain effectively to sensor..... 75

Figure 5.11: Camera and fountain auger installation..... 75

Figure 5.12: Raw response signals of particle flow and impact-based mass flow yield monitors 77

Figure 5.13: Distribution of flow rate treatment levels for controlled data set..... 80

Figure 5.14: Grain pile below and above fountain auger..... 81

Figure 5.15: NDVI imagery of 2015 corn and soybean uncontrolled data sets..... 82

Figure 5.16: Modified fountain auger details for simulation 84

Figure 5.17: Load size influence on pixel displacement..... 85

Figure 5.18: Load size influence on pixel displacement grouped by mass flow rate treatment levels 85

Figure 5.19: Pixel line displacement rate across mass flow rate for controlled data..... 87

Figure 5.20: Pixel displacement rate across mass flow rate for uncontrolled data..... 91

Figure 5.21: Volumetric yield estimation for 2015 harvest season 93

Figure 5.22: Distribution of test weight for corn during harvest 2015 96

Figure 5.23: Impact-based mass flow yield monitor performance in uncontrolled data 97

Figure 5.24: Average impact-based mass flow sensor response in uncontrolled data..... 98

Figure 5.25: DEM analysis of the modified fountain auger with simulated grain particles 100

Figure 5.26: Time series of DEM simulation showing decreased velocity on the bottom of the fountain auger as the auger rotates 101

Figure 5.27: Estimate of fountain auger velocity profile difference from DEM simulation..... 101

Figure 6.1: Sensor face blockage and image quality issues during field harvest exposure .. 104

Figure B.1: Impact-based mass flow sensor response to variable corn mass flow rate..... 120

Figure B.2: Calibration type comparison for 12 kg s^{-1} corn mass flow rate set point 121

LIST OF TABLES

Table 2.1: Official U.S. Grain Standards 23

Table 4.1: Impact-based mass flow yield monitor component serial numbers 28

Table 4.2: Volumetric flow yield monitor component serial numbers 29

Table 4.3: Mass flow rate treatment levels for yield monitor evaluation 32

Table 4.4: Paddle type matrix 32

Table 4.5: Data set description for yield monitor evaluation of paddle type 35

Table 4.6: Data set description for yield monitor evaluation of machine orientation 38

Table 4.7: Statistical difference by paddle configuration data set for impact-based mass flow yield monitor 44

Table 4.8: Statistical difference by paddle configuration data set for volumetric flow yield monitor 44

Table 4.9: Statistical differences by specific flow rate range and paddle set for impact-based mass flow yield monitor 48

Table 4.10: Statistical differences by specific flow rate range and paddle set for volumetric flow yield monitor 49

Table 4.11: Statistical difference by machine orientation data set for impact-based mass flow yield monitor 50

Table 4.12: Statistical difference by machine orientation data set for volumetric flow yield monitor 50

Table 4.13: Statistical differences by specific flow rate range and machine orientation for impact-based mass flow yield monitor: 53

Table 4.14: Statistical differences by specific flow rate range and machine orientation for volumetric flow yield monitor 53

Table 5.1: Regression model parameters for cavity power requirement testing..... 65

Table 5.2: Expected mass flow rate of grain into the combine (kg s^{-1}) 83

Table 5.3: Regression model parameters for load size influence on pixel displacement 86

Table 5.4: Pixel line displacement rate regression equation coefficient ANOVA 87

Table 5.5: Pixel displacement rate comparison for fill level respective to fountain auger (shaded indicates different means, 95% CI) 89

Table 5.6: Regression model parameters for pixel displacement rate for uncontrolled data.. 91

Table 5.7: Regression model parameters for volumetric yield estimation 93

Table 5.8: Grain properties for uncontrolled data set 95

Table 5.9: Regression model parameters for impact-based mass flow yield monitor performance 97

Table 5.10: Regression model parameters for average impact-based mass flow sensor response..... 99

Table B.1: Uncertainty budget for mass flow sensor measurement 115

Table B.2: RMSE comparison for test stand and harvest conditions 116

Table B.3: Uncertainty budget for navigation-based velocity sensor evaluated at 5 kph..... 117

Table B.4: Uncertainty budget for grain density evaluated during corn harvest 2015..... 117

Table B.5: Sensitivity of grain yield estimation to input parameter values..... 118

Table C.1 Uncertainty budget for pixel displacement rate measurement..... 123

Table C.2 : RMSE for particle flow test stand and harvest conditions..... 123

LIST OF EQUATIONS

Equation 2.1: Yield estimation from mass flow sensor 6

Equation 2.2: Yield estimation from volumetric flow sensor 6

Equation 5.1: Volumetric flow rate through a cylinderical tube of a known diameter 62

Equation 5.2: Volumetric flow rate estimate in a cylindrical tube using camera images 68

Equation B.1: Root-Mean-Square Error 116

Equation B.2: Total standard uncertainty for mass flow sensor 117

Equation B.3: Grain yield estimation combined standard uncertainty 118

Equation C.1: Yield estimation for particle flow yield monitor 122

Equation C.2: Volumetric flow rate estimation from pixel displacement rate 122

Equation C.3: Particle flow yield estimation combined standard uncertainty 124

ACKNOWLEDGEMENTS

I would like to thank Deere & Company for their financial and equipment support towards this research. I owe a great deal of thanks Dr. Matthew Darr for providing the amazing opportunity to complete this research, as well as guidance and encouragement throughout the graduate program. I would also like to thank Dr. Steven Hoff and Dr. Stuart Birrell for guidance and subject expertise they provided, as well as willingness to serve on my program of study committee.

I am grateful to many faculty and staff of the Agricultural and Biosystems Engineering Department for their support and guidance throughout my time as an undergraduate and graduate student. I am especially thankful to Dr. Robert McNaull, Levi Powell, Ben Covington, Jeff Askey, Chris Hoffman, Brad Kruse, and Koy Vander Leest for their many hours of technical and analytical assistance. Without your assistance, none of this work would have been possible.

I am very fortunate to be surrounded by endearing and supportive family and friends. I am grateful for the continuous support you provide for my research and life-long goals. I would not be where I am today without my beautiful fiancé Lacie and loving family.

Finally, I would like to thank God for the opportunity and strength to perform this research. With God all things are possible.

ABSTRACT

Recent technological innovations such as variable rate seeding and fertilizer application have given farmers the ability to manage large fields as smaller sections with specific application needs. Crop yield data and maps from previous years are the primary source of information from which crop management recommendations and decisions are based upon. Yield monitoring has been widely adopted into current crop production practices since the first commercially successful yield monitor became available more than 20 years ago. Yield monitoring allows for producers to compress the comprehensive list of previous crop input decisions into a single yield measurement value for that area. When combined with soil properties measurements and production inputs, yield monitoring becomes a useful tool to rate performance and increase profits per acre.

Yield data is a useful tool for making crop management decisions, but becomes irrelevant when it is not accurate or reliable. The first goal of this research was to benchmark current yield monitoring solutions to better understand current performance and build performance goals for the next generation of yield monitoring. Two common yield monitors utilizing different methods of yield estimation were selected for benchmarking. Both systems required intensive calibration to achieve accuracy. The volumetric flow yield monitor maintained accuracy across the entire flow range better than the impact-based mass flow yield monitor because of a fundamental measurement system that does not rely entirely upon calibration regression.

A particle flow yield monitor utilizing the advantages of both yield systems was designed and developed for initial performance assessment. Linearity and consistency across a wide range of flow rates for three different crops demonstrated promise for future

development of the system. The design performed in conjunction with an impact-based mass flow yield monitor and maintained flow rate linearity for all three crops. Limitations of the current design were revealed in field harvest conditions and validated using simulation tools. Successful initial performance and yield estimation linearity supports continued development of this technology.

CHAPTER 1. INTRODUCTION

1.1. Project Description

Recent global economic instability and extreme climactic events have resulted in nearly 50% reductions in United States farm income from levels seen just a few years ago (Interagency Agricultural Projections Committee, 2016). Record crop yield and total acres planted, in addition to global competition have attributed to increased stockpiles of grains and decreased crop prices. Lin (2011) suggests that crop diversification may provide a buffer against extreme crop events resulting in total loss and allow for financial protection for producers. A 13-year study by the United States Department of Agriculture, USDA, showed that mono-cropping is becoming increasingly rare, with 84% of planted acres participating in crop rotations in 2010. (United States Department of Agriculture, 2013). This shift in crop production results in smaller windows for harvest and puts pressure on machinery to increase productivity. Crop harvesters must be able to handle a diverse spread of crop types and minimize the time required to prepare the machine for the next crop type to be harvested.

Over the last 20 years, sensing mass flow of grain has become the most common method for determining crop yield. Crop producers must perform a rigorous calibration procedure with their crop harvesters to ensure accuracy of yield estimation, requiring several combine tank loads of grain (Shearer, Fulton, McNeill, Higgins, & Mueller, 1999). Yield monitor accuracy is highly dependent upon the crop properties, harvest conditions, and harvester set-speed for which the calibration was performed (Grisso, Jasa, Schroeder, & Wilcox, 2002). While current yield monitoring systems may provide adequate post-calibration accuracy, it does not support accurate harvesting of multiple crop types without

intensive sensor recalibration. Little research has been conducted on alternatives to the current yield monitoring system that maintains accuracy while reducing calibration.

The goal of this study is to investigate the current technology behind flow-based yield sensing and propose an alternative that allows for multiple-crop harvesting with reduced calibration needs. This technology would provide valuable information to producers and reduced calibration time during harvest season. This project focuses on addressing technology design considerations and evaluating alternative yield sensing performance in harvest conditions.

CHAPTER 2. LITERATURE REVIEW

2.1. Combine Operation

Before modern combines, the only way to harvest field grains was by reaping and threshing the crop. To do so required intensive labor with a great number of workers. Crops would be reaped, gathered together, and would be either transported to a nearby thresher, or a portable model would be brought to the field. The threshing would clean the grain from the chaff. Grains were sold and traded on a whole mass basis. There was no means of yield monitoring crop output. Modern crop harvesters operate on the same two basic principles of reaping and threshing, but have combined them into a stand-alone unit that is self-propelled and can record crop yields on a per area basis (Figure 2.1).

Figure 2.1 : Modern combine with 12-row corn head

Modern harvesters cut and gather crop into the machine using headers specifically designed for that crop. Corn headers are used solely for corn harvesting, while draper and rigid auger headers are capable of handling a wide variety of small grains, such as wheat, rye, canola, and oats. Although headers may differ by technique, the design functionality is the same. When crop enters the header it is cut at the base of the stalk and pulled onto a belt or

auger, where it is conveyed to the feeder house at the center of the header. The feeder house accelerates the crop into the machine using sets of conveyor chains and delivers it to the threshing system. Threshing of grain is performed by a large rotating drum and concave-shaped screens. Grain is separated from stalk residue and seed covers by the rubbing action between the threshing drum and the concave screen. The clearance between the rotating drum and the concave screen, as well as the screen opening size, is adjusted using a hydraulically driven lever arm attached to the concave screen that can be controlled from inside of the combine cab. Concave clearance can impact harvesting performance and ideal settings are variable between different crop types. Stalks, seed covers, and other material that is not separated through the concave screen is pushed to the top of the threshing drum and disposed out of the back of the combine as trash. Grain and other material small enough to make it through the concave screen is delivered to the cleaning shoe assembly (Figure 2.2).

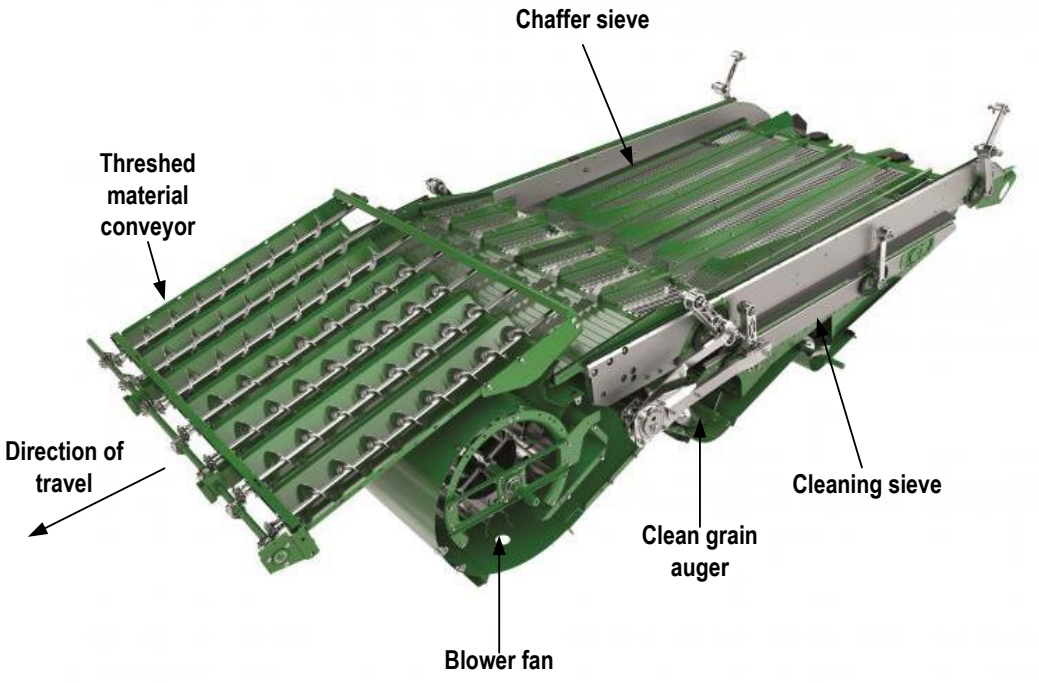

Figure 2.2: Diagram of the cleaning shoe assembly in a combine

Photo Credit: (Deere & Company, 2016)

The cleaning shoe is composed of levels of sieves with angled, finger-like openings and a blower fan to achieve separation of grain from chaff material. Grain is separated using rotary and lateral mechanical movements of the sieve while air is blown through the sieve openings. Grain falls vertically through different levels of sieve tables and is separated from material other than grain, MOG. MOG is blown to the rear of the combine and is reduced in size by a series of chopping knives, before being dispersed behind the machine. The top level sieve is referred to as the chaffer sieve and has a different size of opening than that of the lower level sieve, the cleaning sieve. This is to decrease MOG in the final product. The angle of the sieve openings dictate how much MOG is allowed into the clean grain stream and can be controlled from the combine cab. These settings can be too strict and increase grain loss out of the combine, so original equipment manufacturers have incorporated re-threshing of unseparated material to reduce losses. Material that is to be re-threshed is conveyed back to the threshing rotor and the process is started over. Grain that has been separated from MOG by the cleaning shoe falls to the bottom-most point of the combine, where it is conveyed by the clean grain auger. This is the first point in the combine harvesting process where grain is measurable in quantity. Grain moved horizontally across the combine is carried up to the grain tank on paddles in the clean grain elevator. Clean grain flows through yield monitoring components in the clean grain elevator and into the fountain auger, which accumulates it into the grain tank. Combine harvesters utilize multiple processes to separate and clean grain from harvested crop (Figure 2.3).

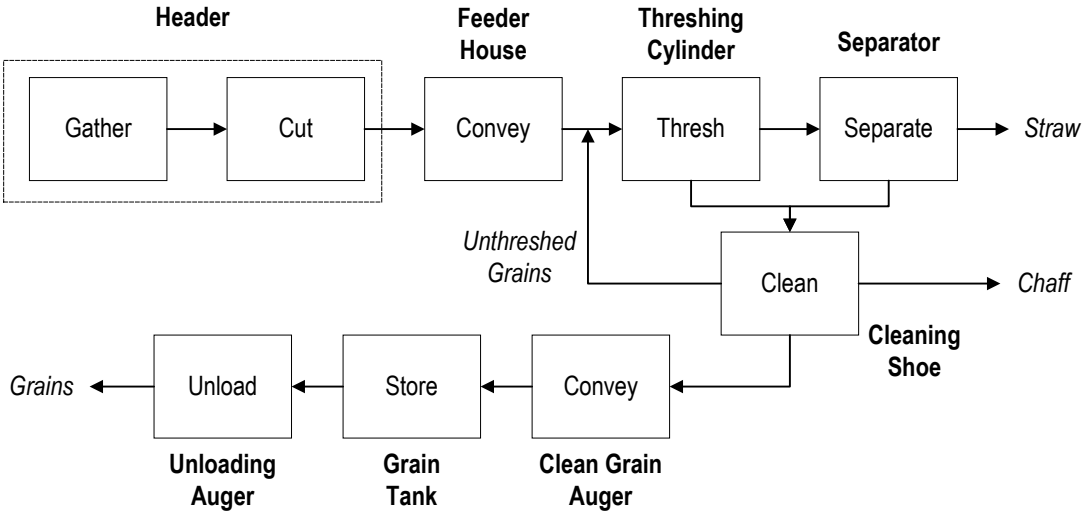

Figure 2.3: Functional process of combine harvesting

Photo Credit: (Grain Harvesting, 2006)

2.2. Components of Yield Monitoring

The purpose of a grain yield monitor is to measure and record in real-time the crop yield per unit area. This can be achieved by measuring either the volume or mass of grain harvested over a fixed period of time using a grain flow sensor and scaling by the combine velocity and size of the crop harvester head. Grain yield is commonly expressed in terms of volume or mass of grain per unit area. In imperial units this is bushels per acre and for the SI system it is metric tons per hectare (Equation 2.1, Equation 2.2).

Equation 2.1: Yield estimation from mass flow sensor

$$Yield = \frac{V}{A} = \frac{\dot{m}}{\rho * \vec{v} * w}$$

Equation 2.2: Yield estimation from volumetric flow sensor

$$Yield = \frac{V}{A} = \frac{\dot{V}}{\vec{v} * w}$$

Yield estimation is a function of mass flow rate ($\dot{m}$) or volumetric flow rate ($\dot{V}$) of grain through the sensor area, test weight or density of the grain being harvested (ρ), crop harvester velocity ($\vec{v}$), and the total width of crop entering the harvester (w). This value can be displayed to the operator with an interface display inside of the harvester cab along with the grain moisture content. These two values represent a direct measurement of crop performance of an area in a given year and can influence major crop decisions.

Adoption of yield monitor technology in the United States has increased significantly during the past decade. The Agricultural Resource Management Survey conducted by the United States Department of Agriculture cited nearly a 20% increase in yield monitor usage in corn production, from 42% in 2005 to 61% in 2010, respectively. Similarly, yield monitor usage increased 18% from 2006 to 2012 for soybean production and 22% from 2004 to 2009 for winter wheat production (USDA Economic Research Service, 2015).

2.2.1. Grain Flow Sensors

Grain flow sensors have been commercially available since the early 1990's. A pioneer of precision agriculture, Al Myers developed the first yield monitor over the course of six years and six prototypes. The final product, Yield Monitor 2000, was one of the first widely adopted precision agriculture technologies by producers (Ag Leader Technology, 2016). Today, producers can select from many different grain flow sensors offered from original equipment manufacturers and aftermarket suppliers. In this section impact, radiation, electromagnetic, metering, and optical sensors will be discussed.

2.2.1.1. Impact-Based Sensing

The most common method used to monitor the flow of grain is impact-based sensing. This method was first employed by Al Myers and is still used today by Ag Leader

Technology (US Patent No. 5,343,761, 1994). Grain is lifted up the clean grain elevators on paddles and expelled from them at the top of the elevator by centrifugal force as the paddles rotate 180° (Shearer, Fulton, McNeill, Higgins, & Mueller, 1999). Grain is subjected to projectile motion until it contacts the impact sensor positioned across from the clean grain elevator. The impact sensor measures the quantity of grain using a strain gage load cell attached to the impact plate. Grain deflecting off of the impact plate causes deformation in the structural components of the load cell and can be measured using a strain gage in a Wheatstone bridge configuration. Varying amounts of grain flow induce different amounts of strain on the impact sensor, which alter the electrical output signal of the sensor. This electrical signal can be calibrated to correspond to different mass flow rates of grain and adjusted to account for changes in elevator speed. After the grain has deflected off of the impact sensor, it falls into the base of the fountain auger and is conveyed into the grain tank (Figure 2.4).

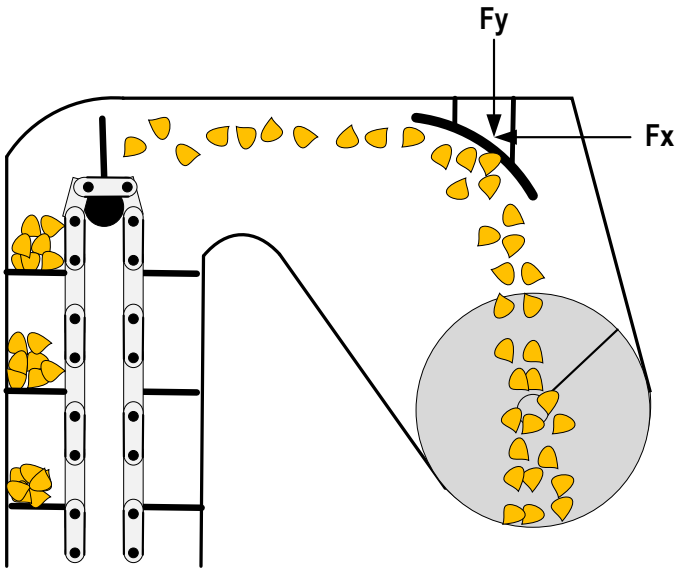

Figure 2.4: Impact-based mass flow sensor after clean grain elevator

2.2.1.2. Radiation-Based Sensing

Radiation-based sensing has been widely utilized in industrial and manufacturing applications for determining mass flow rate of a material. The idea was patented by Jens Overgaard and commercialized into agriculture by Massey Ferguson for grain flow monitoring (Patent No. EP0147452 A1, 1983). Radiometric sensing utilizes a pair of sensors to determine the density of material in a flow stream (Figure 2.5). Each pair of sensors consist of an emitter and detector that are installed opposite each other to enable the gamma source of the emitter to enter the detector. The detector measures the attenuation of gamma radiation as grain flows between the sensor pair. When no grain flow is present the detector measures the full strength of the radiation source, but as material density increases in higher flow rates there is a reduction in radiation signal strength. It is common to mount the sensor pair after the clean grain elevator when grain becomes airborne to limit mechanical inference of the measurement. Since the velocity of the grain is fixed by the clean grain elevator rotational speed, the radiation signal strength is directly proportional to the mass flow rate of grain. Unlike other systems, measurement principles of radiation-based sensors are unaffected by temperature, moisture, or chemical properties of the grain. However, utilization of a gamma source may limit where the sensor can be sold.

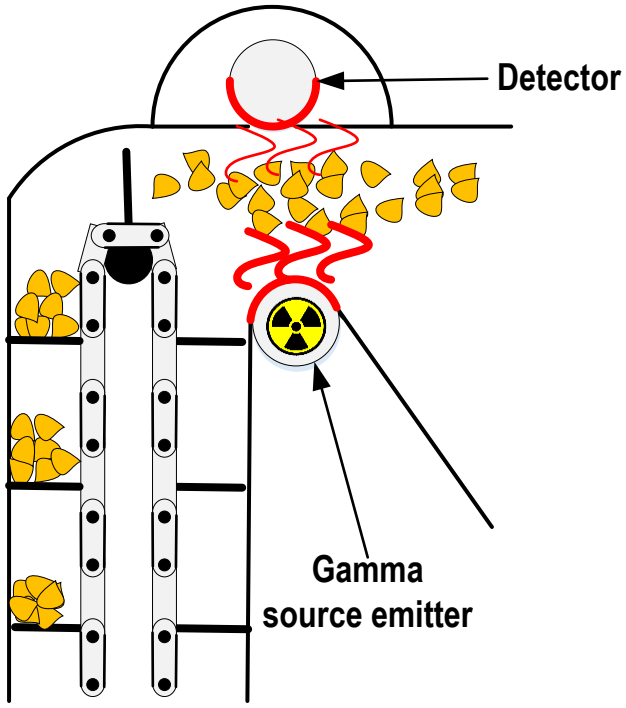

Figure 2.5: Radiation-based mass flow sensor after clean grain elevator

2.2.1.3. Electromagnetic-Based Sensing

Electromagnetic sensing is a non-contact method for determining the flow measurement of dry bulk solids. It is most commonly applied in the food and grain handling industries. A magnetic field is created and channeled into the flow of dielectric grain in a fixed volume. As the velocity or material density of grain changes, the voltage generated is proportionally changed. Since any conductive material will affect the electrical response of the sensor, adoption into precision agriculture has been limited mainly to sensing of grain moisture content.

2.2.1.4. Metering Roll Systems

One of the first yield monitors to utilize volumetric metering of grains was the CLAAS Yield-O-Meter (Patent No. EP0042245 A1, 1981). Metering grain flow sensors consist of a paddle wheel mounted in between the outlet of the clean grain elevator and the

fountain auger (Figure 2.6). The paddle wheel is sectioned into typically four or more fixed volumes. As grain exits the clean grain elevator, it accumulates in one of the sections of the paddles wheels. The section continues to fill with grain until the volume reaches a predetermined sensor set-point. When the sensor is triggered it indicates that the paddle wheel section is full and the entire paddle wheel rotates to begin filling the next empty section. Full sections of grain are emptied into the fountain auger below for conveyance to the grain tank. Grain volume harvested is determined by multiplying the volume of sections on a paddle wheel by the number of paddle wheel revolutions. Density of the grain must be known in order to convert volume of grain harvested into mass.

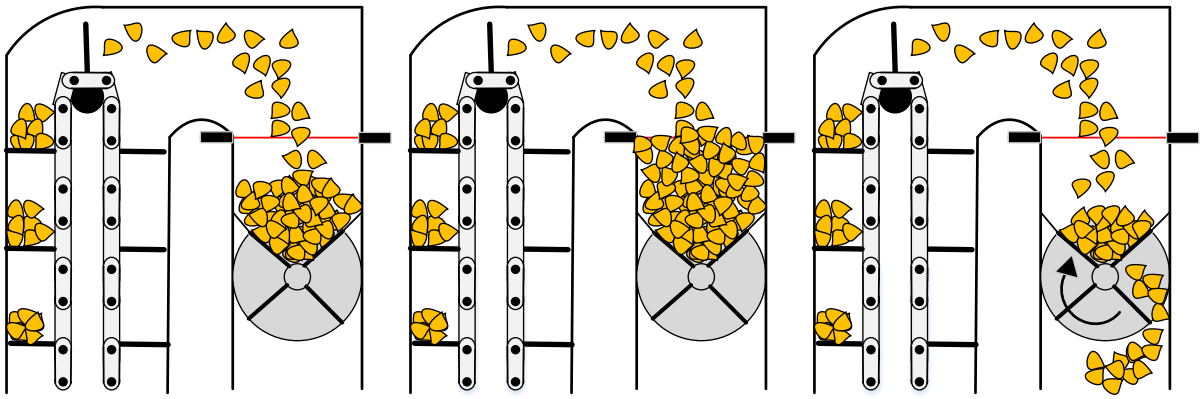

Figure 2.6: Volumetric metering of grain using paddle wheel after clean grain elevator

2.2.1.5. Non-Contact Beam Sensors

Beam sensors are another form of non-contact sensor that perform similarly to radiation-based sensors. These sensors function in pairs as an emitter and detector. An emitter transmits a non-visible beam of light at a detector positioned opposite of it. The beam of light is outside of the visible spectrum of light so as to not be affected by environment or material properties within the installed location. Unlike radiation-based sensing, the light beam is unable to attenuate through grain to get proportionate output measurements.

Therefore, the detector has a binary response to the measurement of the emitted light beam. When the detector measures light transmitted from the emitter a high voltage response is outputted. Alternatively, once the light beam is broken and emittance is no longer detected, a low voltage response is outputted. The timing of light being interrupted can be correlated to the amount of grain being conveyed during that period. A calibration procedure is necessary to determine the frequency of dead band in sensor response due to the clean grain elevator paddles breaking the beam. For this application, it is common to mount these pairs of sensors opposite each other on the clean grain elevator (Figure 2.7).

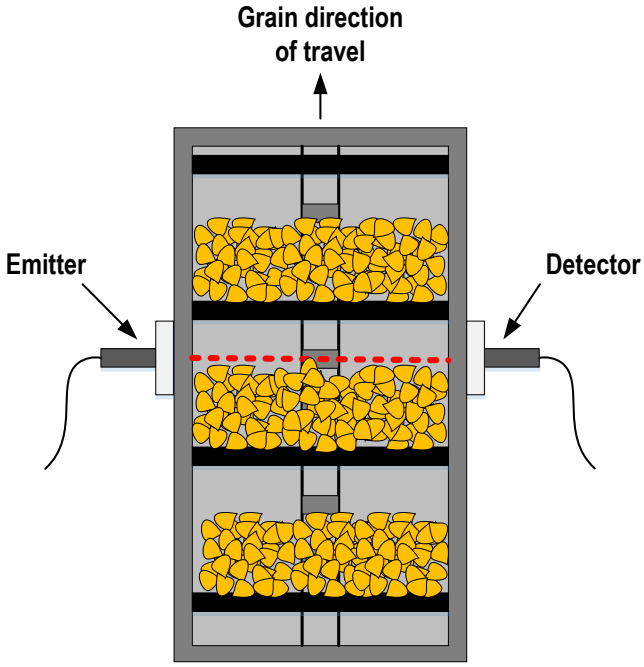

Figure 2.7: Beam volumetric sensor pair installed inside of the clean grain elevator

Since the area of the paddle is fixed, higher crop yields translate to an increased height of the grain pile per paddle. The volume of grain harvested is calculated using the area of a paddle and the height of the grain piled per paddle. The height of the grain pile per paddle can be determined using the clean grain elevator speed and the duration of time that the sensor was in a low voltage state.

2.2.2. Grain Moisture Sensors

Moisture content of grain can vary significantly within a single field. Variation in soil type, growing conditions, ear size, and test weight can cause shifts in moisture content of grain by ten percent or greater (NDSU Agriculture Communication, 2013). Additionally, moisture content of crop in the field will gradually decline throughout a harvest season. Accurate moisture sensors are necessary to assess field performance and scale harvested grain mass to a market standard.

Grain moisture content is determined using capacitive sensors. This iterative process occurs simultaneously with harvesting to determine moisture variation in crop as the combine travels across the field. Capacitive sensors measure voltage potential between two conductive plates. These plates are positioned opposite of one another and offset by a fixed distance to allow an electric field to establish between the two. Sensing range is directly proportional to the size of the capacitive sensor. In most applications, grain is allowed to pass directly over the face of the sensing element. As a conductive material passes over the sensor, the dielectric properties of the material affects the electrical field and output voltage. This change in output voltage signal is calibrated to correlate to different moisture contents for various crops. In the patent, “Grain moisture sensor”, inventors claim the capacitive signal that is affected by clean grain can be related to grain moisture content (US Patent No. 6285198 B1, 1997).

Since sensing range is limited, grain moisture sensors are commonly installed in the clean grain elevator or fountain auger, where a continuous stream of clean grain is available. It is most common to install the moisture sensor on the clean grain elevator for ease of access and maintenance. A vertical chamber is mounted on the side of the clean grain elevator, with

inlet and outlet holes cut into each side of the clean grain elevator. Small samples of clean grain fall off of the elevator paddles and into the sensing chamber. Capacitive measurements of the grain are recorded digitally until the sensing chamber is full. Capacity of the chamber is determined by a photoelectric emitter and detector sensor pair installed near the grain inlet. Once grain reaches the height of the sensor and the chamber is deemed full, an electric motor meters grain back into the clean grain elevator and begins collecting a new sample of grain (Figure 2.8).

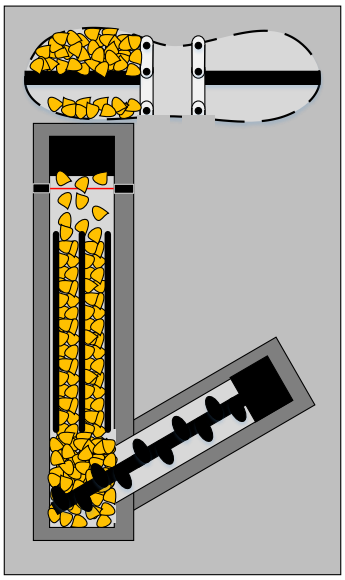

Figure 2.8: Moisture sensor

2.3. Factors Influencing Yield Monitoring Performance

2.3.1. Yield Monitor Calibration Procedure

Manufacturers of yield monitors try to ensure that their system is accurate and precise, however, calibration must be routinely performed to remove errors. During calibration, the combine is not being calibrated for bushels per acre, but rather mass per second or volume per second. Calibration consists of harvesting a sample section of crop that is representative of the field population and calibrating the sensor estimated mass of grain to

the actual mass of grain harvested. The actual mass of grain harvested is obtained using a weigh wagon with digital readout or hauling loads of grain to the nearest scale site. It is widely agreed upon that calibration loads should be between 1,500 and 3,000 kg. The mass of grain harvested and known harvest time can be used to measure mass flow rate estimation error. Each individual load of grain harvested during calibration exemplifies a flow rate of grain that will be observed during the harvest season. Sensor correction can be performed with a single point or multi-point calibration (Figure 2.9).

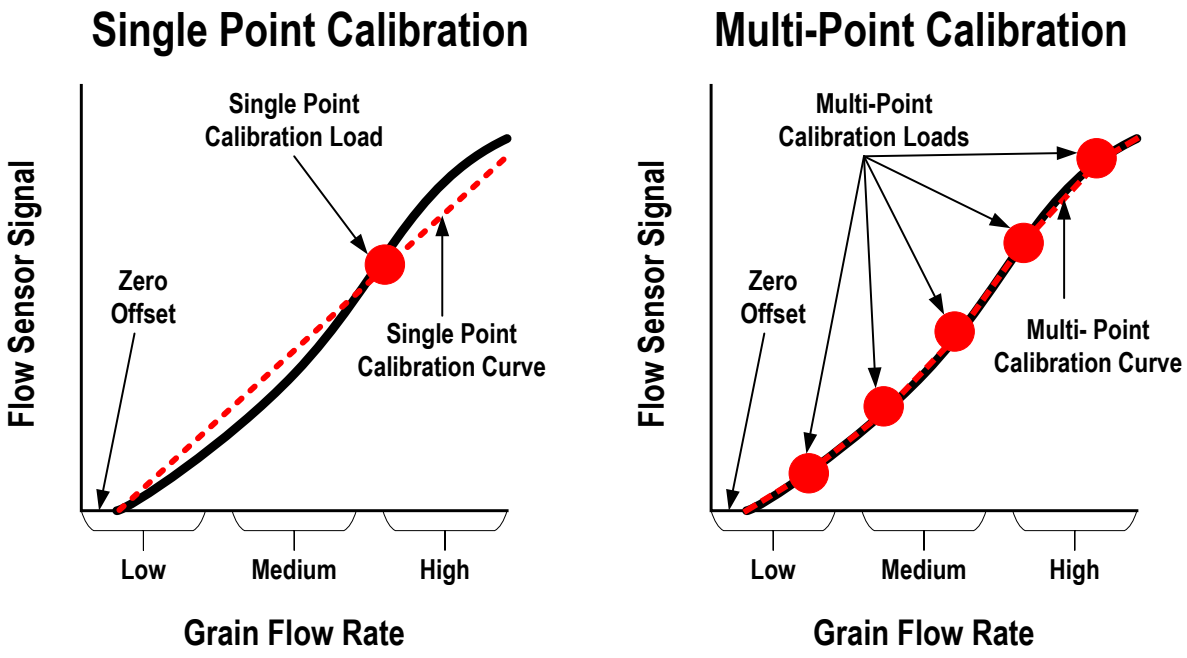

Figure 2.9: Single point calibration vs. multi-point calibration for a yield monitoring system

Single point calibration is simply a straight linear regression from the zero offset reading of the mass flow sensor to the single point calibration load. It is often recommended that the single point calibration load be an average of at least three calibration loads. This allows for a more a representative point to be used, thus further minimizing errors induced during calibration due to incorrect procedure or environmental factors. Single point calibration was widely used during the early years of yield monitor technology. To better

capture the full range of grain flow rates the combine will experience during a harvest season, non-linear, multi-point calibration is a common practice today.

Multi-point calibration involves harvesting between 3 and 6 calibration loads to capture the non-linear response curve of the yield sensor at different flow rates of grain (Neilsen, 2010). There are two methods of obtaining a calibration point at a desired flow rate of grain. The most common method is to harvest consistent, representative sections of crop at a different speed setting for each calibration point. One calibration load should be performed at the normal harvesting speed, then two incremental harvesting speeds above and below the normal. For example, one original equipment manufacturer recommends two calibration loads to be performed at the normal operating speed and then perform 4 additional calibration loads 0.5 mph and 1 mph faster and slower than the normal operating speed (Deere & Company, 2013). The alternative method of multi-point calibration is to perform calibration loads at a consistent harvesting speed while using fractions of the available header width. Harvesting speed should be the normal operating speed. On a 12-row head for example, one calibration load would be performed at full head width of 12 rows and fractional head width calibration loads performed at 10, 8, 6, 4, and 2. It should be noted that for this procedure, there will be left over "clean-up" rows that will be partial header width and will need to be harvested before normal harvesting operation can begin. Both calibration methods will extrapolate for grain mass flow rates that exceed the maximum calibrated range, which will increase the yield estimation error (Burks T. F., Shearer, Fulton, & Sobolik, 2004).

The data coming out of the mass flow sensor is only as accurate as the input environment. Weigh wagons and scales used to measure mass of grain harvested must be accurate and checked regularly. When using a weigh wagon in the field, measurements

should be taken when the machine is static on a level, solid surface. Failure to properly perform weigh wagon measurements will result in inaccurate calibration of the mass flow sensor and flawed data measurements during the harvest season. Mass flow sensor calibration should be performed in uniform, representative crop conditions. Operators should refrain from calibrating when turning around on the headlands, opening up the field, or any areas of the field that will cause intermittent starting and stopping. Calibration of the mass flow sensor is required every year at the start of harvest, as machine wear may have occurred since the last calibration and environmental crop conditions will be different. Additional recalibration may be necessary throughout the harvest season. According to Darr (2015), it is necessary to recalibrate when any of the following criteria are met: crop type changes, grain moisture content changes more than 4%, grain test weight changes more than 5.6 kg hL^{-1} (4 lb bu^{-1}), or field conditions dramatically change. This may result in several calibrations performed per season, but a general expectation for a corn-soybean crop production is 2 calibrations for corn and 1 calibration for soybean during an average year.

In addition to the mass flow sensor calibration, the grain moisture sensor requires calibration for each crop type at least once per season. This calibration procedure involves harvesting a tank load of grain and randomly taking samples from different locations and depths of the grain tank. These two criterion can be met using a grain probe. Once collected and samples are mixed, the average moisture content of the sample can be input into the display for calibration. This correction offset of actual grain moisture content versus the grain moisture sensor estimate is used for all further grain moisture measurements. It is important to note that moisture content does affect the response of the mass flow sensor, but there is no

correction factor between the two variables, only recalibration of the mass flow sensor. This is a known limitation of current yield monitoring systems.

2.3.2. Time Delay of Crop

Grain mass flow and moisture measurements occur in the clean grain elevator after harvested crop has been cleaned and aggregated. Since harvesting is a continuous process, there is a time delay between grain being analyzed by the yield monitoring system and the geographical location of the combine. This lag time for grain delivery can take between 13 and 14 seconds (Chung, Sudduth, & Drummond, 2002). The time delay of crop becomes increasingly important when creating yield maps, which is done by over half of operators that use a yield monitor (USDA Economic Research Service, 2015). Kruse (2015) found similar results using ultraviolet sensors and cameras mounted in the clean grain elevator. Through sensor detection and visual verification of painted ears of corn, the study showed that the time delay from the harvester feeder house to the top of the clean grain elevator varied between 10 and 30 seconds in a skewed right distribution, with mean time delay occurring between 11 and 12 seconds for various grain mass flow rates. The time delay is dependent upon machine settings and mass flow rate of grain. In addition to lag time of grain from entering the combine to the yield monitoring system, there is partial delay of crop from when it enters the head to entering the combine. As crop harvesters have increased in size this issue has become more prevalent. In the same study, Kruse (2015) observed increased time delay on crop entering the head 6 row units away from the feeder house, compared to crop entering 2 and 4 row units from the feeder house. On average, it took 16.7 seconds for sensors to detect grain in the clean grain elevator from the edge of a 12 row corn head, versus 13.3 seconds for grain coming just 2 row units from the feeder house. The variation in time delay

of crop per row unit creates further complications when mapping, resulting in yield smoothing over the width of the header.

2.3.3. Harvester Properties

Sensors used for yield monitoring are subject to harsh conditions and must be robust. Sensors located in the top of the clean grain elevator experience constant mechanical vibration from the harvester. The combine threshing and cleaning systems oscillate at high frequencies to clean grain. Additionally, uneven field terrain and vehicle handling can increase vibration experienced by the yield monitoring sensors. Specifically, impact-based mass flow sensors are most vulnerable to vibration-induced errors due to their method of measurement. Impact-based mass flow sensors utilize two parallel beam load cells to measure the force of grain striking the impact plate and measure the induced vibration by the machine. One study found that the relative error of using a reference parallel beam load cell was less than 2.2%, but could be further reduced to 1.6% when analyzing the harmonic delivery of grain by the clean grain elevator (Zhou, Cong, & Liu, 2014). Other mass and volumetric flow sensors do not have this issue, as their method of measurement is unaffected by vibration.

Strubbe, Missotten, and Baerdemaeker (1996) studied the effect of friction on impact-based mass flow measurement. The study showed that projectile motion characteristics of grain leaving the clean grain elevator is dependent upon exit velocity of the grain due to elevator speed, elevator paddle shape, deflector plate location, and friction properties between the grain and components. Curved elevator paddles and deflector plates are commercially available to concentrate grain flow to the mass flow sensor. The study found

that influences of friction can be minimized if the velocity of the grain is high enough and clean grain elevator speeds satisfy this condition on most combines today.

2.3.4. Operator Errors

In addition to machine parameters, operator decisions can reduce yield monitor accuracy. Abrupt changes in ground speed can induce significant error when considered with time delay of grain travel through the combine. Sudden stopping with grain still being processed through the machine would cause an overestimation in yield over the small area covered. This is a common issue when experiencing crop plugging problems in the header, harvesting headlands of a field, and stopping to unload at field edges. Post-processing techniques can smooth estimations to improve yield map quality (Darr, 2015). Arslan and Colvin (1999) recommend maintaining constant ground speed when harvesting crop. They found that even gradual changes in ground speed from 5 mph to 7 mph caused increases in average individual load error from 3% to 5%. This error can be reduced by maintaining a constant ground speed.

The overall accuracy of yield monitoring systems diminishes as the time step decreases. Evaluating the instantaneous, 1-Hz signal of an impact-based mass flow sensor with consistent grain delivery showed variability as high as 8% (Burks T. F., Shearer, Fulton, & Sobolik, 2003). Yield monitor error variability is not correlated with yield monitor error magnitude and therefore cannot be removed via sensor calibration (Taylor, et al., 2011). Yield monitor instantaneous flow rate is not as accurate as the accumulated mass, especially at low flow rates. This could be caused by surging of grain delivery from the clean grain elevator. To mitigate these types of errors, operators should strive for larger load sizes. Missotten, Strubbe, and Baerdemaeker (1996) noted that the yield monitor estimation error

percentage increases with decreasing harvested area due to operator errors and sensor characteristics. They observed that maximum error could be reduced from 5% to 3% by increasing the harvested area by a factor of 5. When the area was increased to an entire field, the error was further reduced to 1.7%. Operator errors are difficult to control, but the overall impact on yield monitor accuracy can be reduced by harvesting large areas and higher accumulated grain mass.

2.3.5. Environmental Properties

Cropland slopes can cause estimation error for yield monitors from gravitational effects on grain projectile motion and grain pile shifting in the clean grain elevator. Both mass and volumetric based flow sensors are affected by slope changes in a field. Kettle and Peterson (1998) studied the performance of impact-based mass flow sensors on sloped terrain. Field slopes varied from 6% to 9%. The study concluded that the yield monitoring system was affected by field slopes and that a slope calibration factor may help to correct yield estimation. The yield monitor system overestimated yields when harvesting down slope by 36.8% and underestimated yields on upward slope harvesting by 12.5%. The average error induced by slopes on impact-based mass flow sensors will vary per machine type and settings.

Similar results were shown in a lab study that analyzed the effect of pitch and roll on an impact-based yield monitor system (Fulton, Sobolik, Shearer, Higgins, & Burks, 2009). The tests were performed at common slopes that a combine would experience in the field ranging from 0% to 15%. The results indicated that roll had minimal effects on accumulated mass estimates from the yield monitoring systems with errors ranging from -3.5% to 3.5%. Roll had an adverse effect on yield monitor performance with accumulated mass estimate

errors ranging from -6.4% to 5.5%. The investigation further concluded that a linear correlation exists between yield monitor error and slope that can used to remove error induced by slope. Mass flow rate errors were significantly reduced when the slope correction factor was introduced. This is an important correction factor, as conditions vary extensively from field-to-field.

Field properties such as soil type and texture have high spatial variability. This can lead to a major impact on yield and plant stand through soil moisture, early growing season temperature, and compaction. Yield and weather variations over time can take several years to become stable. In most cases, it will take between 4 and 6 years for a field to establish an average yield expectation (Colvin, Jaynes, Karlen, Laird, & Ambuel, 1997). In a multiple crop rotation, yield can be normalized to a scale that is comparable over multiple years. Since field properties can change abruptly within a field, current yield monitoring systems will smooth over some of the finite differences as grain is aggregated through the harvester (Figure 2.10).

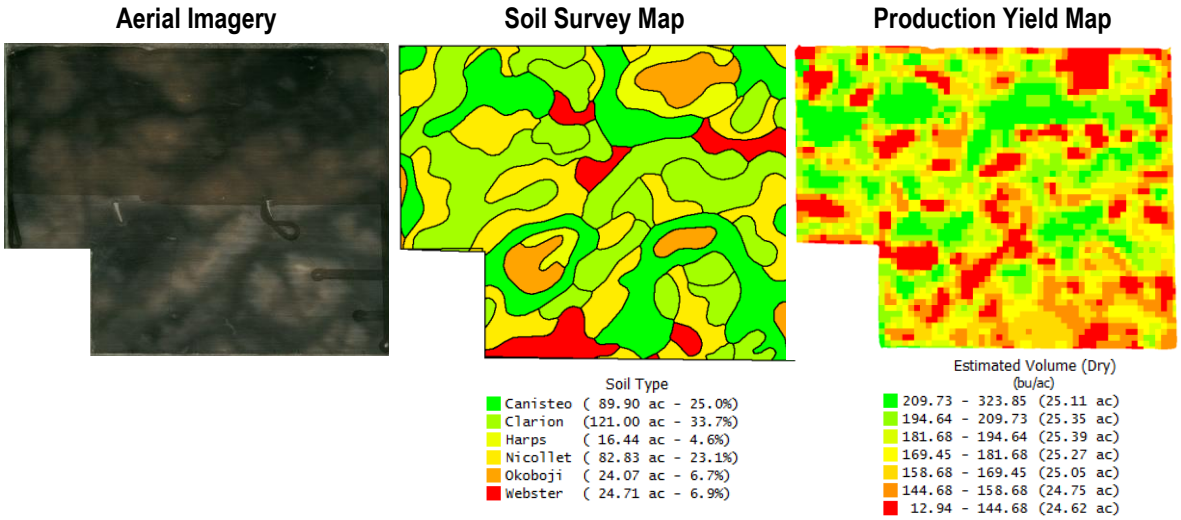

Figure 2.10: Reflection of different field properties and soil types into production yield map

Grain moisture content can also vary significantly within a field and can impact yield monitor performance. There is currently no correction to the mass flow sensor for grain moisture content variation. One study found that moisture content of corn in a field varied by as much as 10 percentage points in the same day (Pierce, et al., 1997). This variation can lead to error and necessary recalibration. A 1% error in moisture content will lead to a yield estimation error of 0.17 MT ha^{-1} (2.5 bu ac^{-1}) (Taylor, et al., 2011).

2.3.6. Crop Test Weight Properties

Test weight is a measure of grain bulk density and is used in the agricultural industry as an indicator of grain quality. Test weight can be measured using the USDA manual test weight apparatus or with a grain analysis computer. Units commonly associated with test weight are pounds per Winchester bushel. The United States Grain Standards Act of 1916 established specifications regarding grain test weights and has been amended periodically by the United States Department of Agriculture (Table 2.1).

Table 2.1: Official U.S. Grain Standards

Grain	Grade	Standard Bushel Weight (lb bu^{-1})	Standard Grain Moisture Content (%)	Maximium Limits of Damaged Kernals (%)	Maximum Limits of Broken Material (%)
Corn	U.S. No. 1	56.0	15.5	3.0	2.0
Soybeans	U.S. No. 1	N/A[a]	13.0	2.0	1.0
Hard Red Spring Wheat	U.S. No. 1	58.0	13.5	2.0	3.0
Oats	U.S. No. 1	36.0	14.0	0.1	2.0
Barley	U.S. No. 1	47.0	14.5	2.0	4.0

[a] *Test weight for soybeans is no longer part of the U.S. grade standards as of 2007*

Since grain is traded on a mass basis, mass flow sensors are minimally affected by changes in test weight. Volumetric flow sensors convert grain volume to mass using test weight. This can lead to errors if the grain test weight is not checked periodically. To reduce systemic errors, test weight should be corrected for volumetric yield systems four to five

times per day (Blackmore & Moore, 1999). As the number of recalibrations increases, the sensor becomes more accurate for the current crop conditions.

2.4. Conclusion

Grain yield monitoring technology provides real-time collection of crop yield metrics to benefit producers as a source of decision validation. Several technologies have become available in the past decade that offer mass or volumetric flow as solutions for accurate yield monitoring. Current yield monitoring technologies require intensive calibration to cover the range of variable conditions that will be observed during a harvest season and accuracy is limited to the conditions upon which the calibration was performed. Production agriculture has shown a need for an improved yield monitor technology that reduces the input requirements of obtaining accurate yield data and is less sensitive to environmental and machine changes. This research will analyze the design considerations and performance of an innovative non-contact method of yield estimation. This concept will allow for less dependency upon calibration, while reducing the impact of environmental and physical changes of crop.

CHAPTER 3. OVERVIEW OF RESEARCH OBJECTIVES

3.1. Research Objectives

The long-term goal of this research was to provide users with a more accurate method of yield monitoring that will maintain accuracy across a variety of harvesting conditions with reduced calibration requirements than what is standard on impact-based yield monitoring systems used today. Current yield monitoring systems are calibration intensive and are unreliable when conditions and crop type change. The short-term goal of this research was to identify a measurement method with an output signal proportional to grain flow rate through the combine. Specifically this included:

1. Benchmark the performance of commercially available yield monitoring systems and evaluate the effects of combine properties on yield estimation accuracy.
2. Design and quantify the initial performance of an alternative yield monitoring system based on image tracking grain particles.

CHAPTER 4. YIELD MONITORING TECHNOLOGY BENCHMARK

4.1. Introduction

There are several yield monitoring solutions commercially available to producers that claim increased accuracy of yield data, simplified calibration, and ease of use. The long-term goal of this research is to provide users with a more accurate method of yield monitoring that will maintain accuracy across a variety of harvesting conditions with reduced calibration requirements than what is required currently. Benchmarking available yield monitoring systems was necessary in order to define performance goals, as well as identify advantages and disadvantages of each system.

Two commercial yield monitors were selected for evaluation. A yield monitor measures yield using a proxy signal for mass or volumetric grain flow rate. The most commonly used mass flow yield monitor utilizes an impact-based mass flow sensor to measure flow rate from grain impulses against an impact plate. The impact-based mass flow yield monitor is the most widely used yield monitor on harvesters today. A beam-based volumetric flow yield monitor was selected as the second system to benchmark performance because of its popularity for aftermarket installation. Each system utilized different methods of yield sensing, which allowed comparative analysis of the technologies. The main objectives of this chapter are to:

- Evaluate accuracy and consistency of mass flow and volumetric flow yield monitors under treatment factors of mass flow rate, clean grain elevator paddle type, and machine orientation.
- Identify the advantages and failure modes of each yield system for consideration for the next generation of yield monitoring technology.

4.2. Materials and Methods

4.2.1. Combine Test Stand

Experiments were completed using a yield monitor test stand. A class 7 combine was positioned so that grain could be precisely metered into the auger bed at set mass flow rates (Figure 4.1). Corn purchased from a local elevator was metered through the gates of a scaled axle grain wagon. Corn could be recycled from the combine back into the grain wagon for repetitive testing using the unloading auger. Corn mass flow rates were implemented through remote control of linear actuated doors on the grain wagon. Maximum achievable mass flow rate exceeded 50 kg s^{-1}. The test stand had been previously evaluated and proven to provide an accurate ground truth mass flow rate to compare commercially available yield monitor systems (Risius, 2014).

Figure 4.1: Combine test stand

Corn used for experimental testing was consistently at 15% moisture content and ranged in test weight from 56 to 58 lb bu^{-1}. Preliminary testing revealed that as grain was

repetitively recycled through the test stand it would deteriorate over time. The degree of deterioration and the effect on yield monitor estimation accuracy was unknown. Samples were collected throughout testing using a 6 slot grain probe that allowed a sample depth of 1 m in the grain tank. A single sample was composed of five to six grain probes randomly collected from the grain wagon. Samples were mixed in a one-gallon bag and weighed. Measurement of the percentage broken corn and foreign material (BCFM) was performed using a Carter-Day XT7 Dockage Tester. No foreign material was introduced between replicates, BCFM could be directly correlated to deterioration due to grain recycling.

4.2.2. Yield Monitors

In this section, the two yield monitoring systems under evaluation are presented. Each system differs in sensing method and location on the machine. Both yield monitors were evaluated simultaneously using the test stand.

4.2.2.1. Impact-Based Mass Flow Yield Monitor

The mass flow based system under evaluation was an Ag Leader yield monitor available as standard equipment on all John Deere combines beginning in 2012. The yield monitor system consisted of several components including the impact-based mass flow sensor, grain moisture sensor, and internal software in the John Deere display (Table 4.1). The system came preinstalled from the factory with the mass flow sensor mounted at the top of the clean grain elevator.

Table 4.1: Impact-based mass flow yield monitor component serial numbers

Component	Mass Flow Sensor	Moisture Sensor	Display
Serial Number	1850014886	2010510014	PCGU2UD439650

4.2.2.2. Beam-Based Volumetric Flow Yield Monitor

The volumetric flow based system under evaluation was a SmartYield™ Pro yield monitor manufactured by Raven Industries. The system was comprised of a beam-based volumetric flow sensor, grain moisture sensor, processing controller, and external display that allowed aftermarket installation on any combine (Table 4.2).

Table 4.2: Volumetric flow yield monitor component serial numbers

Component	Volumetric Flow Sensor	Moisture Sensor	Controller Module	Display
Serial Number	01351E	010046	001017	600531

The beam-based volumetric flow sensor was installed on the upper region of the clean grain elevator above the grain moisture sensor. The controller module was mounted to the side of the combine. Since experiments were conducted on a stationary combine, a program was used to simulate the dynamic GPS signal required by the controller. The external display was installed in the cab next to the John Deere display so that accumulated load weight estimations could be compared between the two yield monitors (Figure 4.2).

Figure 4.2: SmartYield Pro yield monitor beam-based volumetric flow sensor and display, respectively.

4.2.2.3. Pre-Testing Calibration

Several calibrations were performed on the yield monitors prior to the experiment. Clean grain elevator speed was set to 450 RPM at zero-flow conditions and monitored on the CAN bus throughout testing. Both yield systems were calibrated for machine orientation by following the manufacturer recommended procedures. Static, level position was maintained until calibration was completed. A vibration calibration was performed for the impact-based mass flow yield monitor to reduce systematic error at zero-flow conditions. Vibration calibration was performed through the John Deere display with the separator and feeder house engaged at full engine RPM. Similarly, a zero-flow calibration was performed for the volumetric flow yield monitor to record the sensor response from empty elevator paddles. Both vibration and zero-flow calibrations record the sensor response at no flow conditions so that it could be internally processed out of the final signal in real-time. Calibration of the mass flow sensor was performed in adherence to standard operating procedure (Deere & Company, 2013). Five grain mass flow rates were selected from field observed flow rates to collect calibration loads and evaluate yield monitor performance. Three of these five were selected to also be collected as a calibration load for the volumetric flow yield monitor. Per manufacturer recommendation, one of the three represented either low, medium, or high mass flow rate from the distribution. Accumulated load size target for calibration and evaluation testing was 2,500 kg. The calibration curve of the volumetric yield monitor was updated immediately after a calibration load was collected, which differs from the impact-based mass flow yield monitor that updates the curve after all loads have been collected. Following flow sensor calibration, both systems were ready for evaluation.

4.2.3. Mass Flow Rate of Grain

Mass flow rate of grain was selected as a treatment factor to evaluate the yield monitor performance. Mass flow was measurable using the scaled axle grain wagon and metering system previously described. To select treatment levels of mass flow rate, analysis was conducted into the distribution of mass flow rate on combines. The normal distributions were observed from nearly 2,000 hours of mass flow sensor data recorded from the Controller Area Network (CAN) bus on combine harvesters in a harvest operation (Figure 4.3).

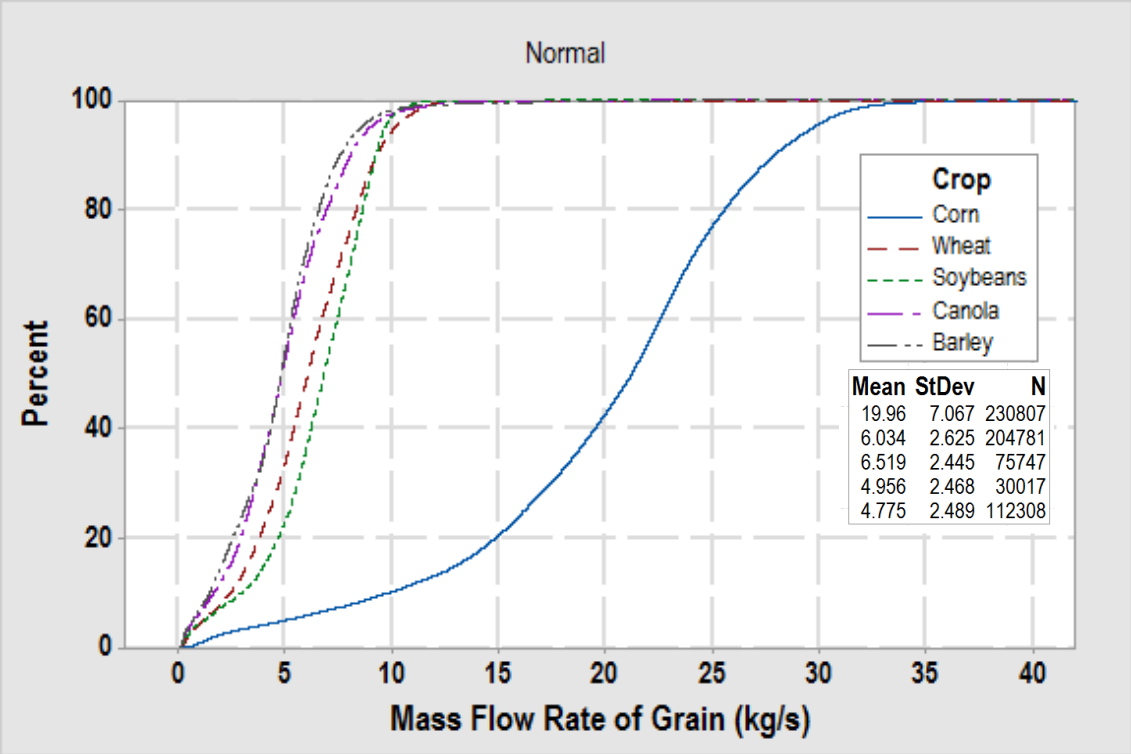

Figure 4.3: Cumulative distribution of mass flow rate sensor data for different crops

The distribution of mass flow rate was much broader for corn than it was for other crops. Emphasis was placed on flow rates for small grains when selecting treatment levels to evaluate yield monitor performance. Impact-based mass flow yield monitor performance in

corn at higher flow rates has already been well documented (McNaull, 2016). Treatment levels spanning two standard deviations for small grains and one standard deviation for corn were targeted (Table 4.3).

Table 4.3: Mass flow rate treatment levels for yield monitor evaluation

	Treatment levels: mass flow rate (kg s^{-1})	
Flow rate CDF target	**Small grains**	**Large grains**
-2-sigma	2	5
-1-sigma	4	10
Mean	5	15
+1-sigma	8	20
+2-sigma	10	25

4.2.4. Clean Grain Elevator Paddle Type

The presentation of grain to the sensors for both mass and volumetric flow yield monitors is controlled by the clean grain elevator. Several different configurations of paddle shape and type are commercially available. Clean grain elevator paddle type was selected as a treatment factor to identify how grain presentation to the yield monitors may impact performance. The paddle chain, elevator drive sprocket, and elevator assembly remained unchanged between different paddle types. The paddle material and shape were the only variables altered that define a different type of paddle and corresponding data set (Table 4.4).

Table 4.4: Paddle type matrix

Paddle set ID no.	Material	Material stiffness	Estimated previous separator run time (h)	Paddle shape
1	Recycled tire carcass	Flexible	250	Cupped
2	Recycled tire carcass	Flexible	616	Flat
3	HDPE plastic	Rigid	5	Flat
4	Belt conveyor rubber	Flexible	0	Flat

Paddle sets 1 and 2 were taken from two John Deere combines that had several harvest seasons of use. They were commercially available paddles made of flexible, rubber ply from recycled tires. Consistency in shape from paddle-to-paddle was poor with several paddles deformed from normal wear and tear. The shape of paddle set 1 was cupped, concave upward that allowed grain to pile in the center of the paddle when the clean grain elevator was running. Paddle set 2 featured a mostly flat shape with some inconsistencies per paddle. Paddle set 3 was a rigid plastic paddle that was consistently flat. The mounting to the elevator chain was the same for all paddle sets. Unlike the rubber paddles, paddle set 3 did not flex when contact was made with the clean grain auger. Instead, the elevator chain would pull slightly away from the elevator drive sprocket. Paddle set 4 was a different type of rubber than paddle sets 1 and 2. Layers of belted rubber kept the paddle shape consistent and flat. The flexible material allowed for the paddles to bend when rotating around the drive sprocket and clean grain auger. The different paddle sets formed four treatment levels to evaluate the yield monitor systems at different mass flow rates (Figure 4.4).

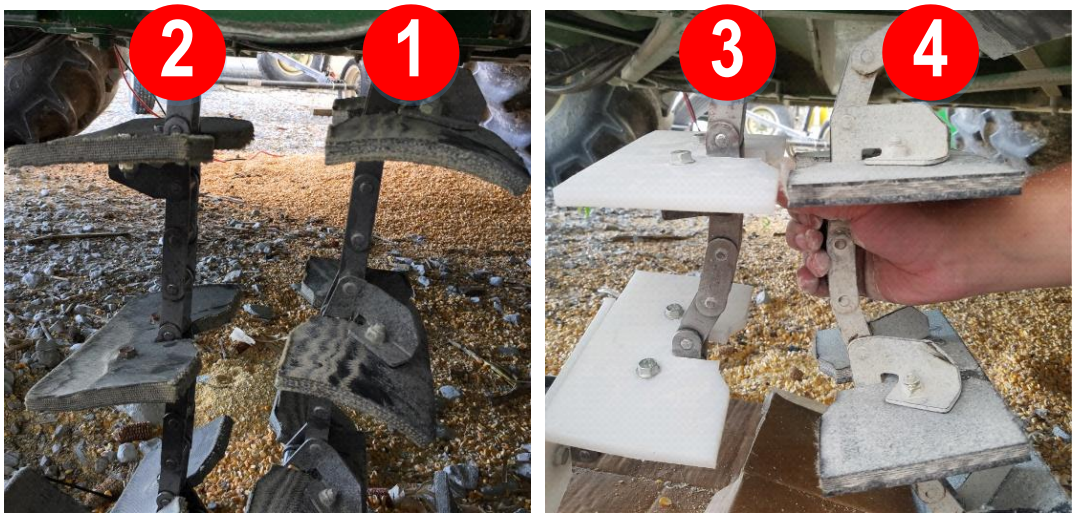

Figure 4.4: Paddle set configurations and respective ID numbers

Eight tests were completed on four different elevator paddle configurations (Table 4.5). Paddle configurations were installed by swapping the clean grain elevator chain for another with paddles already installed. Clearance between the edges of the paddle and the clean grain elevator walls were verified to be within manufacturer specification for all paddle sets. Elevators chains were tensioned to manufacturer specification. Dry corn was sourced from a local grain elevator and swapped for a new batch for each data set, or when grain reached the threshold of dockage for BCFM. Calibration was performed for both yield monitor systems to their respective recommended procedures for each data set. Yield monitors were tested at mass flow rate treatment levels outside of the calibrated range for data sets B, E, F, G, and H to observe the impact on estimation accuracy. All other mass flow rate treatment levels are within the calibrated range of flow.

Table 4.5: Data set description for yield monitor evaluation of paddle type

Data set	Paddle set ID no.	Mass flow rate (kg s^{-1})	Replicates
A	1	5	5
		10	5
		15	5
		20	5
		25	5
B	1	5 [a]	3
		10	3
		15	3
		20	3
		25	3
C	2	10	2
		15	2
		20	4
		25	2
D	2	10	4
		15	4
		25	4
E	3	5 [a]	4
		10	4
		15	4
		20	4
F	3	2 [a]	2
		4	4
		8	4
		10	4
G	4	5 [a]	4
		10	4
		15	4
		20	4
		25	4
H	4	5 [a]	4
		10	4
		15	4
		25	4

[a] *Mass flow rate was not characterized in yield monitor calibration*

4.2.5. Machine Orientation

Combine orientation affects how grain piles in the clean grain elevator and induces gravitation effects on the projectile motion of grain leaving the paddle. Machine orientation was selected as a treatment factor to gain a better understanding of the implication of pitch and roll on yield monitor performance. Machine pitch referred to the axial orientation of the combine. The fore position was represented by the crop head or the front of the combine. The aft position was represented by the rear of the combine. Pitch was defined as positive for downward rotation of the head. Machine roll refers to the transverse orientation of the combine. A clockwise transverse rotation of the combine was defined as a positive angle rotation (Figure 4.5).

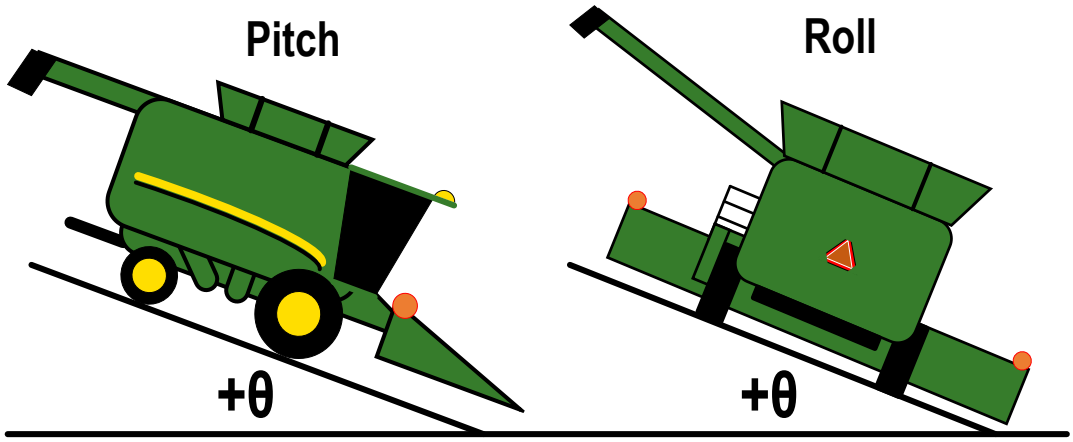

Figure 4.5: Combine pitch and roll orientation

The combine was oriented for testing by driving up on blocks. For roll orientation, one of the front drive wheel was blocked for positive rotation. The rear steering wheels had linkage that allowed the machine to orient without needing a block. Each of the rear steering wheels were blocked up for forward pitch of the combine. Orientation angle for pitch and roll were set using a digital level and monitored during testing using the yield monitor controllers.

Data analysis of combine orientation during harvest conditions was used as a basis of determination of pitch and roll angle for testing. Again utilizing the harvester CAN bus database, the mean angle for combine pitch and roll during harvest was nearly zero with similar standard deviation sizes of 2.1° and 2.3°, respectively (Figure 4.6).

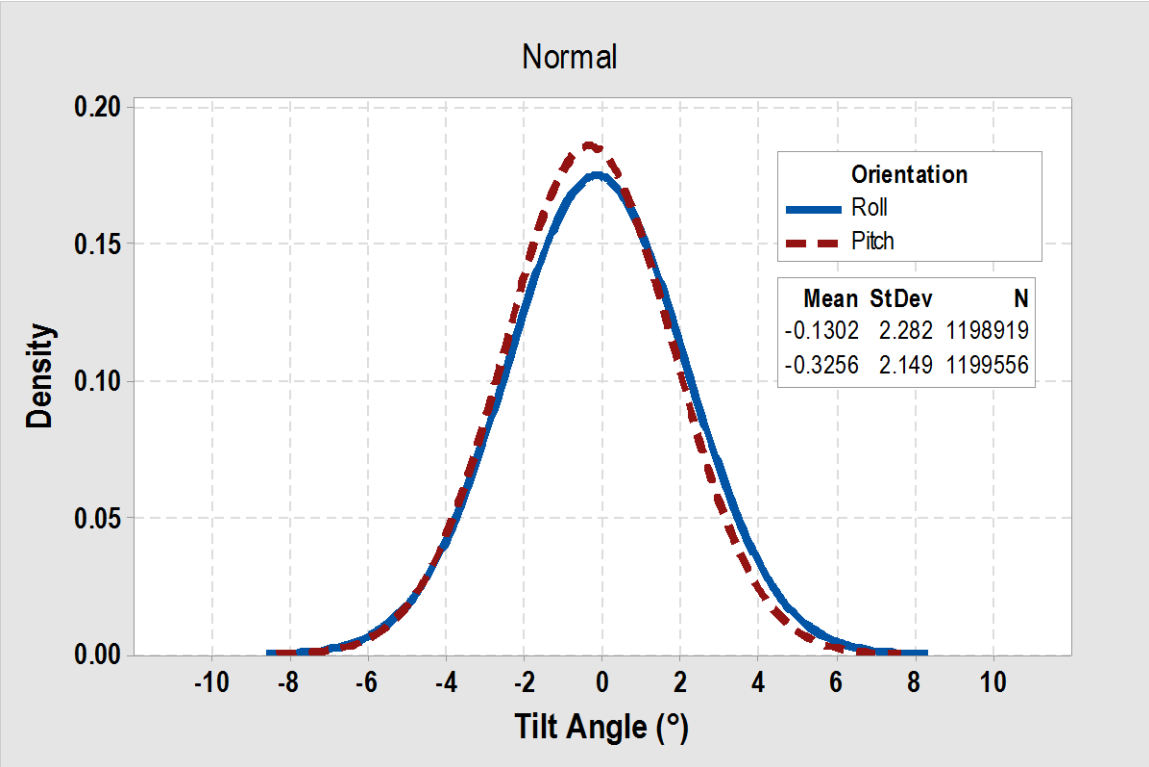

Figure 4.6: Distribution of combine pitch and roll angle during harvest

Analysis included common crop types from both small and large grains across a range of flow rates. Based on these results, a combine pitch and roll angle of 3 degrees was deemed ideal to test at because it encompassed 86% of orientation distributions. Level, 3 degree pitch, and 3 degree roll treatment levels were tested at different mass flow rates to observe the effect of machine orientation on yield monitor performance (Table 4.6). Both yield systems were calibrated on level terrain at mass flow rates spread across the distribution of interest. The combine was then reoriented to the outlined treatment levels with no recalibration to observe accuracy shift. Yield monitors were evaluated at the same mass flow

rates that calibration was completed at. Data sets E and J included one mass flow rate below the calibration range to observe performance shifts. Paddle set 3 was used for all machine orientation replicates because it was the most consistent, flat paddle set. Using the same paddle set for all treatment levels ensured validity regarding accuracy shifts between orientations.

Table 4.6: Data set description for yield monitor evaluation of machine orientation

Data set	Pitch Angle (°)	Roll Angle (°)	Mass flow rate (kg s^{-1})	Replicates
E	0	0	5 [a]	4
			10	4
			15	4
			20	4
I	0	3	10	4
			15	4
			20	4
J	3	0	5 [a]	4
			10	4
			15	4
			20	4

[a] *Mass flow rate was not characterized in yield monitor calibration*

4.2.6. Methodology for Yield Monitor Evaluation

The instantaneous response from the impact-based mass flow yield monitor and corresponding grain wagon weight were recorded at 1 Hz frequency. Instantaneous output from the volumetric flow yield monitor was not available, as the system was completely self-contained. Grain conveyance and the location of grain entry into the combine induced approximately a 10 second delay for grain to leave the wagon and reach the mass flow sensor at the top of the clean grain elevator. For these two reasons, estimated load weight of the respective yield monitoring systems was compared against the displaced load weight

measured by the grain wagon scale. Analysis of accumulated load weight mitigated the effect of time delay and allowed for direct comparison of the two yield systems. Three specific metrics were used to evaluate the accumulated load estimation performance of calibrated mass flow and volumetric flow yield monitors:

- The overall mean error per data set.
- Variability of error per data set.
- True mean error of flow rate ranges within a data set.

Harvest conditions fluctuate throughout a crop field and cause changes in grain flow rate, moisture, and test weight. The performance impact of moisture and test weight were reduced by using dry, consistent corn. Therefore, flow rate of grain was combined with other treatment factors of elevator paddle configuration and machine orientation to observe the effect on yield monitor estimation accuracy. Analysis of the overall mean error was used to compare yield monitor performance for each level of elevator paddle configuration and machine orientation across all levels of mass flow rate. This method isolated the shift in performance between paddle type and orientation direction.

The analysis of the variability of all error per data set focused on the repeatability and accuracy of yield monitors evaluated at mass flow rates that they were calibrated for. This method exposed error induced by levels of paddle configuration and machine orientation across all levels of mass flow rate. Lower overall variability was desired more than lower overall mean error, as the former indicated repeatability and was less susceptible to random error. Bias error in a sensor is easier to correct for than inherit, random error.

The true mean error of flow rate ranges was analyzed to evaluate performance impact of each level of mass flow rate on levels of elevator paddle configuration and machine

orientation. Confidence intervals evaluated the range of the true mean yield monitor error per mass flow rate set point. Preliminary testing with the test stand revealed that it was not possible to replicate a precise mass flow rate every time. As a result, true mean error would be evaluated for a range of flow rates rather than a specific flow rate setting. Flow rate ranges were determined post-testing by appropriately dividing the observed flow rates (Figure 4.7). Flow rate ranges were divided at natural breaks and included calibration points: 3 to 9, 9 to 15, 15 to 21, and 21 to 27 kg/s.

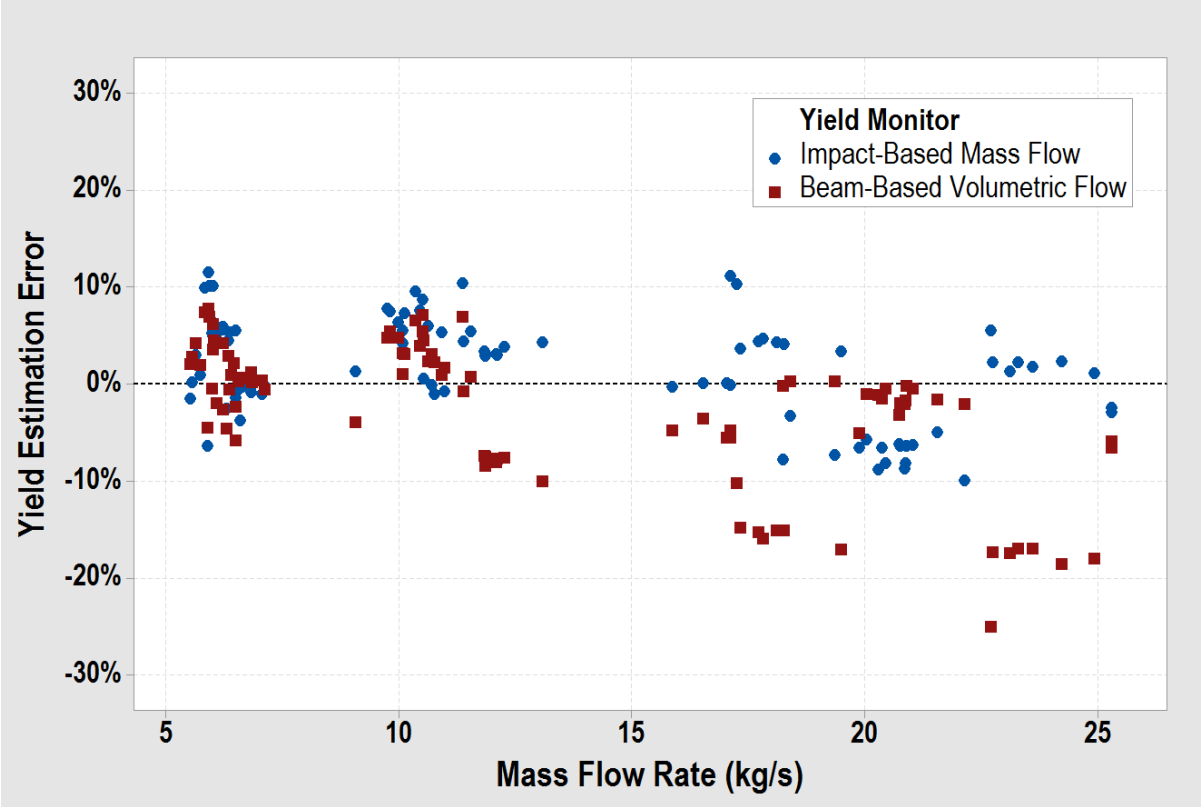

Figure 4.7: Yield estimation error at observed mass flow rates within the calibrated range

4.3. Results and Discussion

4.3.1. Grain Deterioration

As corn was recycled back and forth from the scaled grain wagon to the combine during yield monitor evaluation, it began to degrade. A test repetition consisted of a 2,500 kg load of corn metered at a constant flow rate from the grain wagon, into the combine, and back into the grain wagon using the unloading auger. Excessive flow rates, vibration, and conveyance of corn using augers caused corn to shatter during yield monitor evaluation. Percent broken corn was measured using USDA standard operating procedure. Corn deteriorated linearly at 0.5% per 10 repetitions (Figure 4.8). Assessment revealed that 92% of the observed variation in percent broken material could be explained by the simple linear model.

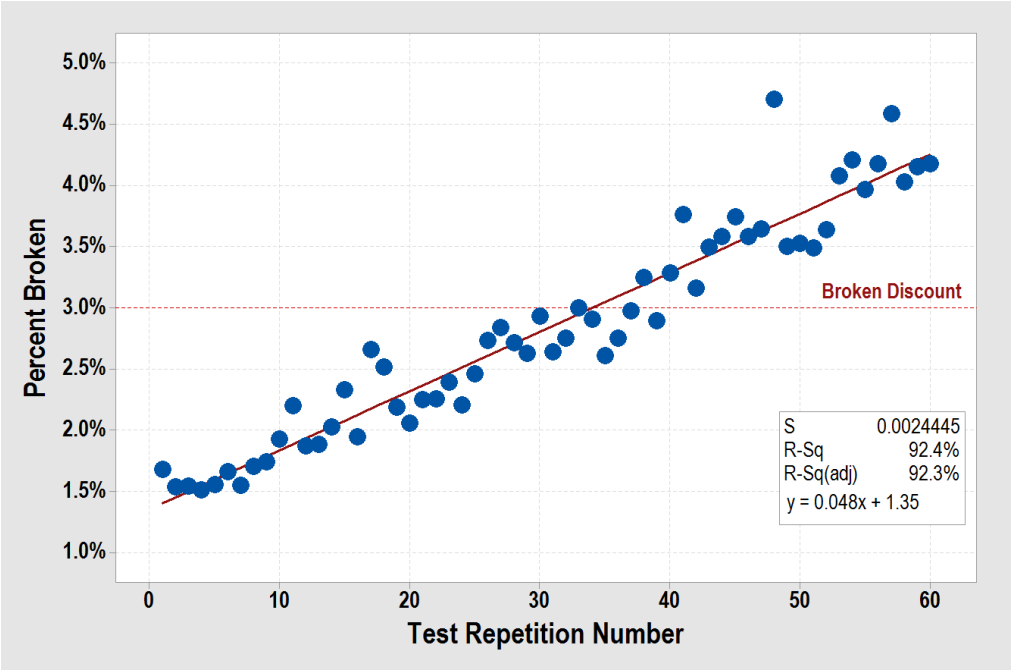

Figure 4.8: Corn deterioration during test stand repetitions

Discount on BCFM for incoming corn at central Iowa elevators is typically $0.02 per bushel per percentage point over 3% (Bern, Hurburgh, & Brumm, 2014). New corn was

sourced from a local elevator every 30 loads to limit damaged grain discount and keep quality representative of field harvest. Yield monitor accuracy was recorded with sample collection to ensure that grain deterioration was not affecting performance. Paddle set 1 was used for all grain deterioration repetitions. No definitive trends in estimation accuracy as grain deteriorates was found for either yield system (Figure 4.9).

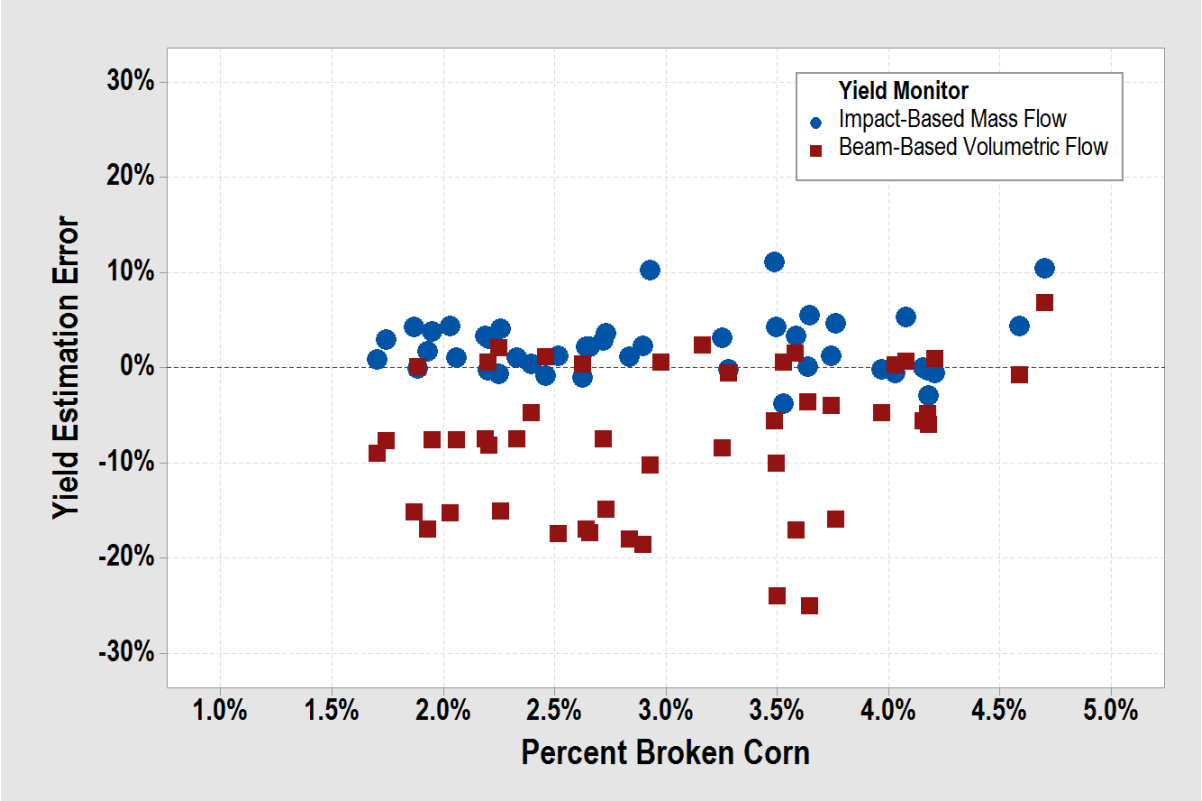

Figure 4.9: Yield monitor accuracy as corn deteriorates during test stand repetitions

4.3.2. Performance Impact of Paddle Configuration

The analysis of mean error focused on percent difference between the yield monitor estimated mass of grain metered into the combine and the mass displaced from the scaled axle grain wagon. Ideally, a yield monitor would produce a mean error of zero for grain flow rates within the calibrated range. Analysis of mean error was completed for paddle configuration data sets using flow rates that the yield monitors were calibrated for. Examination of the calibrated flow rate range allowed for statistical comparisons between treatment levels.

The paddle configuration had little effect on the estimation error for the impact-based mass flow yield monitor. Estimation error of data set F using poly paddles was found to be statistically significant to the estimation error, however this can be attributed to evaluation at exceptionally lower mass flow rates than other data sets (Table 4.7). Impact-based mass flow yield monitor performance was poorer for mass flow rates less than 5 kg s^{-1} compared to the higher rates. Calibration was difficult for lower mass flow rates due to sensor response limitations. Absolute estimation error for data sets other than F ranged from 0% to 4% and is in agreement with previous research. It was inferred that impact-based mass flow yield monitors are less susceptible to performance error due to clean grain elevator paddle configuration. Paddles project grain across a volume to the sensor, which may explain some reasoning for the lack of influence on impact-based mass flow yield monitor performance.

Table 4.7: Statistical difference by paddle configuration data set for impact-based mass flow yield monitor

Data set	Paddle set ID	Replicates	Estimation Error Mean	Estimation Error Std. Dev.	Tukey Grouping		
A	1	25	2.1%	2.4%	A		
B	1	12	3.8%	4.3%	A		
C	2	10	0.3%	2.6%	A		
D	2	12	-0.3%	4.9%	A		
E	3	12	1.1%	6.8%	A		
F	3	12	-52%	42%		B	
G	4	16	3.4%	8.8%	A		
H	4	12	0.5%	5.3%	A		

Influence of paddle configuration was evident for the volumetric flow yield monitor. The paddle configuration was found to be statistically significant to the estimation error (Table 4.8). Paddle set 2 (data sets C and D), 3 (data sets E and F), and 4 (data sets G and H) were found to not be statistically different from each other, however they were found to be different from paddle set 1 (data sets A and B). The inclusion of data set F in Tukey group B could be attributed the lower flow rates at which the data set was performed.

Table 4.8: Statistical difference by paddle configuration data set for volumetric flow yield monitor

Data set	Paddle set ID	Replicates	Estimation Error Mean	Estimation Error Std. Dev.	Tukey Grouping		
A	1	25	-9.1%	6.5%			C
B	1	12	-8.9%	9.6%		B	C
C	2	10	-3.0%	3.0%	A	B	C
D	2	12	1.2%	3.3%	A		
E	3	12	-0.2%	1.8%	A		
F	3	12	-2.6%	7.8%	A	B	
G	4	16	3.7%	4.1%	A		
H	4	12	2.2%	2.4%	A		

Paddle set 1 was found to be statistically different from other paddle configurations for volumetric flow yield monitors. Outlined in Table 4.4, these paddles were cupped upward so that grain collected in the center of the paddle. Individual paddle shape and consistency throughout the paddle set effected performance of volumetric flow yield monitors greater than impact-based mass flow yield monitors. The cause of this came from the presentation of grain to the sensor and the sensing technology. For the impact-based mass flow yield monitor, grain is propelled across the top of the clean grain elevator and into an impact sensor (Figure 2.4). Impact-based sensors correlate the force of the grain impact to a mass flow rate through calibration and regression. All paddle configurations tested allowed grain to leave the paddle and impact the sensor in a similar way, resulting in comparable yield estimation performance. When mass flow rate was diminished exceptionally in data set F, performance was reduced. It was hypothesized that this was the threshold where the grain trajectory and relationship with the sensor changed. The beam sensor of the volumetric flow yield monitor, positioned on the side of the clean grain elevator, was more susceptible to changes in paddle configuration because the sensing method relies upon the characteristics of grain delivery. Calibration characterized the beam breakage time to volumetric flow rates of grain. The yield monitor operated under the assumption that when the beam breaks, grain loading across the entire paddle is uniform. Misshaped paddles and poor paddle-to-paddle consistency changed the grain profile and loading on the paddle, resulting in increased estimation error for data sets A and B. The estimation error was negative because the yield monitor was underestimating the amount of grain displaced. Misshaped paddles allowed grain to hide from the beam sensor, compared to paddle ID no. 3 which uniformly displayed on the paddle. Paddle loading visual aids were created using the elevator rotational speed and

the number of paddles per chain (Figure 4.10). For the standard elevator configuration, approximately 17 paddles passed the sensing regions of the yield monitors per second. Calibration does not correct paddle sensitivity for the volumetric flow yield monitor if the presentation of grain to the sensor is flawed.

Figure 4.10: Grain pile loading on paddle ID no. 1 and 3 for 5 kg s^{-1} mass flow rate, respectively

The overall standard deviation across all flow rates was compared between data sets to evaluate the effect of paddle configuration on the repeatability of the yield monitoring systems. The variability of the impact-based mass flow yield monitor estimation error was between 2% and 9% for all paddle configurations, excluding data set F (Figure 4.11). The variability increased substantially to a 1-sigma standard deviation of 42% for data set F. This concurred with analysis of overall mean error that the estimation performance was reduced due to low flow rate calibration. Data sets G and H had larger variability than data sets A, B, C, and D although the mean estimation errors were comparable. Further research would need to be conducted to determine root cause.

Data sets A, B, and F had the largest variability for the volumetric flow yield monitor. Increased variability for data set F was likely the result of low flow calibration and presentation of grain to the sensor. Exceptionally low flow rates were tested within data set

F. If the grain mass flow rate was low enough that a paddle was not completely filled with grain, the yield monitor would overestimate yield under the assumption that paddles are completely filled with grain to the measured height. Research showed that the mass flow rate threshold of complete coverage of paddle area with corn was 2 kg s^{-1}. This was a level that data set F was evaluated at. Increased variability for data sets A and B was a result of misshaped and inconsistent paddles. All other data sets contained a 1-sigma standard deviation less than 5%.

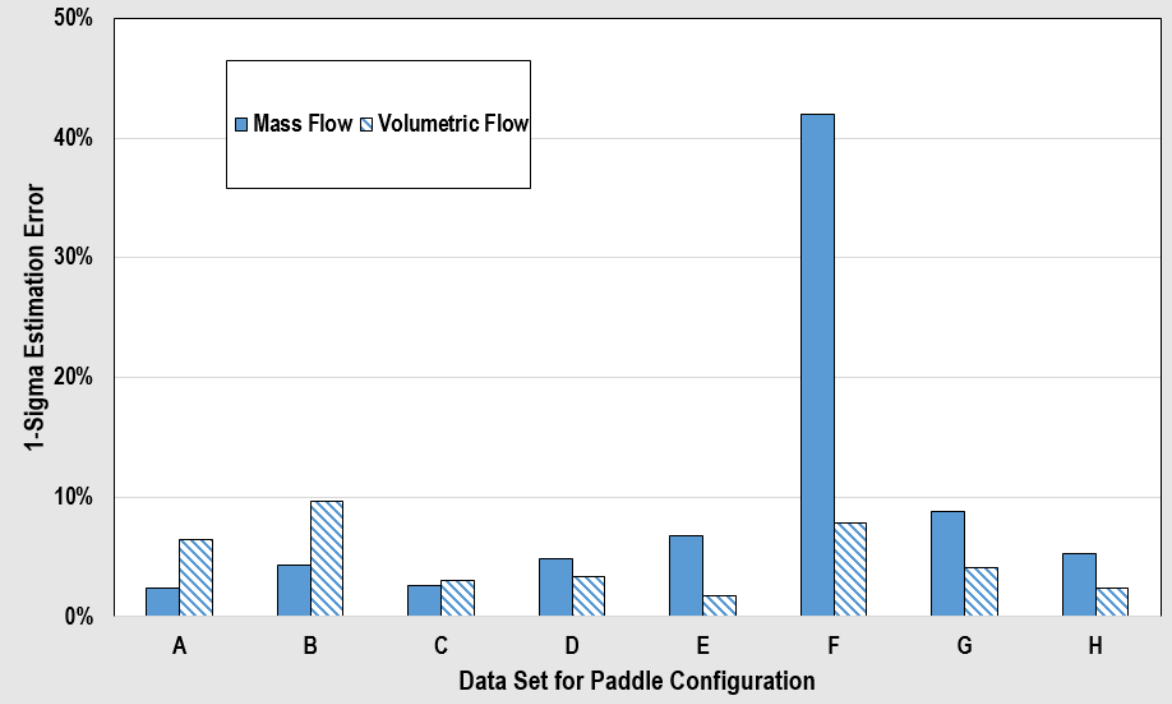

Figure 4.11: Standard deviation of yield monitor estimation error across all flow rates

The true mean error for four flow rate ranges was analyzed for each paddle configuration. As described, each paddle configuration was used in two data sets (Table 4.5). True mean error for the impact-based mass flow yield monitor ranged from -8% to +7% across all flow ranges and paddle configurations (Table 4.9). Paddle set 1 had three flow ranges that were found to not be statistically different from one another. Paddle sets 2, 3, and 4 had comparable flat shaped paddles and had at least two flow rate ranges that were found

not to be statistically different. Paddle sets 3 and 4 had two groups of paired flow rates and showed poorer estimation accuracy at higher mass flow rate. The impact-based mass flow yield monitor demonstrated comparable performance across all paddle types, however statistical difference was found between flow rates. Repeatable results across the entire calibrated flow range is fundamental in obtaining accurate yield measurement. Bias error that offsets the yield estimation across all flow rates is easier to correct than random error and variability between flow ranges.

Table 4.9: Statistical differences by specific flow rate range and paddle set for impact-based mass flow yield monitor

Paddle set ID	Flow Range (kg s^{-1})	Estimation Error		Tukey Grouping						
		Mean	Std. Dev.							
1	5-9	-1.0%	1.3%			C	D	E	F	
	9-15	3.9%	2.6%	A	B	C				
	15-21	5.7%	3.1%	A	B					
	21-27	2.3%	1.5%	A	B	C	D	E		
2	5-9	3.4%	3.2%	A	B	C	D			
	9-15	1.4%	2.8%		B	C	D	E		
	15-21	-2.8%	3.4%					E	F	G
	21-27	-3.5%	1.3%				D	E	F	G
3	5-9	2.0%	4.8%		B	C	D	E		
	9-15	6.0%	0.91%	A	B					
	15-21	-8.1%	0.64%							G
	21-27	NA	NA							
4	5-9	5.5%	5.4%	A	B					
	9-15	7.3%	1.65	A						
	15-21	-6.5%	1.9%						F	G
	21-27	-8.1%	2.6%						F	G

True mean error for the volumetric flow yield monitor ranged -18% to 5% across all flow ranges and paddle set configurations (Table 4.10). True mean error for flat paddle sets 2, 3, and 4 ranged from -5% to +5%. Paddle set 1 had the largest error range with nearly zero

yield estimation error at lower flow rates and the largest error at the higher flow rates. Flow ranges 15-21 and 21-27 kg s^{-1} were found to be significantly different from flow ranges for all paddle configurations. This was attributed to the shape and consistency of the paddles. Misshaped paddles allowed grain to settle in areas of the paddle where the sensor could not accurately measure. Consistency of each paddle affected the zero flow tare and resulting accumulated load estimations. At least two flow ranges from paddle sets 2, 3, and 4 were found to not be significantly different from each other within the same paddle set. Similar results as the impact-based mass flow yield monitor of two groups of statistical significance per paddle configuration were found. Three of the four paddle configurations are were found to not be statistically different for the 5-9, 9-15, and 15-21 kg s^{-1} ranges.

Table 4.10: Statistical differences by specific flow rate range and paddle set for volumetric flow yield monitor

Paddle set ID	Flow Range (kg s^{-1})	Estimation Error		Tukey Grouping								
		Mean	Std. Dev.									
1	5-9	0.61%	0.84%	A	B	C	D	E				
	9-15	-6.0%	5.1%							G		
	15-21	-13%	3.8%								H	
	21-27	-18%	2.9%									I
2	5-9	2.7%	1.8%	A	B	C						
	9-15	1.9%	1.8%	A	B	C	D					
	15-21	-4.2%	1.3%						F	G		
	21-27	-4.7%	2.7%					E	F	G		
3	5-9	-2.9%	1.9%				D	E	F	G		
	9-15	1.8%	1.0%	A	B	C	D	E				
	15-21	0.40%	0.59%		B	C	D	E	F			
	21-27	NA	NA									
4	5-9	4.9%	2.5%	A	B							
	9-15	5.1%	1.3%	A								
	15-21	-1.1%	0.91%			C	D	E	F			
	21-27	-1.3%	1.2%	A	B	C	D	E	F	G		

4.3.3. Performance Impact of Machine Orientation

The overall mean error, variability, and mean error per flow rate range were analyzed to evaluate the impact of machine orientation on yield monitor performance. Estimation error was found to not be statistically different by machine orientation for the impact-based mass flow yield monitor, although overall mean error increased from level to roll and pitch orientation (Table 4.11). Mean error produced for roll and pitch orientations was 3.2% and 5.0%. Results were in agreement with previously reported results by Fulton et al. (2009).

Table 4.11: Statistical difference by machine orientation data set for impact-based mass flow yield monitor

			Estimation Error		
Data set	**Orientation**	**Replicates**	**Mean**	**Std. Dev.**	**Tukey Grouping**
E	Level	12	1.1%	6.8%	A
I	3° Roll	12	3.2%	6.8%	A
J	3° Pitch	10	5.0%	7.6%	A

Estimation error was found to be statistically different by machine orientation for the volumetric flow yield monitor (Table 4.12). Yield monitor performance was highly accurate for level orientation with mean error nearly zero. Data set I, rolled orientation, produced the largest mean error of 11%, while pitched orientation was less severe to estimation accuracy.

Table 4.12: Statistical difference by machine orientation data set for volumetric flow yield monitor

			Estimation Error			
Data set		**Replicates**	**Mean**	**Std. Dev.**	**Tukey Grouping**	
E	Level	12	-0.2%	1.8%		C
I	3° Roll	12	11%	2.1%	A	
J	3° Pitch	10	6.7%	1.5%		B

Both rolled and pitched machine orientation caused the volumetric flow yield monitor to overestimate the mass of the accumulated load. Overestimation stems from the measuring method of the sensor. Changes in machine orientation caused uneven loading on elevator paddles and overestimation of grain flow (Figure 4.12). When the combine was rolled, grain piled to one side of the elevator paddle. The yield system estimated grain flow under the assumption that when the sensing beam was broken, grain pile height was consistent all the way across the elevator paddle. Since grain height varied, overestimation occurred. Similar results were observed for machine pitch, however with lower mean error. The clean grain elevator allowed grain to pile towards the front of the paddle for pitched machine orientation. Beam sensor installation allowed for the approximate center of the pile to be measured and pile height to be averaged between both sides of the pile, resulting in less error for pitched orientation. The severity of grain piling to one side of the paddle is dependent upon the degree of machine pitch or roll and angle of repose of the grain.

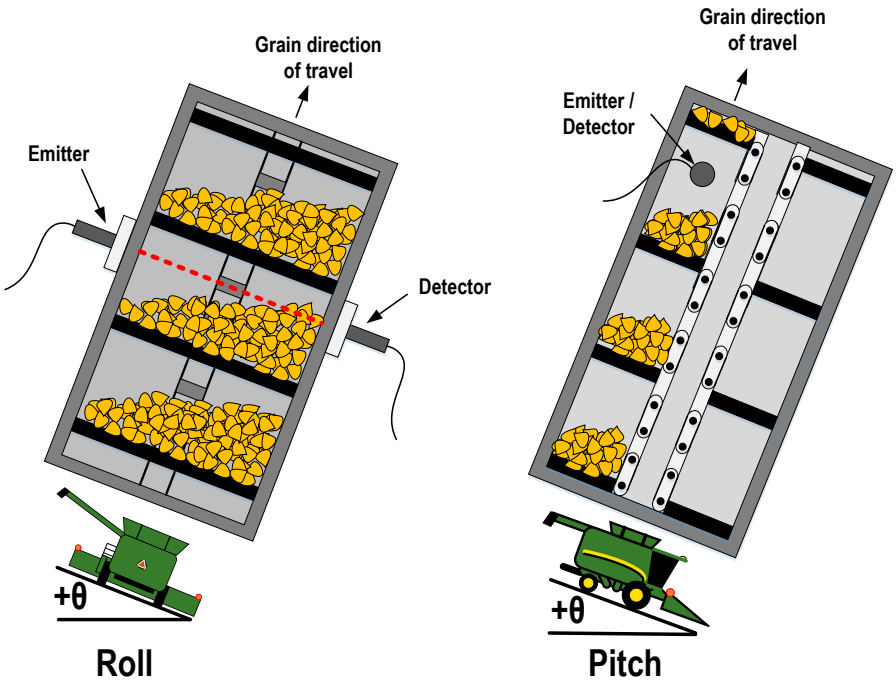

Figure 4.12: Machine orientation impact on grain pile in clean grain elevator

The repeatability of the yield systems was analyzed using the overall standard deviation across all flow ranges. Standard deviation was consistent between the data sets for each of the yield monitors, likely because evaluation was completed with the same paddle set. Rigid, flat paddles from paddle set 3 were used for all machine orientation data sets to isolate orientation as the treatment factor. The variability in yield estimation was greater for the impact-based mass flow yield monitor than the volumetric flow yield monitor. Increased variability of the impact-based mass flow yield monitor was expected based on paddle configuration results. Volumetric flow yield monitor results had average error standard deviation less than 2% for the three data sets. Repeatability across all flow ranges is a key metric of yield monitor performance and allows for simple estimation offset adjustment based on machine orientation. The controller module should have corrected yield estimation using the pre-test slope calibration, but it is unclear why the system did not compensate.

Analysis of the true mean error showed that there was significant difference between machine orientation and estimation error for different ranges of flow rates for the impact-based mass flow yield monitor (Table 4.13). In general, similar performance was achieved at each mass flow rate for the three machine orientations. For all data sets, flow rate range 15-21 kg s^{-1} was found to be statistically significant to the other two flow ranges. Flow rate ranges 5-9 and 15-21 kg s^{-1} were found not to be statistically significant between each orientation data sets. It was inferred from similar performance for the three data sets that the impact-based mass flow yield monitor was less susceptible to performance degradation from changes in machine orientation.

Table 4.13: Statistical differences by specific flow rate range and machine orientation for impact-based mass flow yield monitor:

Data set	Orientation	Flow Range (kg s^{-1})	Estimation Error		Tukey Grouping		
			Mean	Std. Dev.			
E	Level	5-9	5.4%	0.21%		B	
		9-15	6.0%	0.91%		B	
		15-21	-8.1%	0.64%			C
I	3° Roll	5-9	5.5%	4.7%		B	
		9-15	9.9%	0.89%	A	B	
		15-21	-4.8%	0.57%			C
J	3° Pitch	5-9	6.8%	2.2%		B	
		9-15	13%	0.53%	A		
		15-21	-4.6%	0.38%			C

Volumetric flow yield monitor estimation error was found to be statistically significant for different machine orientations, but not for flow rate within the same orientation data set (Table 4.14). Although different orientations shifted mean performance, variability of error within flow rate ranges was less than 3%. The volumetric yield monitor performed more uniformly across flow rates than the impact-based mass flow yield monitor.

Table 4.14: Statistical differences by specific flow rate range and machine orientation for volumetric flow yield monitor

Data set	Orientation	Flow Range (kg s^{-1})	Estimation Error		Tukey Grouping			
			Mean	Std. Dev.				
E	Level	5-9	-1.9%	0.96%				D
		9-15	1.8%	1.0%			C	
		15-21	-0.40%	0.59%			C	D
I	3° Roll	5-9	10.8%	3.3%	A			
		9-15	12.3%	0.50%	A			
		15-21	10.9%	0.87%	A			
J	3° Pitch	5-9	5.8%	0.35%		B		
		9-15	8.6%	0.53%	A	B		
		15-21	5.6%	0.91%		B		

4.3.4. Performance of Non-Calibrated Flow Rates

Manufacturers recommend recalibration of yield monitors when crop conditions change and no longer are represented by the current calibration factors. It is difficult to get exposure to all anticipated crop conditions in a single yield monitor calibration, so it is often necessary for a producer to calibrate multiple times throughout a season to maintain accuracy. Even so, a calibration will not encase all of the continuous range of flow rates a field may have. In this section, yield monitor performance was analyzed for flow rates that were below the range of calibration.

Absolute yield estimation error increased significantly for flow rates that were outside of the calibrated range (Figure 4.13). Estimation error was analyzed across all paddle configurations on level orientation. The impact-based mass flow yield monitor consistently underestimated the mass displaced from the scaled grain wagon. The impact-based mass flow yield monitor estimated the flow rate of grain using regression from the calibration loads. Flow rates evaluated outside of the calibrated range are estimated using extrapolation and subject to error. Extrapolation of flow rates becomes increasingly difficult when a non-linear relationship exists between the yield sensor and flow rate. The dramatic drop-off of estimation accuracy for flow rates outside of the calibrated range suggested a non-linear relationship existed for the impact-based mass flow sensor, which places higher priority in maintaining a calibration suitable to the current harvesting environment. Non-linearity of impact-based yield sensors across a wide flow range has been well-documented by previous research. The impact-based mass flow yield monitor performance declined as flow rate decreased, with a low of -100% error. Presentation quality of grain to the mass flow sensor is drastically reduced at lower flow rates, making it difficult to record grain impulses.

Calibration was difficult and time consuming at lower flow rates due to diminished sensor response. Calibration loads were often rejected after target load size had been reached due to estimated accumulated mass not measuring within the manufacturer tolerance range.

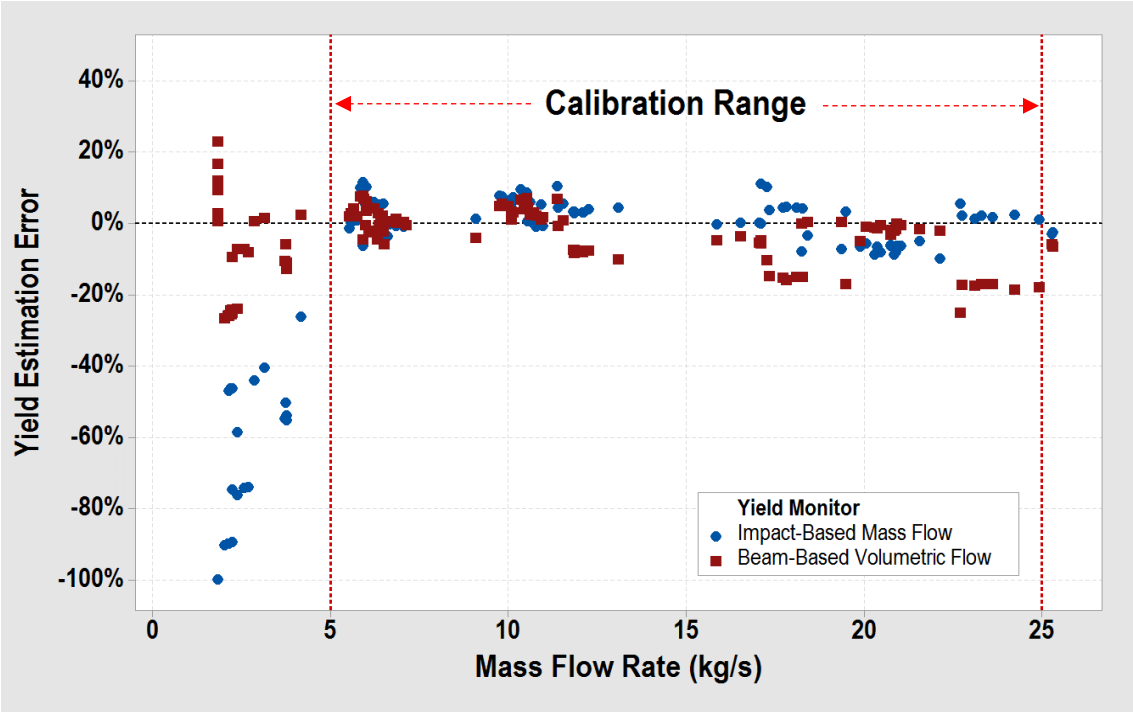

Figure 4.13: Yield monitor accuracy for flow rates outside of calibration range

The volumetric flow yield monitor performance diminished as uncalibrated flow rates were introduced, although not as significantly as the impact-based mass flow yield monitor. The volumetric flow yield monitor used regression of calibration loads to estimate flow rate, however it also utilized fundamental measurement principles. The beam-based volumetric sensor estimated the volume of grain on a paddle using the beam break time, paddle dimensions, and clean grain elevator speed. A basic yield estimation equation was formed and regression used to correct for bias error, moisture, and grain quality. This translated to decreased mean error for flow rates below the calibrated range compared to the impact-based mass flow yield monitor. The increased variability of positive and negative estimation error

came from different paddle configurations. As different paddle configurations were evaluated, accuracy at lower flow rates reflected the presentation quality of grain to the beam-based volumetric sensor and echoed the necessity for consistent grain presentation from the paddle.

4.4. Conclusions

The accuracy and variability of two commercial yield monitors that utilize different measurement principles were evaluated using a combine test stand. Accumulated grain weights were compared between the systems, as the unprocessed signals were unavailable. The mean error and variability across all flow rates and mean error between flow ranges were used as performance metrics for evaluation.

The impact-based mass flow yield monitor used a mass flow sensor installed at the top of the clean grain elevator to measure impulses as grain is projected from the clean grain elevator paddles. Yield estimation accuracy was reliant upon calibration for the different treatment levels. Clean grain elevator paddle configuration and machine orientation were not statistically significant to yield estimation error. The impact-based mass flow yield monitor performance was found to have higher variability across all flow ranges during testing. Average variability was 5% for flow rates expected of large grains. Performance was dramatically reduced for flow rates typical of small grains and flow rates that were outside of the calibrated range. Absolute errors ranging from 30% to 100% were observed for flow rates less than 5 kg s^{-1}. Improper calibration and load rejection were common for low flow rates. Poor performance at low flow rates was caused by the diminished sensor response and inability to measure small grain impulses. Reliance solely on regression of calibration loads allows for error influence for crop conditions that are beyond the scope of the most recent

calibration. The impact-based mass flow yield monitor performed well when the system experienced conditions for which it was calibrated for, but accuracy deteriorated when evaluation stepped outside of those conditions. In a sensing environment where crop conditions vary continuously, there is a calibration paradox for the most widely used yield monitoring system.

The volumetric flow yield monitor used a beam-based volumetric flow sensor installed on the side of the clean grain elevator to measure grain fill height per paddle. Volumetric grain flow rate was determined using a fundamental equation with inputs of paddle dimension, fill height, and clean grain elevator speed. Grain test weight was used for conversion between accumulated grain volume and mass and was controlled in the test stand using consistent bulk grain. Both clean grain elevator paddle configuration and machine orientation were found to be statistically significant to yield estimation error. Cupped, misshaped paddles had mean estimation error of 9% and mean standard deviation of 8%. All other data sets featuring flat, consistent paddles had a mean estimation error of 0.2% and mean standard deviation of 4%. Yield estimation performance for level, rolled, and pitched machine orientations were found to be statistically different from each other. Absolute mean error for each of the orientations was 0.2%, 11%, and 7%, respectively with a standard deviation of 2%. Influence of paddle configuration and machine orientation on yield estimation accuracy highlighted the sensitivity of grain presentation to beam-based volumetric sensors. Grain shifting, exceptionally low flow rates, and non-level piling in the clean grain elevator created a difficult sensing environment. The volumetric flow yield monitor was more accurate than the impact-based mass flow yield monitor at flow rates typical of small grains and conditions not covered by calibration. The use of the fundamental

measurement method and equation allows for less dependency on calibration, but is still required to correct for crop and machine specific parameters.

Each yield monitoring system exemplified qualities that are ideal for maintenance of yield estimation accuracy. Compliance across machine parameters and crop conditions, reduced variability between flow ranges, and the move towards a fundamental measurement method of yield estimation will allow for increased performance for a larger crop matrix. Although the impact-based mass flow rate was less susceptible to errors induced by paddle type and machine orientation than the volumetric flow yield monitor, it was subject to more inherit error across the flow rate range. Random error and variability across flow rate ranges reinforces the need for regular re-calibration of the sensor, which adds inefficiency during harvest. Additionally, the estimation error skyrocketed when flow rates outside of the calibrated range and less than 5 kg s^{-1} were experienced. This becomes a problem with field exposure where conditions cannot be controlled. Small grains such as wheat, soybean, canola, and barley regularly contain flow rates within this area of concern. The volumetric flow yield monitor was more susceptible to error induced from changes of the machine rather than inherit error, giving it an advantage if design changes can be made to control those aspects. Design control of the presentation characteristics of grain to the sensor and inherit linearity in sensor response allow potential for predictability of sensor performance in different crop environments. The next generation of yield monitoring technology has the potential for wide market adoption through increased accuracy, less calibration dependency, and maintenance of performance.

CHAPTER 5. PARTICLE FLOW YIELD MONITORING

5.1. Introduction

Combines are capable of performing several complex operations as they harvest grain from a field. Using telematics and cellular services, vast quantities of data from combines are available almost instantaneously for producers to make decisions with. As farm field size has increased, precision agriculture technology has helped to increase productivity and profitability by allowing fields to be managed on a smaller scale. Variable rate fertilizer application and seeding rates are just a couple of examples of available precision agriculture technology. Yield maps have become the standard tool for building production plans for future crop years. Yield monitoring systems must be accurate to ensure validity of producer decisions.

The objective of this research was to propose a yield monitoring system that maintains accuracy with limited calibration requirements. Maintaining accuracy of the system requires moving to a fundamental system of yield measurement. Impact-based yield monitoring relies entirely upon regression of a calibration curve to fit the mass flow sensor response signal to the actual mass flow rate of grain. The system is built upon a foundation of factor dependent analysis and error is induced when conditions are experienced that do not directly fit into the model. Additionally, standard uncertainty of the mass flow sensor further increases error. In large grains such as corn this is not a major issue where higher flow rates are common, but in small grains the relative error of the mass flow sensor standard uncertainty can be 30% or greater. Yield monitoring using a fundamental system of measurement can lead to increased accuracy and less need for system calibration.

Volumetric grain flow was selected as the measurement method for determining crop yield. Both mass and volumetric yield estimation methods require test weight as in input to convert to accumulated volume or mass per unit area. Volumetric flow rate uses a fundamental measurement method that records the velocity through a known cross sectional area, the density of objects traveling at a fixed velocity, or the volume displaced during a fixed time step. The latter is the only method that has been used previously in volumetric yield measurement systems and is found today in systems using metering roll and non-contact beam sensors. A camera was selected as a sensor to measure velocity of grain as it traveled through an area on the combine. Velocity was obtained through measurement of grain displacement between image frames. The particle flow yield monitor was used to quantify the volumetric flow rate of grain passing through the combine and the accuracy of this system in different harvesting conditions.

The intention of this section is to identify design considerations of a particle flow yield monitor to measure volumetric flow rate of grains so that crop yield can accurately be predicted. Mechanical requirements, camera location, and imaging specifications will be discussed. Once determined, initial performance assessment of a particle flow yield monitor across different crop conditions and flow rates will be analyzed. Specific objectives of the particle flow yield monitor design and evaluation process are listed below:

1. Identify specifications and locations of a particle flow yield monitor to ensure mechanical requirements are met for grain velocity measurement.
2. Assess the initial performance of a particle flow yield monitor across different crop types and compare with commercial yield monitoring systems.

5.2. Materials and Methods

5.2.1. Mechanical Requirements

5.2.1.1. Grain Cavity Volume

The selected volumetric flow sensing method uses a camera to measure the velocity of grain as it travels through the combine. In order to convert this velocity to volumetric flow, the cross sectional area of the grain must be known. This value is not consistent on crop harvesters, as the cross sectional area of grain flow through the combine is proportional to the grain flow at that particular time. If all grain passing through the combine was channeled through a 0.3 m (12 in.) tube, the grain velocity measured would change as a function of the fill level and volumetric flow rate through the tube (Figure 5.1).

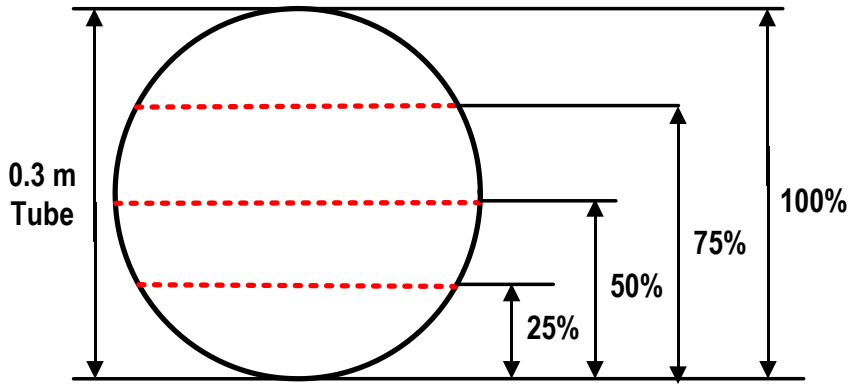

		Volumetric Flow Rate of Grain (m^3/s)									
		0.003	0.006	0.008	0.011	0.014	0.021	0.028	0.035	0.042	0.049
Filled Cavity Area (%)	25%	0.15	0.30	0.46	0.61	0.76	1.14	1.52	1.90	2.28	2.66
	50%	0.08	0.15	0.23	0.30	0.38	0.57	0.76	0.95	1.14	1.33
	75%	0.05	0.10	0.15	0.20	0.25	0.38	0.51	0.63	0.76	0.89
	100%	0.04	0.08	0.11	0.15	0.19	0.29	0.38	0.48	0.57	0.67

Figure 5.1: Filled cavity area and volumetric flow rate impact on grain velocity

Since both filled cavity area and volumetric flow rate of grain can vary in a combine, velocity measurement alone is unsuccessful to estimate volumetric flow rate of grain. In fact,

there are several repeated measurements of velocity for different combinations of cavity area and volumetric flow rate. However, if the filled cavity area in a tube remains fixed then there is a direct relationship between the velocity ($\vec{v}$) and the volumetric flow rate of grain ($\dot{V}$). The relationship is also linear if the velocity of grain is uniform across the entire cross sectional area (A) of a known diameter (D).

Equation 5.1: Volumetric flow rate through a cylinderical tube of a known diameter

$$\dot{V} = \vec{v} * A = \vec{v} * \frac{\pi * D^2}{4}$$

5.2.1.2. Power Requirements to Push Full Grain Cavity Volume

Maintaining a consistent and full cavity of grain requires a volume where grain is allowed to accumulate. This can be done either vertically or horizontally through conveyance of grain into a section with closed sides where grain accumulates and pushes through to the exit. Filling a grain cavity introduces new unknowns regarding the power requirements to push a full volume of grain. To quantify the power requirements of a conveyance system with a pile up region, a test stand was constructed (Figure 5.2). The test stand consisted of a hopper and auger oriented horizontally with a section of auger flighting removed. Different lengths of auger flighting were removed to determine the relationship between cavity volume and power required to push grain through the section. The relationship between grain volume and the power requirement to push it through a cavity is a function of conveyance orientation, cavity size, and grain properties, such as type, moisture, and density. Since the goal of initial testing was to simply define relative power requirements with increased cavity size, dry corn was sourced from a local elevator at storage moisture and recycled throughout testing.

Figure 5.2 : Auger test stand for determination of cavity power requirement

Tests were conducted at target grain mass flow rates ranging from 1 to 35 kg s^{-1}. For each mass flow rate, corn was metered out of a grain cart with scaled axles and conveyed into the grain inlet area of the horizontal test stand. Auger rotation was powered using a hydraulic motor and initially set to 450 RPM to simulate typical combine auger rotational speed. Motor rotational speed and auger rotational speed were recorded using GS1005 cherry Hall Effect speed sensors. Motor pressure was also recorded using a pressure sensor. Hydraulic motor flow rate was calculated by combining hydraulic motor displacement and rotational speed, which was used with motor pressure to find the power requirements to convey target mass flow rates of grain (Figure 5.3, Table 5.1).

The results of the power requirement test showed that incorporation of a grain cavity region in a cylindrical auger tube increased the power required to operate the auger. For the test with no cavity volume, the original auger with complete flighting along the entire length of the shaft was used. Subsequent tests were performed with a cavity length of 0.6 m. The

cavity was in a cylindrical tube of 0.30 m diameter. Pushing grain through a full cavity of 0.6 m in length at the maximum flow rate tested resulted in a power requirement increase from the control of nearly 60%. For the no cavity and 0.6 m cavity, a self-contained hydraulic power unit was used to turn the auger. Since the cavity length used for experimental data collection will be less than 0.6 m, the power required to push grain through a cavity is closely aligned with the power requirements of a full auger. Therefore, power requirements to form and maintain a full cavity of grain in a fixed volume is not a major concern. The power required to push grain through a cavity will increase as the orientation of the auger and direction of grain flow change.

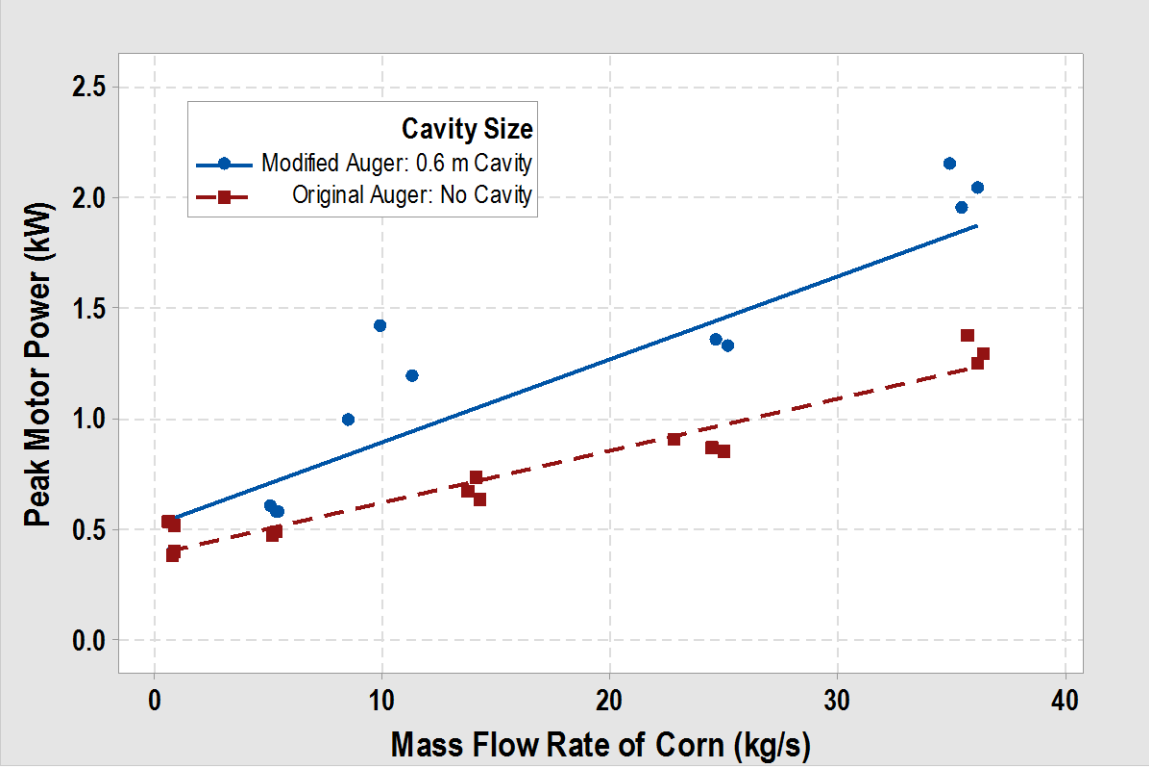

Figure 5.3: Power requirement to push grain cavity for range of grain mass flow rates

Table 5.1: Regression model parameters for cavity power requirement testing

Cavity Size	Regression Model	Regression Parameters		Coefficient of Determination
		β_0	β_1	r^2
0.6 m	Linear	0.514	0.034	78.2%
No Cavity	Linear	0.386	0.023	94.0%

5.2.2. Camera Flow Measurement

In this section, the measurement technique to estimate the volumetric rate of grain being harvested and methodology of the system are presented. Additionally, criteria for installation location of the system and design considerations to meet mechanical requirements will be discussed. Finally, the data acquisition system and post-collection image processing techniques will be discussed.

5.2.2.1. Camera Specifications

A camera used to record images of grain inside a combine harvester must be robust to withstand harsh environmental properties. The electronic components must be robust enough to withstand fluctuating temperature environments as well as vibrational and impact effects. For these reasons, a camera was provided by the project sponsor that was being used on production combine harvesters (Figure 5.4). The camera was a production part used to record images on the re-threshing elevator to determine grain quality.

Figure 5.4: Camera used to record images of grain

The camera dimensions were 140 mm (5.5 inches) in length, 185 mm (7.25 inches) in width, and 130 mm (5.125 inches) in depth. An aluminum milled housing provided support for securing the camera mounting as well as protection for internal components. To prevent corrosion and damage of sensitive internal components, the camera had an IP67 rating, meaning the housing provided complete protection from dust penetration and temporary immersion in water. Internal purging and pressurization of the camera module with nitrogen gas prevents exposure to dust in addition to hindrance of condensation formation on the inside lens. Before selection of the camera for volumetric grain flow estimation, the project sponsor tested the camera to ensure performance in an environment similar to the proposed application. The face of the camera consisted of a thick glass window that was the focus of the camera. The window resulted in a viewable image area of 75 mm (3 inches) in width by 50 mm (2 inches) in height. Durable, scratch resistant glass was a design requirement as

grain would pass directly over the face of the camera during use. Grain was illuminated as it passed over the face by four LED lights mounted inside of the camera. Image resolution was low to achieve higher framerates up to 60 Hz. Images were captured at dimensions of 720 pixels in width by 480 pixels in height, resulting in a resolution of 346 KP with 24 bit depth. Camera exposure time is fixed at 385 microseconds and has a focal length of 6 mm. One Molex PCB 12 pin printed circuit board header on the side of the camera supplied 24 volt power to the camera and allowed for the data acquisition system to receive recorded images. The harnessing established an Ethernet connection between the camera and the image processing module. Additionally, a M12 5-pin connector could be used to view direct video output of the camera without image processing. This was especially helpful for troubleshooting and camera set-up.

5.2.2.2. Volumetric Flow Algorithm

As mentioned previously, a camera was selected as a sensor to measure the velocity of grain as it flowed through the combine. Images were recorded as grain flowed past the face of the camera. Grain displacement between frames was determined through analysis images recorded at a high capture rate. Displacement in units of image pixels (pixel line displacement, PD) was converted to linear length through use of image dimensions (l), which became velocity ($\vec{v}$) when multiplying by image capture frequency (f, Figure 5.5).

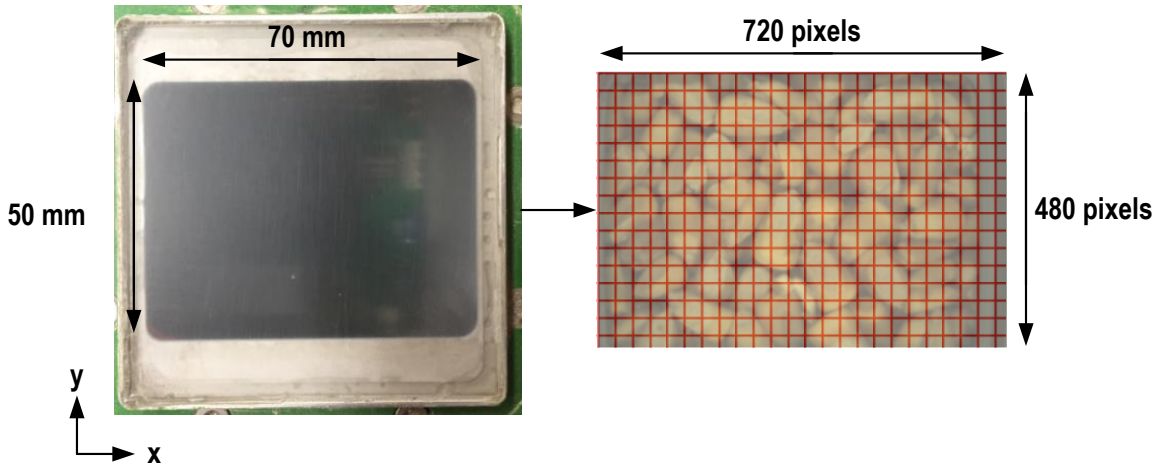

Figure 5.5: Camera face and image dimensions

The camera was installed so that grain flow direction was parallel to the y-axis, therefore it was calculated that image dimensions were 9.6 rows of pixel lines per millimeter. So long as grain flow was controlled and limited to only the y-axis, no additional dimensioning parameters were needed. Under the assumption that the cross sectional area (A) or diameter (D) of the grain stream was constant and known, volumetric flow rate of grain was determined by combining the velocity with the cross sectional area (Equation 5.2). Alternatively, an accumulated volume of grain was estimated by combining total pixels displaced in a test replicate and the cross sectional area.

Equation 5.2: Volumetric flow rate estimate in a cylindrical tube using camera images

$$Volumetric\ Flow\ Rate = \dot{V} = \vec{v} * A = \frac{PD * f}{l} * \frac{\pi * D^2}{4}$$

The algorithm used to process images and detect pixel displacement was provided by the project sponsor from a previous project. The software was developed by the National Robotics Engineering Center at Carnegie Mellon University. Images that were captured at a high frequency were analyzed in order to detect 1-D movement (Figure 5.6). Grain overlap between images was converted to pixel lines displaced and then grain velocity.

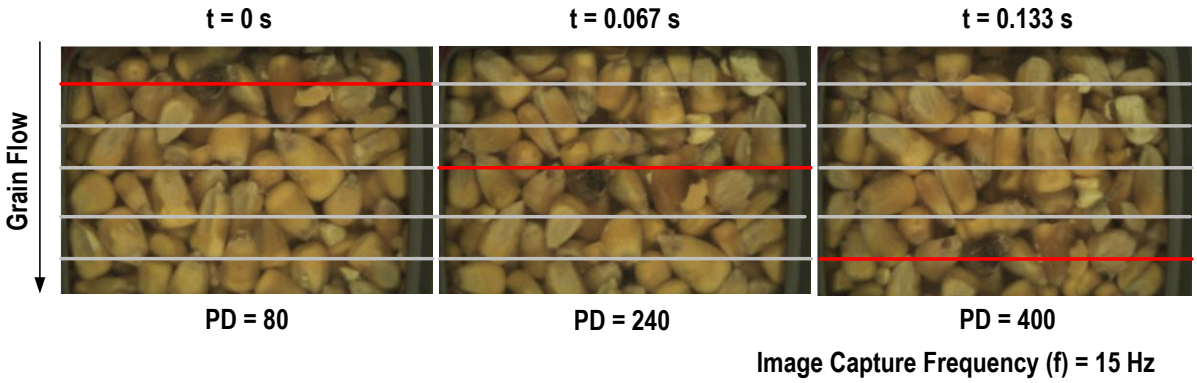

Figure 5.6: Example of image tracking algorithm for corn

5.2.2.3. Camera Installation Considerations

In order to accurately estimate the rate and accumulated volume of grain being harvested, several installation conditions were developed. These criteria are outlined as follows:

- The camera must be installed in a region of the combine that all grain must pass through continuously
- Moderate machine modification will be permitted to maintain consistent cross sectional area of grain flow
- Camera and wiring harness must avoid contact with other mechanically driven components

The camera that was used to record images of the grain must be located where all grain passes through so that a direct correlation to the total volume of grain harvested can be made. After threshing and cleaning, all grain passes through four conveyance regions before exiting the machine. These areas provided opportunity for direct volumetric measurement of grain (Figure 5.7).

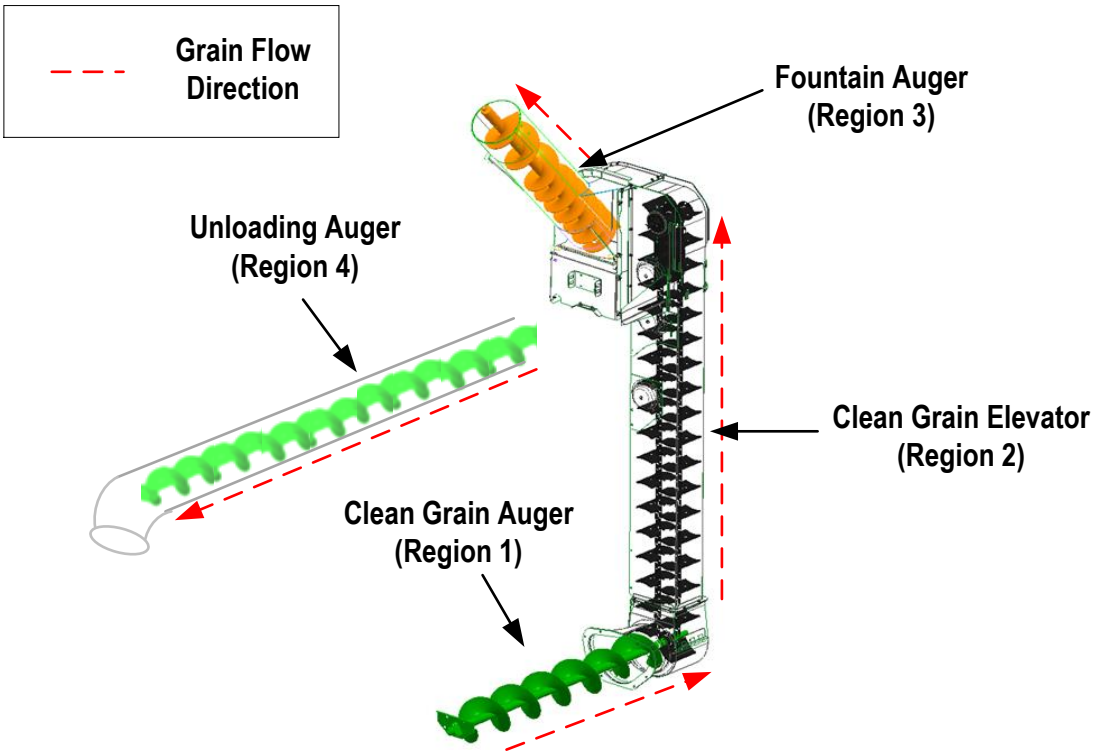

Figure 5.7: Conveyance regions of accumulated grain flow in combine harvester

The first region of accumulated grain conveyance occurred at the bottom-most point of the combine in the clean grain auger. Being the first point of grain accumulation and earlier in the grain stream would allow for the least amount of time delay of yield data. Constraints in this area included geometric limitations caused by the cleaning shoe, blower fan, and horizontal orientation of the auger. The clean grain auger conveyed grain into the clean grain elevator, the second region of accumulated grain flow. Detailed in previous chapters, current yield monitoring technology is installed in the clean grain elevator. Since the current elevator design does not allow for consistent cross sectional area of grain flow, this region was not suitable for the proposed volumetric measurement method. The third region of accumulated grain flow was the fountain auger. The fountain auger conveyed grain at an upward angle orientation to maximize pile size for temporary storage in the grain tank.

This region provided opportunity for monitoring continuous flow of the grain stream with no geometric or mechanical limitations. A protective housing would be needed in this area to shield measurement equipment from grain impacts and pressure from the pile. Furthermore, modification could be made to the auger profile to meet the grain flow characteristics constraint. The final region of accumulated grain flow occurred as the grain was conveyed out of the machine via the unloading auger. The unloading auger was deemed to be an undesirable volumetric monitoring region, as it did not allow for continuous measurement and would greatly increase the time delay of yield monitoring data.

After design review of the four locations of accumulated grain flow, the fountain auger was selected as the camera installation location for initial performance assessment of the particle flow yield monitor. Although the location increased the time delay from the point of harvest to yield measurement, it met all three design criteria and offered the easiest installation.

5.2.2.4. Data Acquisition System

The data acquisition system consisted of three major areas of data management: collection, processing and packaging, and storage (Figure 5.8). An Image Processing Module (IPM) provided by the project sponsor established Ethernet connection between the camera and storage device, supplied 24V power to the camera, and packaged images into a single data log. The IPM could handle up to 60 Hz image capture and support two cameras. An Advantech Data Logger was used to store data. Harvester CAN Bus messages and images were time synced and collected simultaneously. During test stand and initial study work, a Panasonic Toughbook was used to store image logs as an alternative to the Advantech Data Logger. This simplified post-processing techniques when no machine CAN Bus was present.

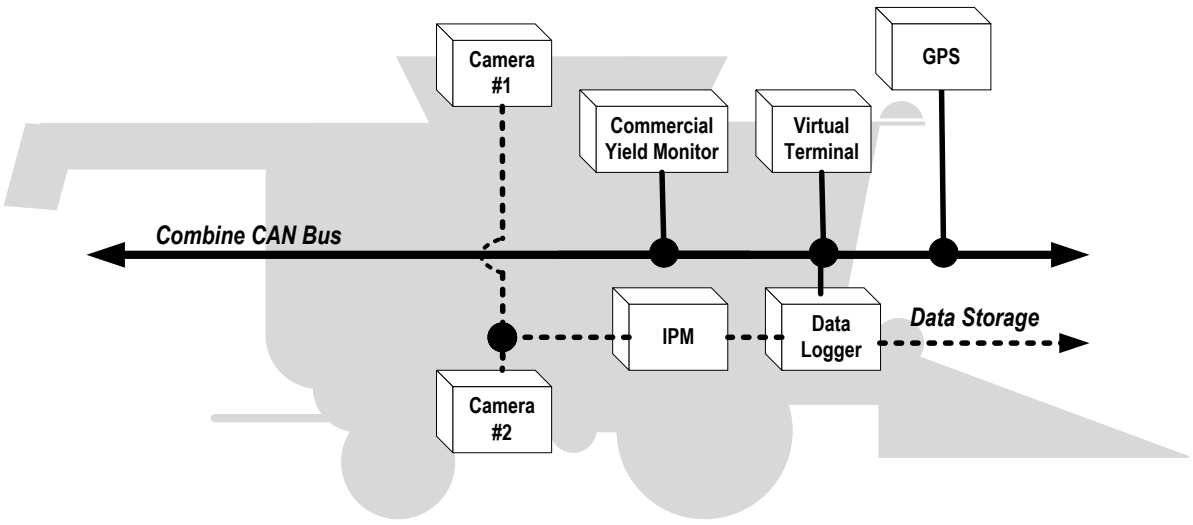

Figure 5.8: Particle flow yield monitor topology diagram

5.2.3. Imaging Frequency

To accurately estimate volumetric flow using particle tracking, a minimum of one pixel line match must occur in two successive images. Therefore a grain particle must have at least two images recorded before leaving the camera screen. If the flow rate of grain exceeds the threshold where less than two images are recorded, volumetric flow rate cannot be estimated because the pixel line displacement and thus grain velocity can no longer be accurately estimated. Without a minimum of two images, the algorithm will be unable to track exactly how much the last image of grain was displaced. For most small grains, this will not be an issue as mass flow rates seldom exceed 10 kg/s. However, for corn the image capture frequency must be high enough to measure the larger flow rate range observed by the crop. Theoretically, the flow rate of the grain through the machine is driven by the crop yield and speed of the machine. At standard test weight for corn, image capture frequency of 15 to 30 Hz would be required to measure the entire flow rate range of corn through a 0.3 m (12 in.) tube in the combine (Figure 5.9).

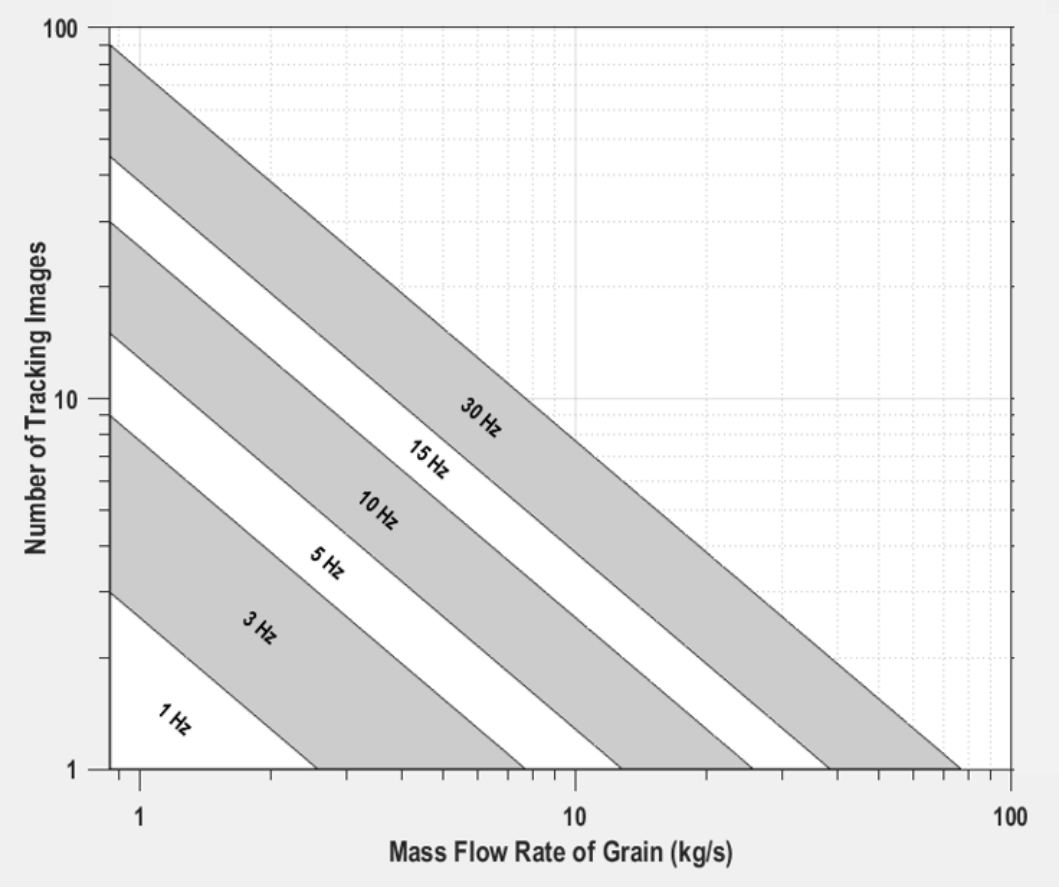

Figure 5.9: Number of images of a grain particle before parting the camera face for flow rate ranges and imaging frequencies

An imaging frequency of 30 Hz was selected to properly cover the flow rates of small and large grains. Lower imaging frequencies supported flow rates of small crops, but lacked upper-tail flow rate distribution coverage for corn. The 30 Hz imaging frequency supported up to 80 kg s^{-1} mass flow rate, based on standard grain density through a 0.3 m cylindrical tube.

5.2.4. Combine, Sump, and Fountain Auger

Test stand and field harvest experiments were completed using a class 8 combine. The test stand consisted of a scaled axle grain wagon positioned so that grain could be

precisely metered to simulate grain harvest flow rates (Risius, 2014). A 16-row corn head and 12 m draper head were used to harvest in-field grains.

The fountain auger was modified to meet the location and mechanical design constraints. Grain conveyed up the clean grain elevator is exposed to commercial yield monitoring components before being dumped into the sump of the fountain auger. A plate was fabricated and installed on the back of the sump housing to prevent grain from spilling over into the back of the grain tank. The back plate ensured that nearly all of the harvested grain was conveyed through the fountain auger. The auger flighting was cut back 25 cm to maintain a consistent cross sectional area. Grain would bubble out of the top of the fountain auger and maintain a full cavity in the section of tube. Preliminary testing with the modified fountain auger showed that grain swirled excessively from the axial rotation of the auger. The particle flow yield monitor could only measure linear grain displacement past the camera face. To mitigate swirling effects, grain deflection baffles were welded axially into the top of the fountain auger and the final revolution of auger flighting was tapered. Each baffle was 22 cm in length and extended 5 cm towards the center of the auger. The tapered auger flighting helped to diminish grain pulsing caused by the vertical orientation of grain movement (Figure 5.10). The camera for the particle flow yield monitor was installed at the top of the fountain auger, offset from the bottom center. Offset orientation improved image quality by minimizing measurement of smaller grain particles and dirt along the bottom of the grain stream. A protective housing helped deflect grain and shield DAQ cables. The camera was positioned to record images of grain in the full cavity area of the auger tube (Figure 5.11).

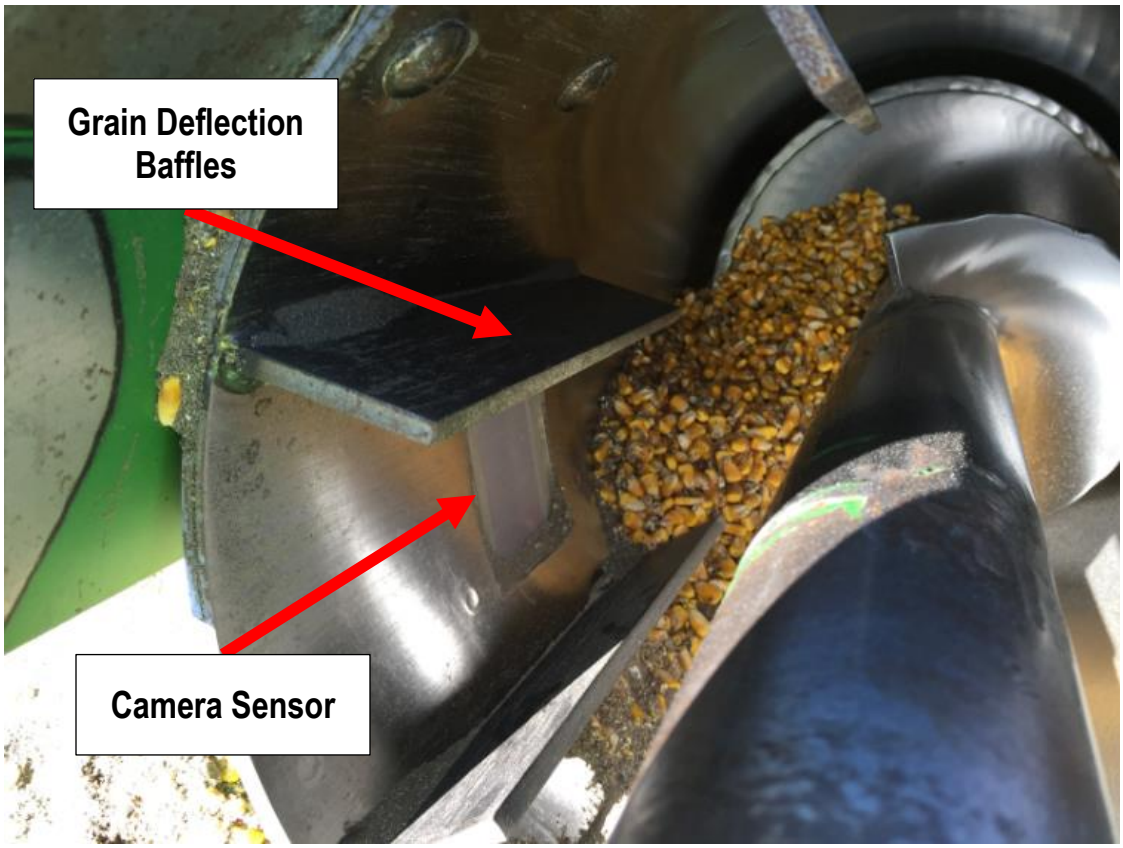

Figure 5.10: Fountain auger modifications of baffles, sump, and tapered auger to deliver grain effectively to sensor

Figure 5.11: Camera and fountain auger installation

5.2.5. Development of a Predictive Volumetric Yield Algorithm

5.2.5.1. Pixel Displacement Filtering Metrics

Pixel displacement was measured as a proxy for the velocity of grain through a cylindrical tube of constant cross sectional area, thus obtaining a volumetric flow estimate. The pixel displacement signal was analyzed in MATLAB and used input parameters to determine if grain is flowing and the mechanical requirement of a constant cross sectional area has been met. The raw output signal was filtered using two performance metrics to capture grain flow only when the sump area was full. These performance metrics were defined and implemented into post-processing scripts (Figure 5.12).

- Impact-based mass flow sensor response: the upstream response of the factory-installed impact-based mass flow yield monitor was used as an indicator of grain flow for harvest time and pixel displacement signal filtering.
- Minimum pixel displacement rate: a minimum threshold was established for pixel displacement rate based on observed noise in the system when no grain is flowing past the sensor.

The impact-based mass flow sensor response was available from the CAN Bus. CAN data and images were recorded in real time so that they were time-synced for analysis of respective response. Pixel displacement rate could be filtered using only the time-synced CAN data from the same replicate. The minimum pixel displacement rate was determined through analysis at zero-flow conditions and implemented uniformly across all test replicates.

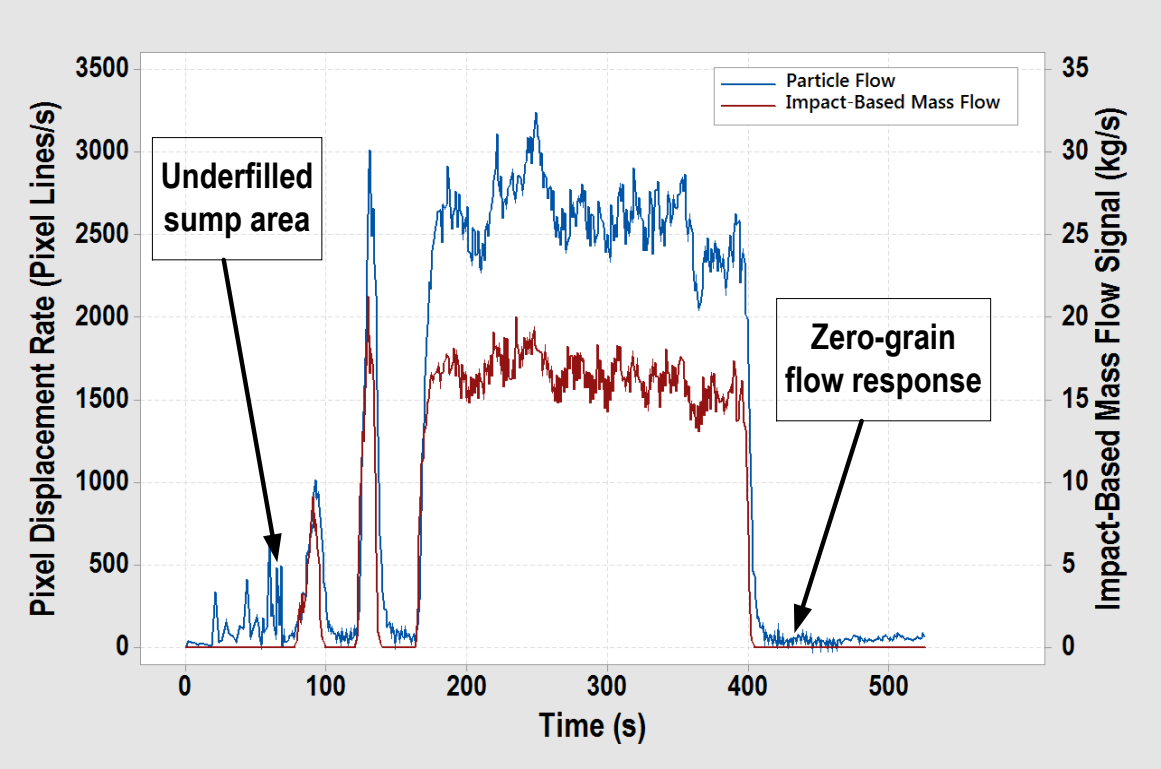

Figure 5.12: Raw response signals of particle flow and impact-based mass flow yield monitors

Filtering the pixel displacement signal based on the response of the impact-based mass flow sensor allowed for most failure conditions due to mechanical requirements to be filtered out. Grain was removed from the fountain auger and the sump area emptied when the unloading auger was engaged. This caused abrupt spikes in the pixel displacement rate signal at the beginning of a test replicate when the fountain auger refilled the sump. Since the impact-based mass flow sensor was installed directly above the base of the fountain auger, the pixel displacement signal could be filtered with minimal time delay effects.

Analysis of the pixel displacement response at zero-grain flow conditions gave an indication of a starting point for a minimum threshold for pixel displacement rate. The test was designed to mimic test stand and harvest environments for the sensor. The cumulative distribution of pixel displacement rate with no grain flow found the 99th percentile to be 38.8

pixel lines per second. Therefore, a minimum threshold for pixel displacement of 40 pixel lines per second was deemed acceptable for test stand and harvest conditions.

The filtering metrics were applied to all data sets that had time-synced CAN messages available. A ground truth start and stop harvesting time was applied to each test replicate by manually parsing sensor response in MATLAB. The normalized difference of accumulated pixel lines displaced between the ground truth and filtered results was analyzed. Of 132 test replicates, there was a mean percent difference of accumulated pixel lines displaced between the ground truth and filtered results of 0.8% with a standard deviation of 2%. The minimal difference in pixel line displacement was deemed insignificant for initial performance assessment, therefore filtered data was used for algorithm development.

5.2.5.2. Predictive Volumetric Yield Algorithm

Initial performance of the particle flow yield monitor was assessed using readily available signals. Total pixel line displacement was compared with accumulated grain mass to assess linearity across load size for the same crop. Grain mass was measured using grain carts with calibrated load cells on the axles. Theoretically, as load size increases the number of pixel lines displaced should increase at a constant rate. Linearity is desirable for applications across crop types and harvester sizes. Additionally, pixel displacement rate was compared with mass flow rate for model assessment across a range of mass flow rates. Each was a metric formed using a total grain flow time. This was readily accessible during test stand work by monitoring scale weight, but not for field harvest. The impact-based mass flow sensor on the combine was used as an indicator for start and stop time of grain flow through the machine because of its location in the grain stream.

The predictive volumetric yield algorithm built upon principles of linearity established by the two previous assessment methods. The algorithm combined the pixel displacement signal and harvest time to estimate a total harvested volume of grain (Equation 5.2). The displacement signal also allowed for a real-time yield estimation using combine input parameters (Equation 2.2). The estimated volume harvested can be evaluated against a ground truth volume harvested using the accumulated mass of grain harvested and test weight of the grain. While properties and test weight are relatively constant in a test stand environment where grain is recycled continuously, harvest conditions can vary excessively and required grain sampling for test weight.

5.2.6. Description of Data Sets

The design of experiments for controlled test stand and uncontrolled field harvest data was developed to evaluate initial performance and feasibility. The first objective was to collect controlled ground truth flow rate of grain and pixel displacement data to aid in the development of a predictive volumetric flow algorithm. Response linearity across multiple crops and flow rates would be evaluated. The second objective was to assess performance of the predictive algorithm in harvest conditions where crop conditions vary naturally across the field. Adjustment of ground speed between test replicates induced greater variation in flow rates without compromising yield estimation. This allowed for more thorough exposure to the range of crop flow rate distributions than normal yield variation in a field could provide. Real-time harvest allowed for the predictive algorithm to be developed for accuracy using ground truth harvested mass and compared against NDVI and commercial yield systems. Each data set was discussed and outlined in respective sections.

5.2.6.1. Controlled Data Set

Controlled data was collected using a test stand to meter grain at predetermined mass flow rates (Risius, 2014). The test stand utilized a grain wagon with scaled axles and actuated doors to repeatedly test flow ranges. With the camera sensor installed on the fountain auger, pixel line displacement between image frames caused by grain flow was measured. Consistent flow throughout a test replicate determined expected pixel displacement rates for corresponding ground truth mass flow rates. Corn was sourced from a local elevator every 30 replicates to maintain consistency of grain properties during data collection. Pixel displacement data was recorded for mass flow rates ranging from 5 to 30 kg s^{-1} in a randomly selected order. Treatment levels were selected at 5, 10, 15, 20, 25, and 30 kg s^{-1} to simulate the spread of flow rates for small and large grains (Figure 5.13).

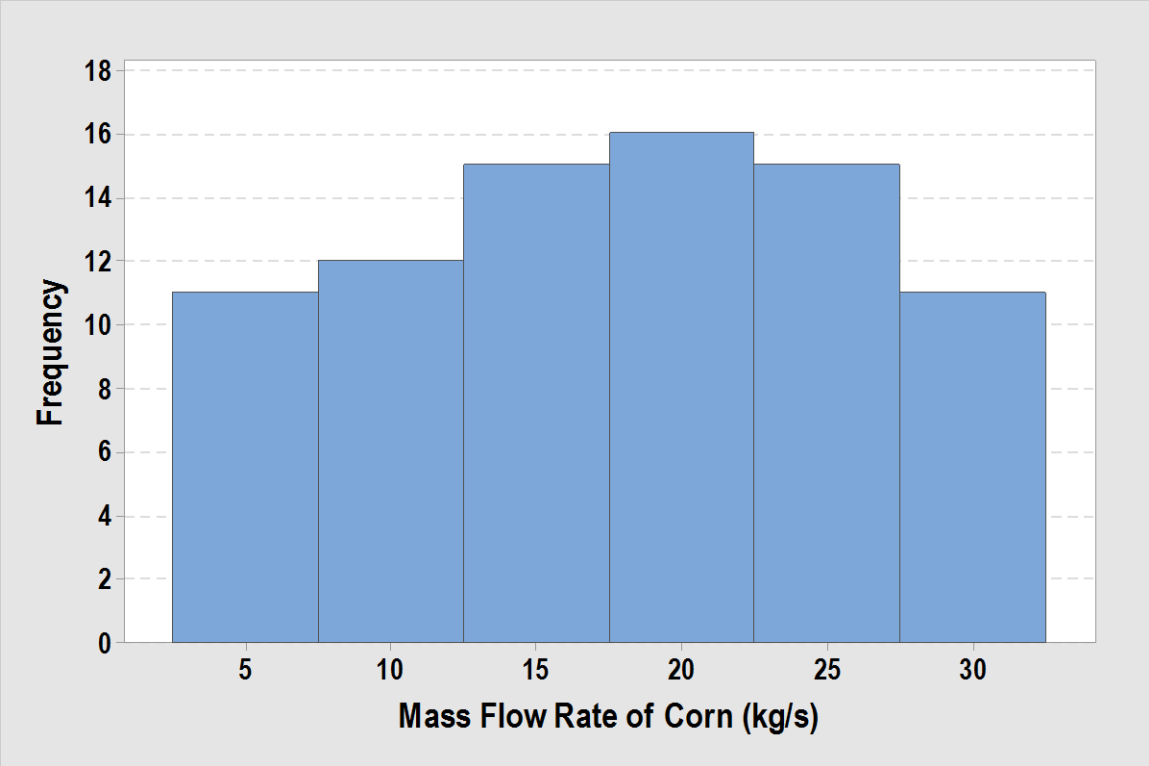

Figure 5.13: Distribution of flow rate treatment levels for controlled data set

High capacity grain tanks up to 14.1 m^3 (400 bu) are becoming more common as machinery size increases. Load size impact on accumulated pixel line displacement was selected as a second treatment factor for controlled data. Additionally, the influence of load size on pixel displacement rate was studied. As the combine harvests grain, the fountain auger dumps grain into the center of the tank until it is completely submerged and then continues to push grain to the top of the pile until capacity is reached. Given the location of yield measurement, the effect of pushing grain above the fountain auger on pixel displacement measurement was analyzed for algorithm development. Preliminary testing revealed mass requirements of 4,000 kg for grain piling to reach the bottom of the fountain auger and an additional 2,000 kg of pushing grain over the sensor to reach tank capacity. Pixel displacement rate was recorded for piling grain below and above the camera sensor at mass flow rates defined in this section (Figure 5.14).

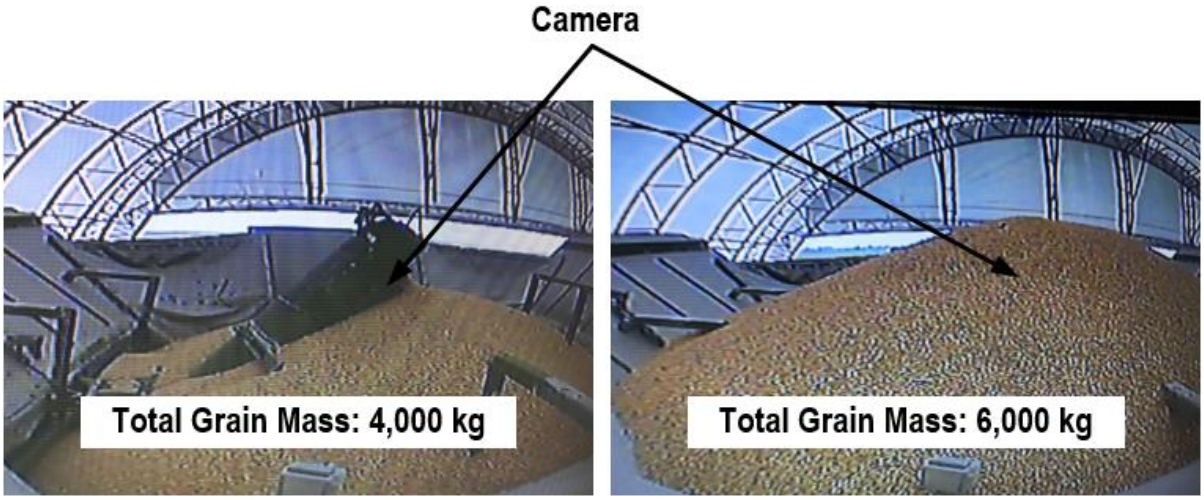

Figure 5.14: Grain pile below and above fountain auger

5.2.6.2. Uncontrolled Data Set

Uncontrolled data consisted of entire crop fields that had a wide spectrum of flow rates available for predictive volume algorithm evaluation. These fields were selected using

NDVI imagery taken during the growing season. A corn, soybean, and wheat field were selected for 2015 harvest to test yield monitor performance (Figure 5.15).

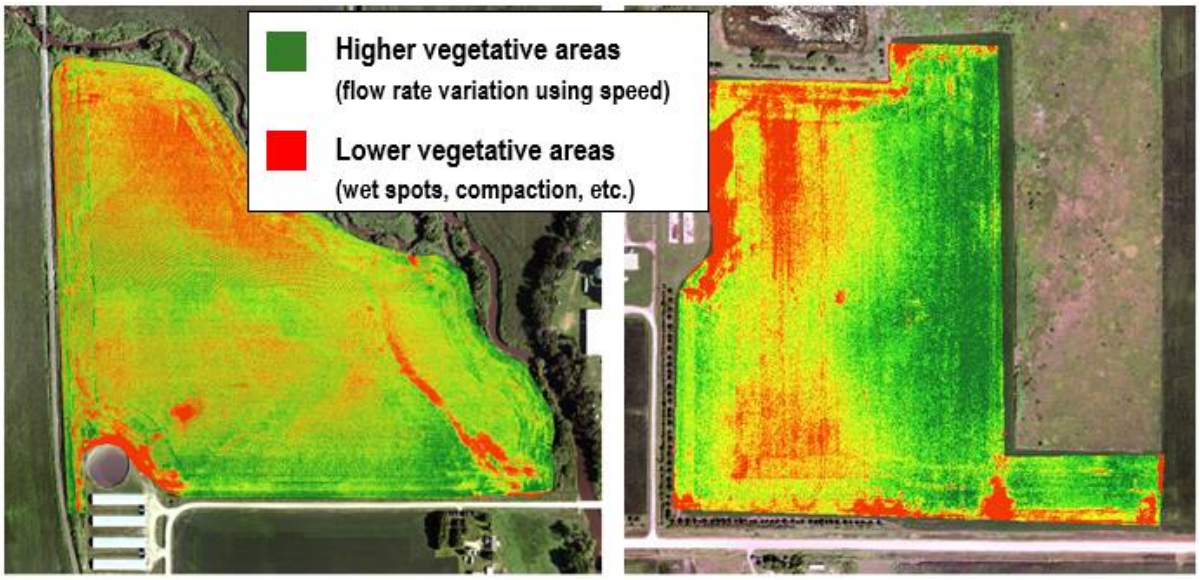

Figure 5.15: NDVI imagery of 2015 corn and soybean uncontrolled data sets

Underdeveloped areas of crop produced lower flow rates through the machine when ground speed was held constant. To increase the exposure across the flow rate distribution in areas of relatively consistent crop yield, ground speed was changed between test replicates. Since ground speed and flow rate are coupled variables, yield estimation would not be effected. Treatment levels of 1, 2, 3 and 4 mph were selected to push different flow rates through the combine (Table 5.2). Higher ground speeds were not necessary because they would result in mass flow rates that were beyond the range of the normal distribution per crop type and poor MOG-grain separation.

Table 5.2: Expected mass flow rate of grain into the combine (kg s^{-1})

		Crop Yield, MT/h (Bu/Ac)					
		3 (50)	6 (100)	9 (150)	12 (200)	15 (250)	18 (300)
Combine Speed kph (mph)	1.7 (1.0)	1.7	3.4	5.1	6.9	8.6	10
	3.2 (2.0)	3.4	6.9	10	14	17	21
	4.8 (3.0)	5.1	10	15	21	26	31
	6.4 (4.0)	6.9	14	21	27	34	41
	8.0 (5.0)	8.6	17	26	34	43	51
	9.7 (6.0)	10	21	31	41	51	62
	11.3 (7.0)	12	24	36	48	60	72
	12.9 (8.0)	14	27	41	55	69	82

5.2.7. Model Assessment

Discrete element method (DEM) software was used to model interactions and flow characteristics of grain particles as they flow through the modified fountain auger. DEM was used as a tool to validate observances from uncontrolled data and support decisions to improve yield monitoring performance for future design iterations. DEM is a group of numerical methods used for simulating the motion and interactions of a large number of small particles. Material geometry and properties are incorporated into analysis on the macroscopic and molecular levels to determine motion of particles as they are contacted by other particles. This can become quite complex when dealing with grains, where particle interactions can reach the millions for even a small simulation. Material properties for grain (Gonzalez-Montellano, Llana, Fuentes, & Ayuga, 2011) and application of DEM simulation within the grain industry have been well documented.

The modified fountain auger was modeled using CAD software to simulate the results of field testing as closely as possible (Figure 5.16). Round particles were chosen to simulate corn and used estimates for standard dimensioning and properties. Flow rates less than 10 kg s^{-1} were simulated to limit processing requirements and time to completion.

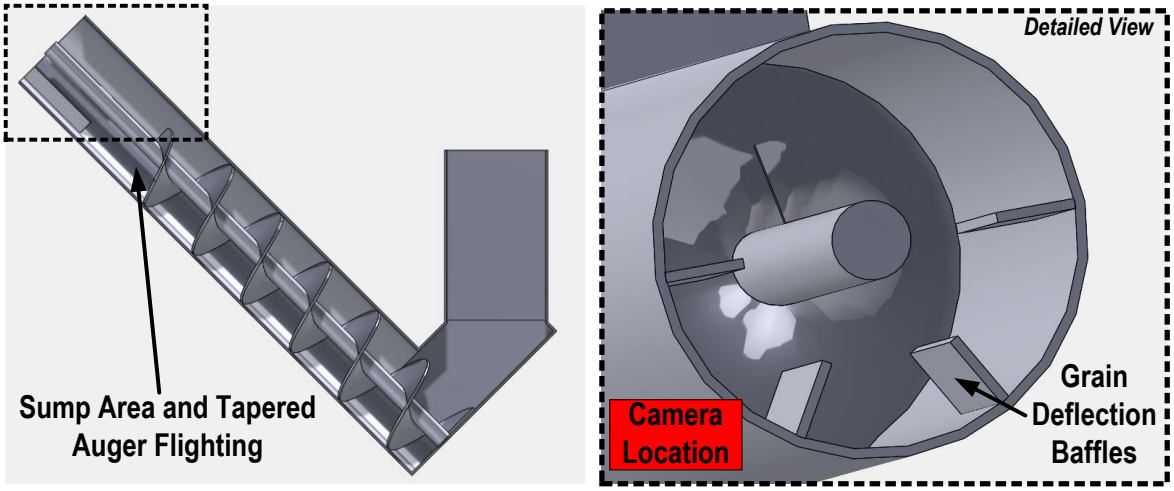

Figure 5.16: Modified fountain auger details for simulation

5.3. Results and Discussion

5.3.1. Performance with Controlled Data

The initial performance assessment of the particle flow yield monitor focused on feasibility to estimate flow from pixel displacement and relationship across the expected range of flow rates for corn. A test stand allowed for experimental control over grain properties and flow rate treatment levels to directly assess performance impact from treatment factors. Results from controlled data with load size, flow rate, and fill level treatment factors will be presented in this section.

5.3.1.1. Performance across Load Size

Increased total pixel line displacement had a positive correlation to load size. A total of 80 test replicates were collected. Analysis was conducted on all data and found a high degree of variability between the accumulated pixel lines displaced per load size (Figure 5.17). Further investigation found that the variability was in-fact caused by different treatment levels of mass flow rate (Figure 5.18, Table 5.3). The bias shifting caused by different mass flow rate levels will be discussed later in the chapter.

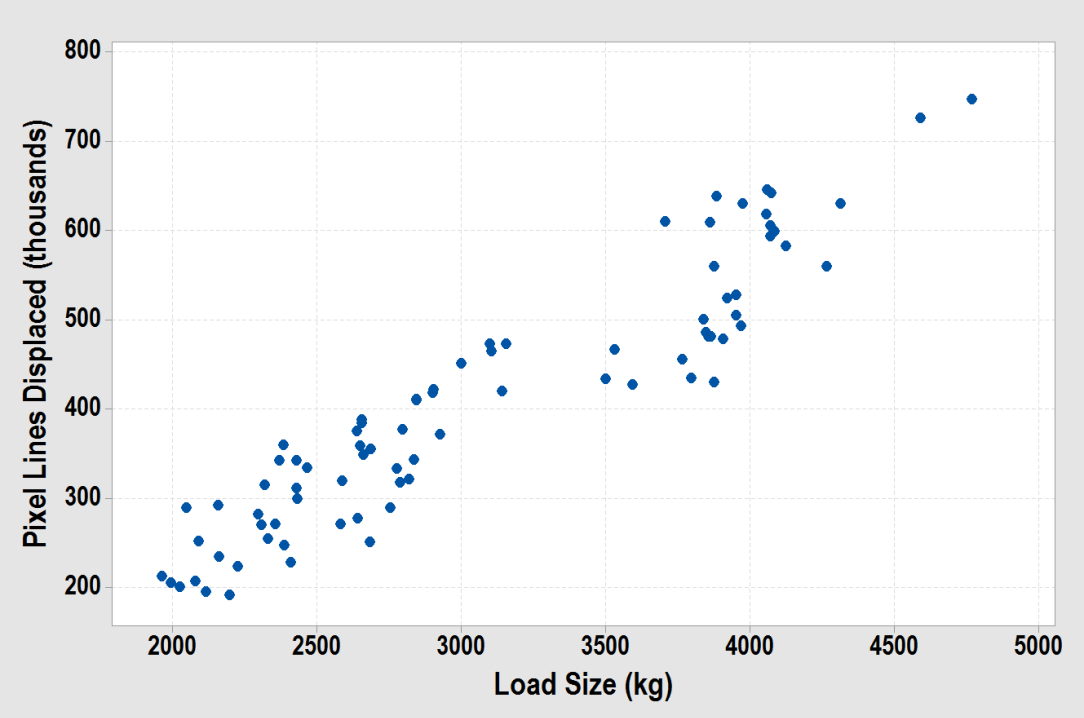

Figure 5.17: Load size influence on pixel displacement

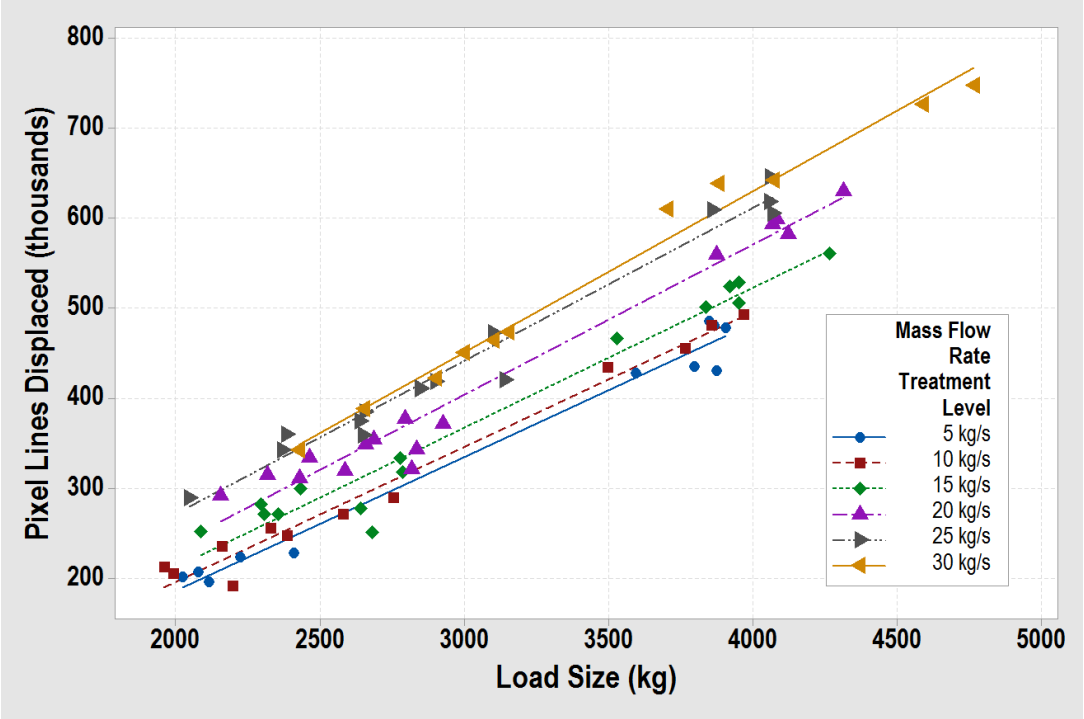

Figure 5.18: Load size influence on pixel displacement grouped by mass flow rate treatment levels

Table 5.3: Regression model parameters for load size influence on pixel displacement

Mass Flow Rate Treatment Level (kg/s)	Regression Parameters		Coefficient of Determination
	β_0	β_1	r^2
Overall	-118,782	170.6	87.4%
5	-102,154	146.4	98.0%
10	-92,451	1468	98.5%
15	-87,652	152.9	95.7%
20	-75,575	163.0	99.1%
25	-82,004	174.3	98.5%
30	-84,049	178.6	98.5%

Overall, a linear relationship existed between pixel lines displaced and load size. Accumulated grain mass was used as a comparison because the signal was readily measurable from the grain wagon. Grain test weight was consistent throughout the experiment, meaning volume and mass are directly relatable by some constant. Further evaluation would be needed to detail the y-intercept as load size approaches zero. Linearity between accumulated signals was encouraging for feasibility of the system.

5.3.1.2. Performance across Mass Flow Rate Range

The relationship between pixel displacement rate and mass flow rate was analyzed during steady state flow conditions. The relationship had low variability and was interpretable for use in a predictive volumetric yield equation. Regression fitting was applied to the model to better understand correlation between the two variables (Figure 5.19, Table 5.4).

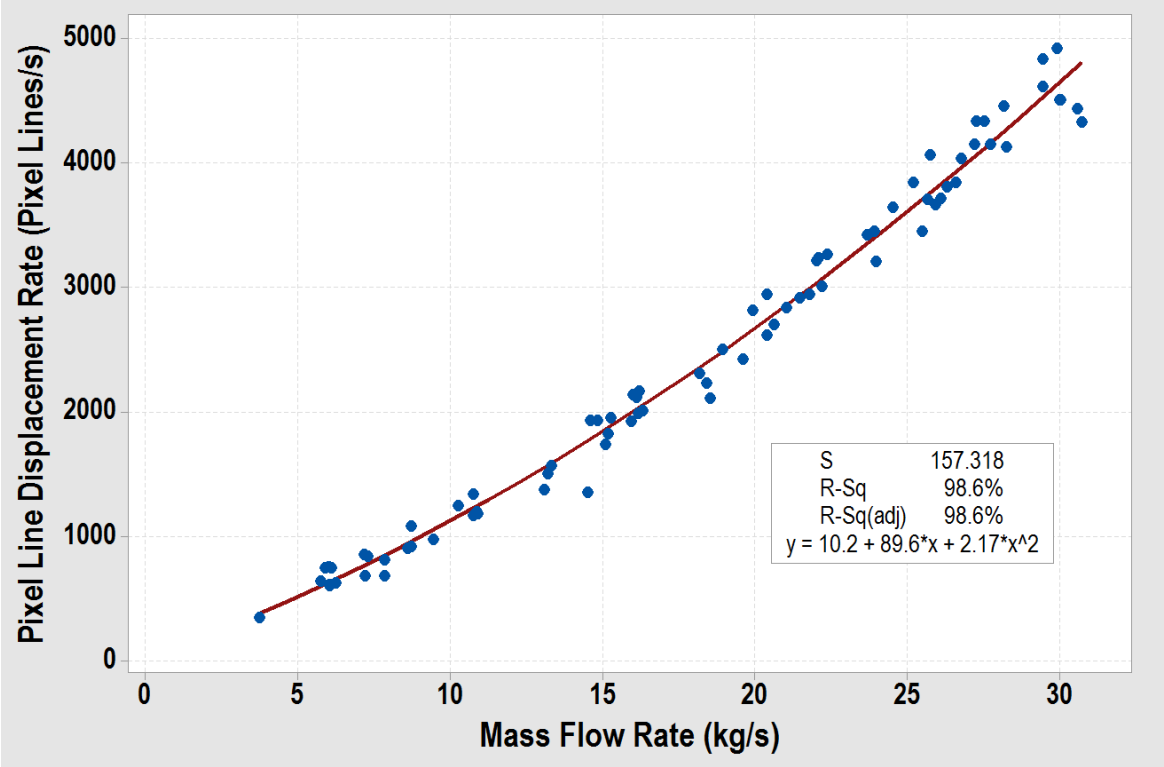

Figure 5.19: Pixel line displacement rate across mass flow rate for controlled data

Table 5.4: Pixel line displacement rate regression equation coefficient ANOVA

Regression Parameter	DF	SS	P-Value	Coefficient Value
Constant	-	-	-	10.2
β_1	1	1.4E+06	< 0.001	89.6
β_2	1	1.1E+06	< 0.001	2.17
Error	77	1.9E+06	0.05	-

Linear and quadratic regressions were applied for model assessment. Both models indicated strong correlations with R^2 values greater than 97%. The quadratic regression model was deemed appropriate for the pixel displacement rate relationship after analysis of residuals. The residuals of the linear model not uniformly scattered and it was clear the quadratic expectation function was necessary. Although it is a non-linear trend, the

relationship between pixel line displacement rate and mass flow rate is very tightly bound with little variation. Inherit sensor response to flow rate is beneficial to the predictive yield equation, especially when considering the system had no previous calibration.

5.3.1.3. Impact of Grain Flow above Sensor

When the grain tank has reached a point that the fountain auger is completely submerged with grain, the fountain auger must push grain to the top of the pile rather than it free flow from the orifice. The influence of the pressure corresponding to grain depth was analyzed to better understand the impact to the sensor mounted on the fountain auger.

A two-sample t-test was used to identify significant difference in true mean pixel displacement rate between grain flow under and overtop the fountain auger for corresponding mass flow rate ranges. The null hypothesis stated that there was no difference of pixel displacement rate between fill levels in the same flow rate category. Flow rate ranges were determined by mass flow rate set point and grouped so that each bin contained a similar quantity of test replicates (Figure 5.13). The two-sample t-test was valid under the assumptions that population standard deviation was unknown and data was normally distributed. Each fill level treatment contained 31 test replicates.

The true mean pixel displacement rate for two flow rate ranges were found to be statistically different from each other. Those flow ranges that contained statistically different pixel displacement rates were for 2.5 to 7.5 kg s^{-1} and 17.5 to 22.5 kg s^{-1} (Table 5.5).

Table 5.5: Pixel displacement rate comparison for fill level respective to fountain auger (shaded indicates different means, 95% CI)

Flow Range (kg s^{-1})	Fill Level to Fountain Auger	Replicates	Mean Pixel Displacement Rate (pixel lines s^{-1})	95% CI for Difference
2.5-7.5	Under	6	761	(-422, -14)
	Over	4	543	
7.5-12.5	Under	4	1249	(-390, 1.3)
	Over	6	1055	
12.5-17.5	Under	7	1940	(-317, 223)
	Over	5	1893	
17.7-22.5	Under	5	3095	(-626, -28)
	Over	6	2768	
22.5-27.5	Under	4	3970	(-812, 204)
	Over	5	3666	
27.5-32.5	Under	5	4631	(-570, 70)
	Over	5	4381	

Mean pixel line displacement rate for all flow ranges shifted downward when the fountain auger began to push grain to the top of the pile. This is likely due to increased back pressure from grain weight and a change in particle interaction as the grain piles above the fountain auger. Flow ranges 7.5-12.5 and 27.5-32.5 kg s^{-1} had upper bounds of the 95% confidence intervals that were near the zero difference threshold. Perhaps if the replicate quantity was increased, the two-sample t-test would find statistical difference of pixel line displacement rate for fill level. Even though only two flow ranges found statistical difference from controlled data evaluation on the test stand, it was deemed appropriate to limit load size to less than 6,000 kg for uncontrolled data collection during the 2015 harvest season. This would increase integrity of data for performance evaluation.

5.3.2. Performance with Uncontrolled Data

After feasibility of the particle flow yield monitor was demonstrated with controlled data, the evaluation of performance focused on field harvest conditions. The uncontrolled data set consisted of corn, soybean, and wheat crops during the 2015 harvest season. Corn and soybean crops were available for full-field harvest, while the wheat field was only partially harvested. Treatment factors of crop type and flow rate were directly measured during field evaluation. Test weight variability and influence on a volumetric yield system were indirectly measured through grain sampling. Volumetric yield estimation and performance across different crop types and flow rates will be presented in this section.

5.3.2.1. Performance across Crop Types

A total of 150 test replicates were collected across corn, soybean, and wheat crops during the 2015 harvest season. 14 test replicates were removed from the data set for analysis due to data acquisition errors and estimation failure due to combine dynamics. Pixel line displacement rate trended linearly with measurable offsets for each crop type (Figure 5.20, Table 5.6). Corn and wheat crops had strong correlation between the pixel line displacement rate and the ground truth mass flow rate. Soybeans had a less-strong correlation between the two variables and was tested at the lowest mass flow rates. Average mass flow rate during the test replicate was estimated using the accumulated harvested mass of grain and the total harvest time from the impact-based mass flow sensor.

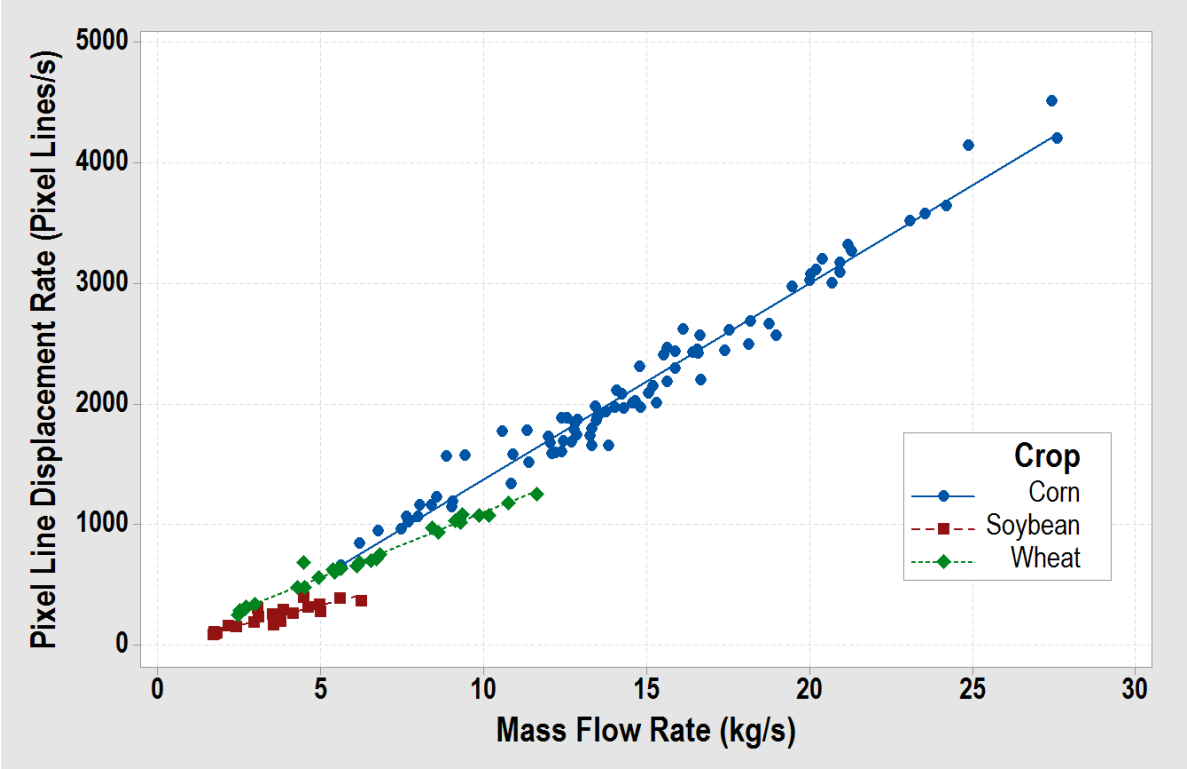

Figure 5.20: Pixel displacement rate across mass flow rate for uncontrolled data

Table 5.6: Regression model parameters for pixel displacement rate for uncontrolled data

Crop Type	Regression Parameters		Coefficient of Determination
	β_0	β_1	r^2
Corn	-256	163	96.9%
Soybean	1.30	65.8	78.6%
Wheat	23.2	108	98.3%

Pixel displacement rate for the respective crops showed similar repeatability as yield estimation. The estimate of the y-intercept parameter for corn was significantly less than the soybean and wheat crops. Although a linear regression shows strong relationship between pixel line displacement rate and mass flow rate, the actual relationship may include higher order terms like the controlled data set. Field evaluation at mass flow rates less than 5 kg s^{-1}

may have better shown the non-linearity as flow rates approach zero, however these data points take much longer to collect. To achieve exceptionally low flow rates with a 16-row corn head means driving less than 1.6 kph (1 mph) and depending on load size can limit data collection to one or two test replicates per hour. Lower flow rate data for corn may have aligned better with soybeans and wheat that had less pixel line displacement response. The estimate for the y-intercept parameters for soybeans and wheat was nearly zero, although the slope estimates were significantly different for corn. This could be attributed to moisture content or test weight properties differences for each grain.

The volumetric yield estimation was calculated using the total pixels displaced during a test replicate. The particle flow yield monitor showed linear regression trends in volumetric yield estimation for the three different crops when compared against the ground truth volume harvested, although the trends are offset from the ideal 1:1 estimation line (Figure 5.21). Coefficients of the linear regression were analyzed to test the significance of each parameter (Table 5.7). Initial regression models included an estimate of the y-intercept, β_0. The P-Values for the y-intercept of each crop regression were found not to be less than the significance level of 0.05. Therefore, the null hypothesis that the y-intercepts were zero could not be rejected. The linear regression model was adjusted for each crop term to force the y-intercept term to zero. Coefficient of determinations improved dramatically for the new model. Load size for corn crop ranged from 1.9 to 10.7 m^3 and contained the largest range of the three crops. This was largely attributed to the time required to obtain larger load sizes due to flow range differences. It takes much longer to collect the same load size for relatively lower yielding small grains of soybean and wheat than relatively higher yielding corn. Soybean and wheat load sizes ranged from 1.6 to 4.9 m^3 and 2.7 to 5.8 m^3, respectively.

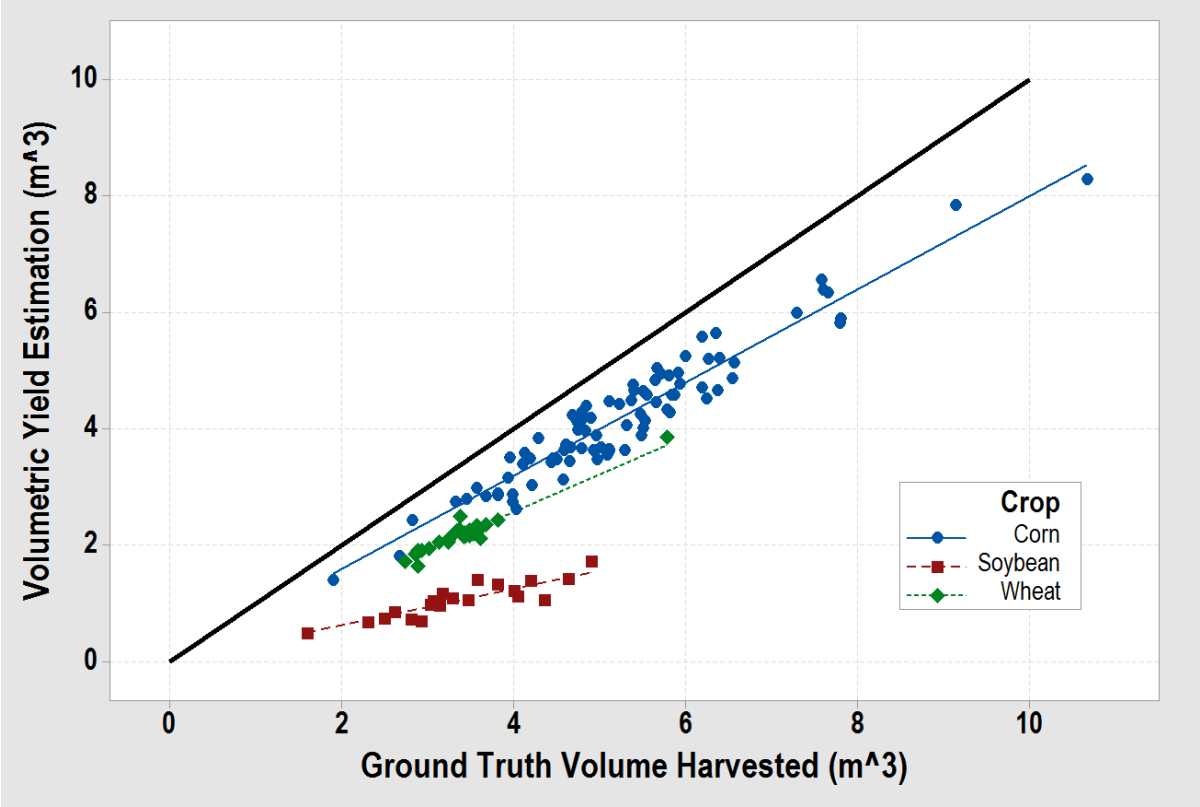

Figure 5.21: Volumetric yield estimation for 2015 harvest season

Table 5.7: Regression model parameters for volumetric yield estimation

	Crop Type	Regression Parameters		Coefficient of Determination	β_0 P-Value
		β_0	β_1	r^2	
Intercept Included	Corn	-0.13	0.82	91.7%	0.36
	Soybean	-0.05	0.33	77.9%	0.73
	Wheat	-0.12	0.68	93.2%	0.30
Intercept Forced to Zero	Corn	0	0.80	99.4%	-
	Soybean	0	0.31	99.8%	-
	Wheat	0	0.64	99.8%	-

Repeatability of yield estimation was impressive across a range of volumes harvested, given that the estimation algorithm is quite simple. Each crop group demonstrates linearity in response as harvested volume increases. Regression y-intercept estimates ranged from -0.05 to -0.13 m^3, which equates to an underestimation at non-harvest state of 40 to 90 kg when standard test weight of respective grains are included. Corn and wheat performed very similarly to each other in estimation accuracy and precision. Soybean performance was offset significantly from the other two crops. This could be attributed to incorrect assumptions about flow properties, grain particle interactions, and cross-sectional velocity for soybean crop. Consistent underestimation of volumetric yield for all crops was likely caused by the unintentional introduction of a non-constant cross-sectional grain velocity profile in the tube. This will be discussed in detail further in the chapter.

5.3.2.2. Test Weight Variability

Since each crop field was harvested in a single day, grain properties for the respective crops were relatively constant and there was no need for yield monitor recalibration. Variation was less than 2 lb bu^{-1} for test weight and 2% for moisture content across all thee crop types (Table 5.8). Grain samples were collected from tank one out of every five test replicates. Test weight and moisture content of corn harvested was nearly equal to official U.S. grain standards (Table 2.1). Corn had the largest variation for test weight, although it also had the largest number of individual samples. Soybean test weight and moisture content was highly consistent across the 12 hectares (30 acres) field. Wheat grain quality was higher than official standards and had the largest variability in moisture content.

Table 5.8: Grain properties for uncontrolled data set

Crop Type	Test Weight (lb bu^{-1})		Moisture Content (%)	
	Mean	**Std. Dev.**	**Mean**	**Std. Dev.**
Corn	55.7	1.7	15.1	1.0
Soybean	57.5	0.2	11.6	0.6
Wheat	60.4	0.6	14.5	1.2

Test weight is an important parameter for volumetric yield systems to convert final volumetric yield estimation to an accumulated mass. Grain is sold and traded on a mass basis to overcome the volumetric variability caused by particle size and quality. Outside of the uncontrolled data set, corn was sampled over the entire 2015 harvest season to better understand the variability of a single crop and the impact this may have on volumetric-to-mass conversion. A total of 127 grain samples were recorded over the harvest season and averaged 55.6 lb bu^{-1} with a standard deviation of 2.4 lb bu^{-1} (Figure 5.22). The 5^{th} and 95^{th} percentiles of test weight were 51.8 and 59.3 lb bu^{-1}, respectively. Although test weight and moisture were consistent for the fields that were evaluated in the uncontrolled data set, a larger distribution was observed for a season long evaluation of more than 400 hectares (1,000 acres). This variation could be driven by different by several different factors including seed hybrids, soil types, and field characteristics such as drainage and tiling. This highlights the importance of continued grain sampling to monitor condition changes and accurately convert volumetric yield data to accumulated mass.

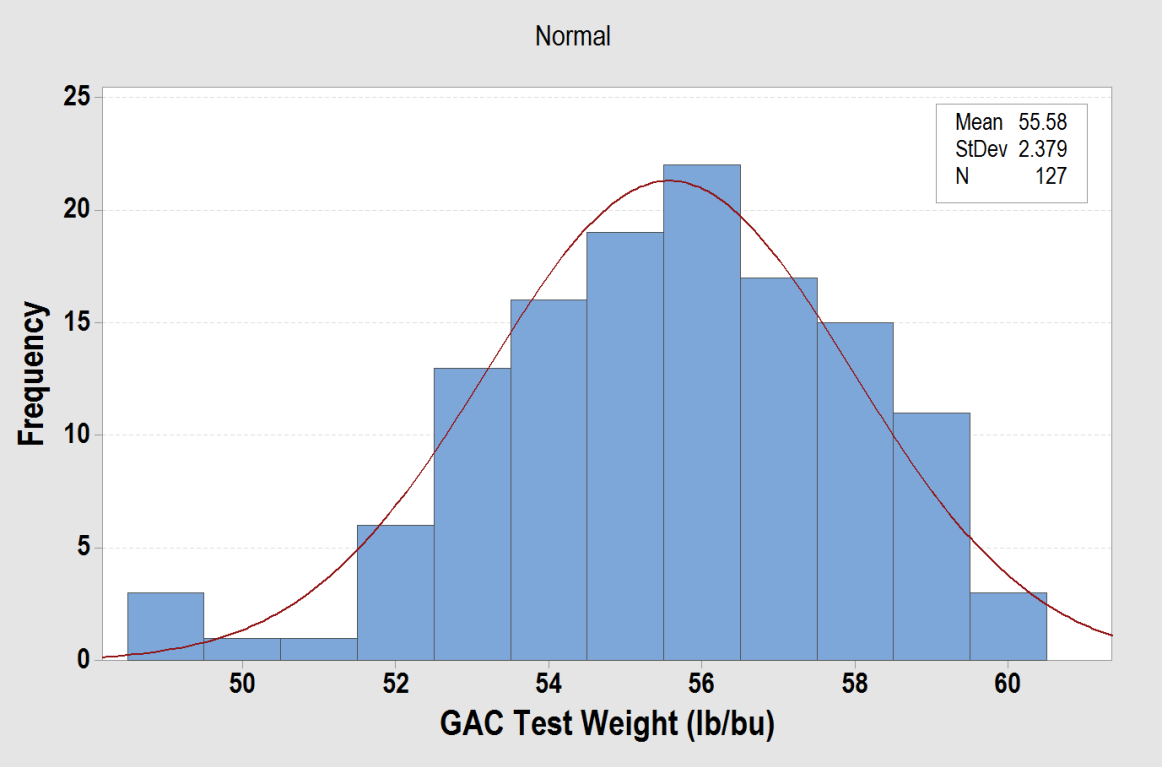

Figure 5.22: Distribution of test weight for corn during harvest 2015

5.3.2.3. Performance of a Commercial Yield System

The impact-based mass flow yield monitor was calibrated for each crop in the field that was being harvested. Performance of estimating accumulated load weights varied between the three crops for the mass flow yield monitor (Figure 5.23, Table 5.9). Performance in corn and soybean crops was linear and consistent across the load size range. Wheat performed much more poorly than the other two crops. This was due to an inability to calibrate the impact-based mass flow yield monitor from rejection of calibration loads, outlined in the previous chapter. Sensor response was not high enough to achieve adequate load size to meet calibration criteria. In contrast, yield response for wheat was linear and showed similar performance to corn for the particle flow yield monitor, but had poor correlation to soybean crop.

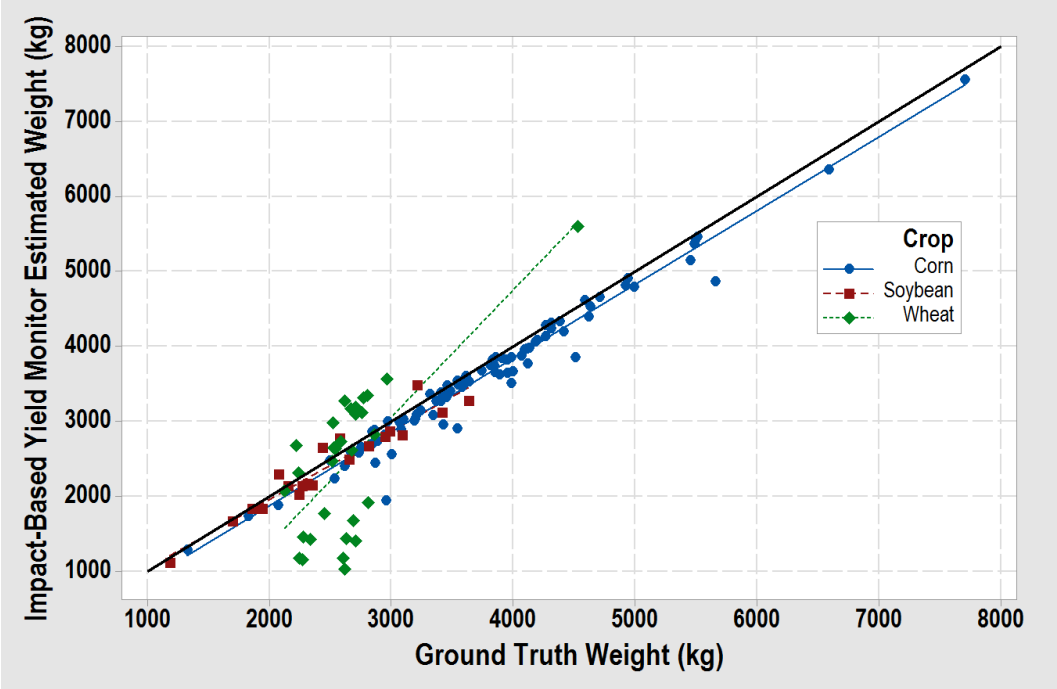

Figure 5.23: Impact-based mass flow yield monitor performance in uncontrolled data

Table 5.9: Regression model parameters for impact-based mass flow yield monitor performance

Crop Type	Regression Parameters		Coefficient of Determination
	β_0	β_1	r^2
Corn	-105	0.986	96.6%
Soybean	121	0.916	91.1%
Wheat	-2030	1.70	49.0%

Variation in raw sensor response was larger for the impact-based mass flow yield monitor than the uncalibrated particle flow yield monitor (Figure 5.24, Table 5.10). The particle flow yield monitor showed different linear trends per crop type, but maintained greater individual correlation than the commercial yield system for corn and wheat. Increased variability in impact-based mass flow sensor response could be attributed to larger variation in test weight and moisture content for corn and wheat. From previous review, grain

properties affect the friction and particle interaction for impact-based sensing. Interestingly, the average mass flow sensor response for wheat showed a 1:1 response to the ground truth, but the overall weight estimate was highly scattered. Even small differences between sensor estimated and actual mass flow rate can result in large relative error for lesser mass flow rates. Large relative error at flow rates typical for small grains, combined with long collection time can drastically increase error of accumulated load weight. Additionally, there may be proprietary internal compensation causing this shift. The impact-based mass flow yield monitor allowed viewing of only the calibrated estimates of mass flow rate and accumulated load weight. Overall, yield estimation from a commercial yield system was adequate when in-field calibrations were used for specific crop types, but improvement is necessary to limit calibration need and maintain accuracy in low-flow grains like wheat.

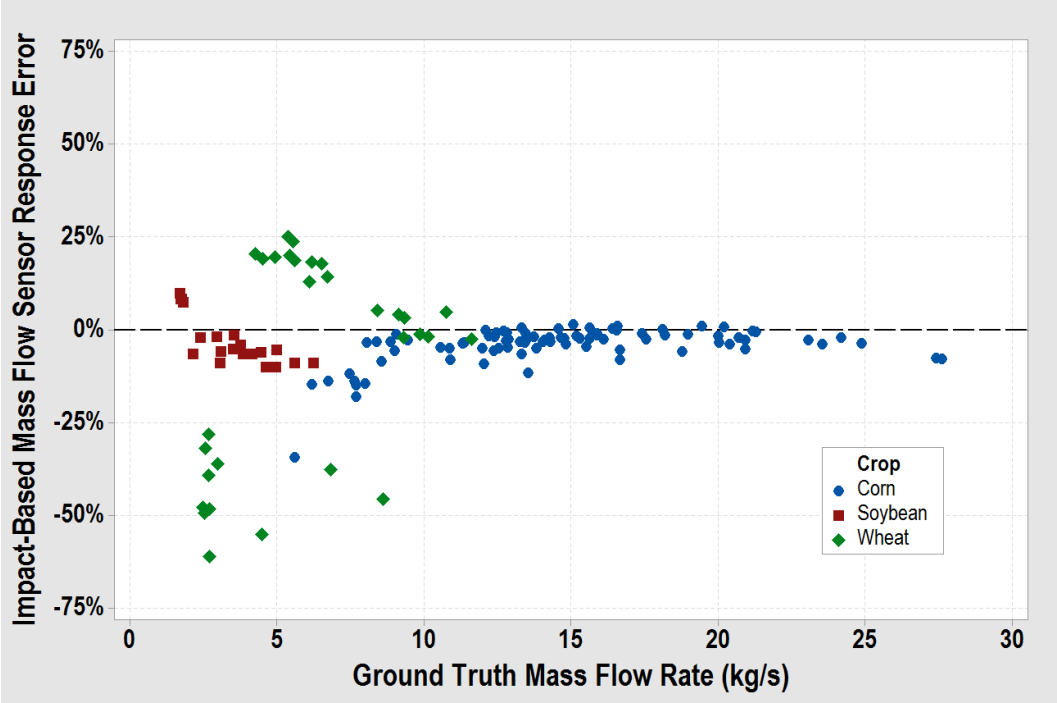

Figure 5.24: Average impact-based mass flow sensor response in uncontrolled data

Table 5.10: Regression model parameters for average impact-based mass flow sensor response

Crop Type	Regression Parameters		Coefficient of Determination
	β_0	β_1	r^2
Corn	2.65	0.845	91.2%
Soybean	0.957	0.869	87.5%
Wheat	-0.467	1.06	84.0%

5.3.3. Model Assessment and Root Cause

The model and methods used for the particle flow yield monitor were reviewed to find cause of consistent underestimation of volumetric yield (Figure 5.21). The algorithm developed by National Robotics Engineering Center to track grain particles was not subject to review since it was a contracted service. The focus of the root cause analysis was on the mechanical environment and flow characteristics of the modified fountain auger. The modified fountain auger included 4 baffles used to deflect grain and keep it from rotating in the angled tube. As the auger rotates, grain is pushed up the incline and into the sump area. For analysis purposes, the fountain auger was divided into two sections: top and bottom. Initial hypothesizing suggested that grain flow would be larger on the bottom of the fountain auger than the top due to gravitation effects pushing grain to the bottom of the auger. Grain was successfully simulated for flow rates less than 10 kg s^{-1} and showed similar results to field harvest (Figure 5.25).

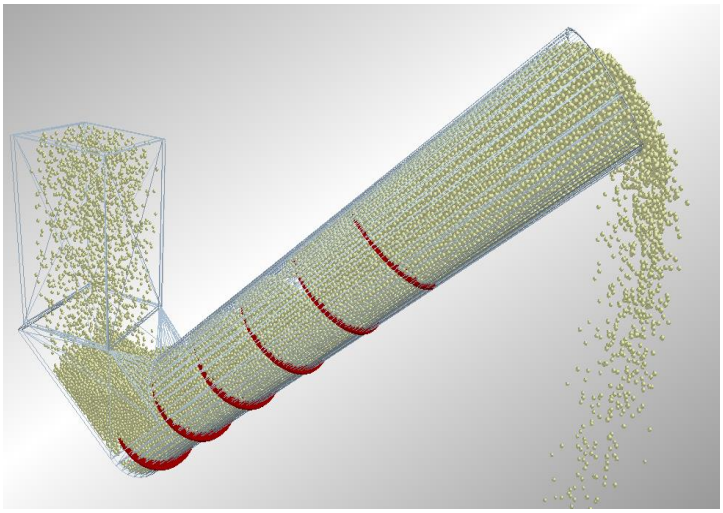

Figure 5.25: DEM analysis of the modified fountain auger with simulated grain particles

Analysis of simulation showed that the grain deflection baffles were the cause of underestimation of yield for the particle flow yield monitor. The sensor was installed on the bottom side of the auger, between the baffles, so that grain would move vertically across the camera face. However, the arc distance between each baffle and the length that the baffle extended towards the center of the auger caused a disturbance to grain flow. The baffles created a path of increased resistance to flow on the bottom-side of the fountain auger and choked grain flow to create an inconsistent velocity profile across the auger tube (Figure 5.26). Simulation showed that as the auger rotated, the velocity on the top region of the auger was larger for an increased time (Figure 5.27). This resulted in a higher flow rate of grain on the top side of the auger. The degree of flow rate difference between the two sections appeared to change with flow rate for the controlled data set (Figure 5.18). The issue of an inconsistent velocity profile across width of the auger would not be apparent in raw pixel displacement data, but would cause underestimation in yield when associating pixel displacement to volume. DEM simulation results supported the claim that observed yield underestimation for uncontrolled data was caused by modifications to the fountain auger. It

was concluded that for future testing, grain deflection baffles were to be distributed evenly around the fountain auger to prevent grain rotation and even resistance across the cross sectional area.

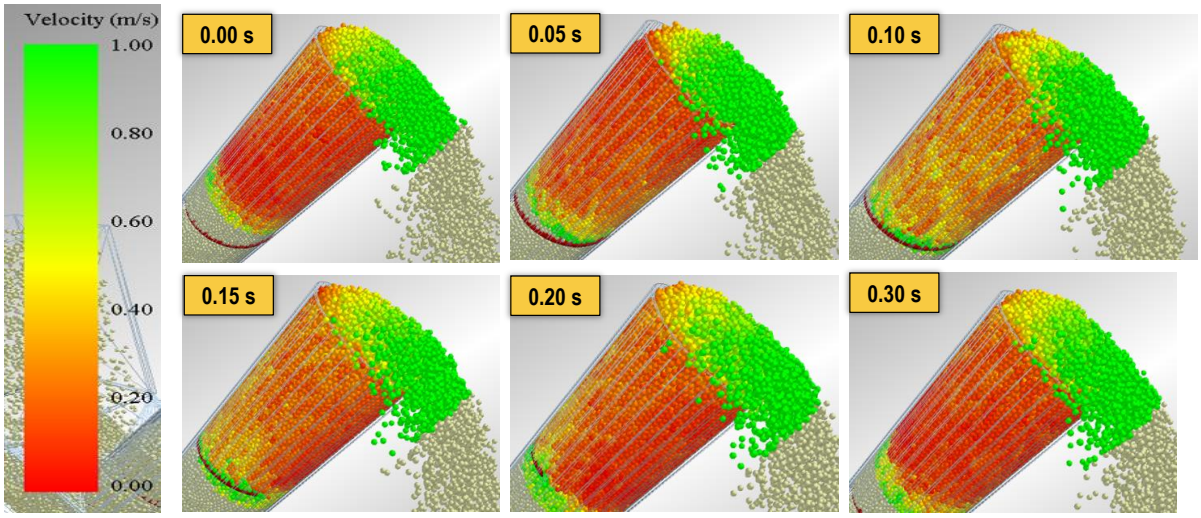

Figure 5.26: Time series of DEM simulation showing decreased velocity on the bottom of the fountain auger as the auger rotates

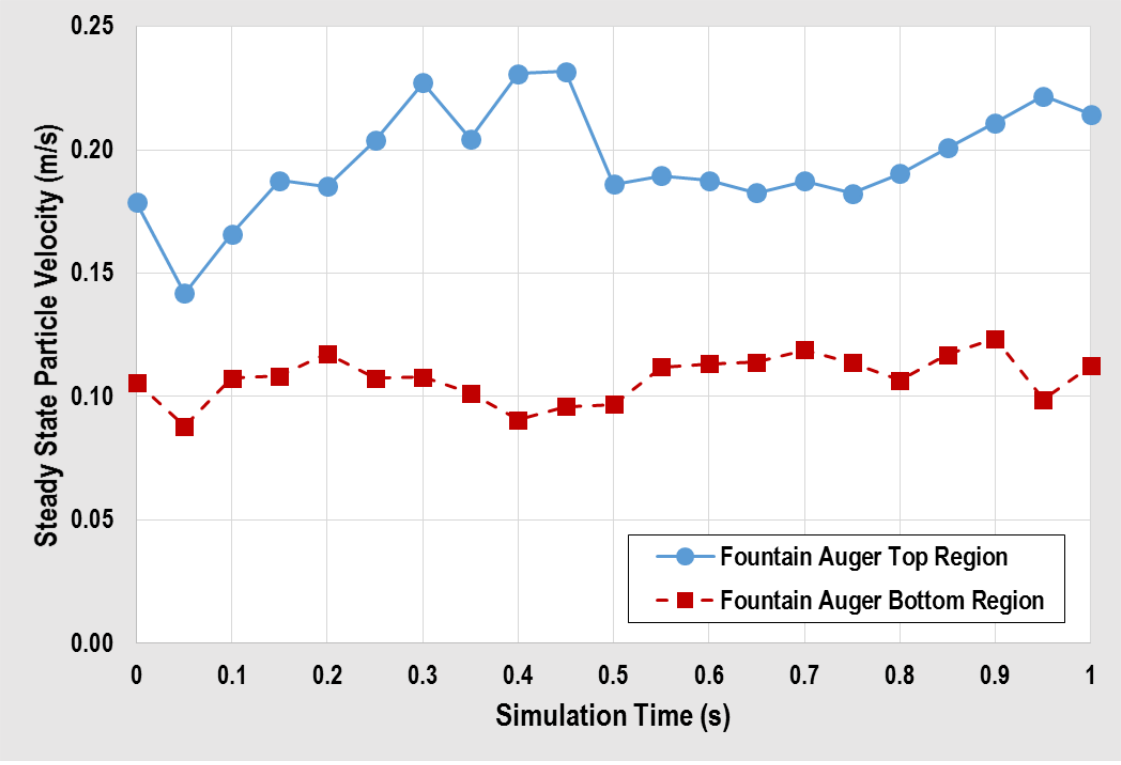

Figure 5.27: Estimate of fountain auger velocity profile difference from DEM simulation

5.4. Conclusions

Exposure to controlled data in the test stand and uncontrolled data during field harvest produced results that demonstrated yield estimation could be made for each crop type tested, so long as the mechanical requirements for the system were met. Yield estimation and sensor response had positive, linear relationships with load size and flow rate intake of the combine. This shows much promise of future development for a system that had no calibration or algorithm adjustment across the corn, soybean, and wheat crops. Minor fabrication to the harvester was necessary to maintain consistent cross sectional area of grain flow. By using DEM software as a tool for root cause analysis, it was determined that these fabrication changes to the fountain auger caused a systematic reduction in grain flow where the sensor was installed, and thus underestimation of yield. The degree to which yield estimation was affected was dependent upon grain properties. The commercial yield monitoring system evaluated was less susceptible to accumulated load weight errors, but showed less linearity of sensor response across the entire flow than the particle flow yield monitor and required in-field calibration for each crop. The initial performance of the particle flow yield monitor showed great potential for a future yield monitoring solution, although design changes should reflect the issues observed with velocity profile of the grain, maintenance of a grain cavity area, and time delay from crop entry to sensor response.

CHAPTER 6. CONCLUSIONS

Benchmarking of two commercial yield systems allowed researchers to gauge performance and understand influence of flow and combine properties that affect yield estimation accuracy. Each system used widely accepted sensor technologies for yield monitoring and showed the pros and cons of each to be considered for the next generation of yield monitoring technology solutions. Reduced or no calibration need, multiple crop support, and accuracy across flow rate and load size are needed in order to provide reliable yield information to producers for use in making crop management decisions. A particle flow yield monitor was developed and evaluated. The system used pixel displacement from image tracking to estimate volumetric flow of grain through a constant cross sectional area. This allowed for a fundamental system of measurement that demonstrated reduced calibration needs, linearity for multiple crop types, and promise for future development work. Although unintentional biasing was introduced into yield estimation, the system showed potential to overcome many of the limitations of current yield monitoring systems.

6.1. Suggestions for Future Testing

Investigation should be made to see if the yield underestimation can be overcome with simple modification to the fountain auger. Additionally, as yield estimation relies on uniform grain flow through a fixed area, research into the flow properties of large and small grains should be considered.

6.2. Suggestions for Future Development

Further design work on achieving the mechanical requirements of the system is needed. Design changes to the clean grain elevator and method of grain conveyance could greatly improve grain presentation to any yield monitoring system. Time delays of 10 to 20

seconds from crop entry to sensor response were common during field evaluation due to filling of the sump area and location of flow measurement. Reduction in time delay could be achieved by relocating the particle flow yield monitor further upstream in the grain cycle. The cross auger shows promise for this type of application. This would require design modification to the current combine cleaning system.

Development of the yield estimation algorithm should be considered to address concerns of image quality. Two documented incidents occurred where the camera face was blocked with debris during field harvest, resulting in inability to track particles or measure yield (Figure 6.1). Integration with the harvester CAN Bus would allow for real-time yield measurement and display warnings of blockage. These cases were isolated incidents and driven by exposure to outlier grain quality conditions.

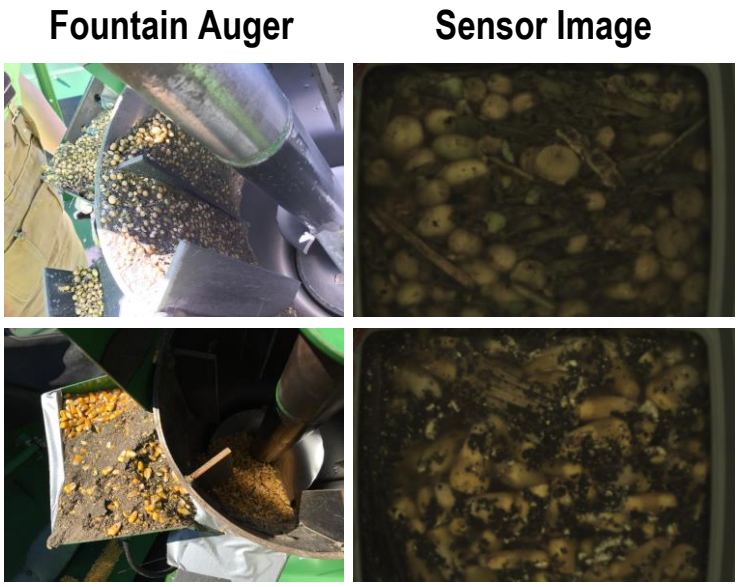

Figure 6.1: Sensor face blockage and image quality issues during field harvest exposure

REFERENCES

Ag Leader Technology. (2016, April 6). *The Evolution of Ag Leader Technology*. Retrieved from Ag Leader Technology: http://www.agleader.com/about/history/

Arslan, S., & Colvin, T. S. (1999). Laboratory performance of a yield monitor. *Applied Engineering in Agriculture, 15*(3), 189-195.

Bern, C. J., Hurburgh, C. R., & Brumm, T. J. (2014). *Managing Grain After Harvest.* Ames, IA: Iowa State University.

Blackmore, S., & Moore, M. (1999). Remedial correction of yield map data. *Precision Agriculture, 1*, 53-66.

Burks, T. F., Shearer, S. A., Fulton, J. P., & Sobolik, C. J. (2003). Combine yield monitor test facility development and initial monitoring test. *Applied Engineering in Agriculture, 19*(1), 5-12.

Burks, T. F., Shearer, S. A., Fulton, J. P., & Sobolik, C. J. (2004). Effects of Time-Varying Inflow Rates on Combine Yield Monitor Accuracy. *Applied Engineering in Agriculture*, 269-275.

Chung, S.-O., Sudduth, K. A., & Drummond, S. T. (2002). Determining Yield Monitoring System Delay Time with Geostatistical and Data Segmentation Approaches. *Transactions of the ASAE, 45*(4), 915-926.

Claydon, J. T. (1981). *Patent No. EP0042245 A1*.

Colvin, T. S., Jaynes, D. B., Karlen, D. L., Laird, D. A., & Ambuel, J. R. (1997). Yield variability within a central Iowa field. *Transactions of the ASAE, 40*(4), 883-889.

Darr, M. (2015). Yield Monitoring Systems. *Iowa State University - TSM 333*. Retrieved May 11, 2016

Deere & Company. (2013, December). *S-Series Combine Calibration Guide.* Retrieved from Sloan Implement Company: http://www.sloans.com/wp-content/uploads/2013/12/S-Series-Calibration-Guide3.pdf

Deere & Company. (2016, March 23). *S-Series Combines*. Retrieved from http://www.deere.com/en_US/products/equipment/grain_harvesting/combines/s_series/s_series.page

Fulton, J. P., Sobolik, C. J., Shearer, S. A., Higgins, S. F., & Burks, T. F. (2009). Grain yield monitor flow sensor accuracy for simulated varying field slopes. *Applied Engineering in Agriculture, 25*(1), 15-21.

Gonzalez-Montellano, C., Llana, D. F., Fuentes, J. M., & Ayuga, F. (2011). Determination of the mechanical properties of corn grains and olive fruits required in DEM simulations. *ASABE Annual International Meeting.* St. Joseph: American Society of Agricultural and Biological Engineers.

Grain Harvesting. (2006). In A. K. Srivastava, C. E. Goering, R. P. Rohrbach, & D. R. Buckmaster, *Engineering Principles of Agricultural Machines* (p. 409). St. Joseph, MN, USA: American Society of Agricultural and Biological Engineers. Retrieved March 23, 2016

Grisso, R. D., Jasa, P. J., Schroeder, M. A., & Wilcox, J. C. (2002). Yield Monitor Accuracy: Successful Farming Magazine Case Study. *Applied Engineering in Agriculture, 18*(2), 147-151. Retrieved February 24, 2016, from http://bsesrv214.bse.vt.edu/grisso/papers/pm2913.pdf

Interagency Agricultural Projections Committee. (2016). *USDA Agricultural Projections to 2025.* World Agricultural Outlook Board, Office of the Chief Economist.

Washington, D.C.: U.S. Department of Agriculture. Retrieved 02 22, 2016, from http://www.usda.gov/oce/commodity/projections/

Kettle, L. Y., & Peterson, C. L. (1998). An evaluation of yield monitors and GPS systems on hillside combines operating on steep slopes in the Palouse. *ASAE Paper No. 981046*. St. Joseph, Michigan: ASAE.

Kruse, B. J. (2015). Quantifying the time delay relationship of corn from ear removal to mass flow measurement on combine harvesters. Unpublished.

Lin, B. B. (2011). Resilience in Agriculture through Crop Diversification: Adaptive Management for Environmental Change. *BioScience, 61*(3), 183-193. Retrieved February 23, 2016, from http://bioscience.oxfordjournals.org/content/61/3/183.full.pdf+html

McNaull, R. P. (2016). Development of a real-time algorithm for automation of the grain yield monitor calibration. *PhD diss*. Ames, IA: Iowa State University, Department of Agricultural and Biosystems Engineering.

Missotten, B., Strubbe, G., & De Baerdemaeker, J. (1996). Accuracy of grain and straw yield mapping. *Precision Agriculture*, 713-722.

Myers, A. (1994, September 6). *US Patent No. 5,343,761*.

NDSU Agriculture Communication. (2013, September 24). *Harvesting, Drying, Storing Corn Could Be Challenging.* Retrieved from NDSU Agriculture Communication: https://www.ag.ndsu.edu/news/newsreleases/2013/sept-23-2013/harvesting-drying-storing-corn-could-be-challenging

Neilsen, R. (2010, August). *Yield Monitor Calibration: Garbage In, Garbage Out.* Retrieved from Purdue University, Department of Agronomy: https://www.agry.purdue.edu/ext/corn/news/timeless/yldmoncalibr.html

Nelson, F. W., Hawk, K. R., Smith, W. F., & Pickett, T. D. (1997, July 3). *US Patent No. 6285198 B1*.

Overgaard, J. (1983). *Patent No. EP0147452 A1*.

Pierce, F. J., Anderson, N. W., Colvin, T. S., Schueller, J. K., Humburg, D. S., & McLaughlin, N. B. (1997). Yield mapping. *Site-Specific Management for Agricultural Systems*, 211-243.

Risius, N. W. (2014). Analysis of a combine grain yield monitoring. *MS thesis*. Ames, IA: Iowa State University, Department of Agricultural and Biosystems Engineering.

Shearer, S. A., Fulton, J. P., McNeill, S. G., Higgins, S. F., & Mueller, T. G. (1999). Elements of Precision Agriculture: Basics of Yield Monitor Installation and Operation. *University of Kentucky Coopertive Extension Service*. Retrieved February 24, 2016, from http://www.bae.uky.edu/precag/PrecisionAg/Exten_pubs/pa1.pdf

Strubbe, G. J., Missotten, B., & Baerdemaeker, J. D. (1996). Mass flow measurement with a curved plate at the exit of an elevator. *Precision Agriculture*, 703-712.

Taylor, R., Fulton, J., Darr, M., Haag, L., Staggenbord, S., Mullenix, D., & McNaull, R. (2011). Using Yield Monitors to Assess On-Farm Test Plots. *ASABE Publication No. 1110690*. St. Joesph, Michigan, USA: American Society of Agricultural and Biological Engineers.

United States Department of Agriculture. (2013, February 27). *Soil Tillage and Crop Rotation*. (S. Wallander, Editor) Retrieved February 23, 2016, from United States

Department of Agriculture: Economic Research Service: http://www.ers.usda.gov/topics/farm-practices-management/crop-livestock-practices/soil-tillage-and-crop-rotation.aspx

USDA Economic Research Service. (2015). *Agricultural Resource Management Survey*. Washington, D.C.: United States Department of Agriculture. Retrieved from http://www.ers.usda.gov/data-products/arms-farm-financial-and-crop-production-practices/arms-data.aspx

Zhou, J., Cong, B., & Liu, C. (2014). Elimination of vibration noise from an impact-type grain mass flow sensor. *Precision Agriculture*, 627-638.

APPENDIX A. YIELD MONITORING PATENT REVIEW

Patent Title: "Method and apparatus for measuring grain mass flow rate in harvesters"

Number: US5343761 A

Filing Date: June 17, 1991

Inventor(s): Allen Myers

Assignee: Allen Myers

Abstract: "A system and method for continuously measuring mass flow rate of grain in a harvester where an impact plate is disposed to be impacted by grain exiting a power driven conveyor which is a normal part of the harvester. The impact plate is mounted on force measuring apparatus which generates an electrical signal proportional to grain impact force. Computing apparatus in electrical communication with the force measuring apparatus calculates the average value of grain impact force, adjusts this value to compensate for the difference between an actual measured operating speed of the conveyor and a constant reference speed, and calculates grain mass flow rate utilizing a mass flow calibration characteristic which relates grain mass flow rate to average grain impact force, where this calibration characteristic is non-linear and has different values for different grain types and different grain moisture contents. Optionally, the operating speed of the conveyor is calculated by analyzing the signal received from the force measuring apparatus to determine a characteristic frequency which is directly proportional to operating speed. Also optionally, electrodes are mounted on the impact plate for generating an electrical signal which is indicative of grain moisture content, and this electrical signal is used in combination with a moisture calibration characteristic to determine grain moisture content. Harvester travel speed is measured and the area rate of harvesting is calculated by multiplying this speed by a preset swath width. Instantaneous crop yield is computed by dividing grain mass flow rate by

area harvesting rate. Total weight of grain harvested and total field area harvested are calculated by integrating grain mass flow rate and area rate of harvesting, respectively. Electronic display apparatus displays measured and calculated values to the harvester operator, while an electronic memory device stores calculated values from multiple field areas. Optionally, the memory device is removable from the grain mass flow measuring system on a harvester to provide convenient transfer of data to a remote computing device."

Claim(s):

1. "A system for measuring mass flow rate of grain exiting a power driven conveying means in a harvester."
2. "A system for measuring mass flow rate of grain exiting a paddle type chain conveyor in a harvester, said system comprising: an impact plate positioned to be impacted by grain exiting said conveyor, force measuring means utilizing at least four strain gauges positioned on a load beam for producing an electrical signal proportional only to the impact force exerted on said impact plate by said grain and is independent of the position of said impact force on said impact plate, and computing means in electrical communication with said force measuring means for calculating grain mass flow rate by determining a value which is representative of said impact force and by utilizing a mass flow calibration characteristic which relates said grain mass flow rate to said value."

Patent Title: “Measuring the flow of grain in a combine harvester”

Number: EP0147452 A1

Filing Date: June 21, 1983

Inventor(s): Jens Overgaard

Assignee: Dronningborg Maskinfabrik A/S

Abstract: “To perform a continuous measurement of mass flow rate of grain in a combine harvester with a signal transmitter and a signal detector arranged on their respective sides of a passageway of flow of grains, using a source of radiation to beta radiation, gamma, as signal emitters. Because the attenuation effect of the grain flow rate on these rays is practically independent of variable factors other than the density of the grain flow, the detector output signal is a precise expression of this density. Knowing the velocity of the flow of grain and the cross section of the passage, the mass flow rate can thus be calculated with an equally high accuracy.”

Claim(s):

1. “Use of measurement of attenuation or another change of beta rays, gamma rays or X-rays transmitted through or refracted by a flow of material for continuous measuring of the mass flow of threshed grain which passes through a passage in a combine harvester.”
2. “Use of a piece of americium 241 as a radiation source.”

Patent Title: "Crop metering device for combine harvesters"

Number: EP0042245 A1

Filing Date: June 9, 1981

Inventor(s): Jeffrey Thomas Claydon

Assignee: Claydon Yield-O-Meter Limited

Abstract: "A crop metering device for measuring by volume the clean crop yield of a combine harvester during harvesting, wherein a trap is located in the clean crop flow to build up a head of clean crop, and a paddle wheel or analogous device successively releases known volumes of crop at a rate which tends to maintain a predetermined head of crop above the trap. A sensor determines when the head of crop has built up to the predetermined level, and initiates successive operations of the paddle wheel or analogous crop releasing device. The volumes released are counted by a switch or the like to determine yield in relation to time or harvested area. A weighing device may be incorporated to enable an on-board computer to effect a volume to weight conversion."

Claim(s):

1. "A crop metering device for combine harvesters, located in the clean crop flow, and characterized by the combination of a trap for creating the build-up of a head of clean crop, a sensor for determining when the head has built up to a predetermined level, means responsive to the sensor for initiating release of successive volumes of crop from the built up head thereof, and means for measuring the volumetric rate of release which tends to maintain said head at the predetermined level."

Patent Title: “Grain moisture sensor”

Number: US6285198 B1

Filing Date: July 3, 1997

Inventor(s): Frederick William Nelson, Kent Robert Hawk, Wayne Farrior Smith, Terence Daniel Pickett

Assignee: Deere & Company

Abstract: “A moisture sensor for an agricultural combine comprises a chamber having an inlet and an outlet and a paddle wheel flow controller located adjacent to the outlet. The paddle wheel flow controller is rotated by an electric motor which is controlled by an electronic controller. Grain from the clean grain elevator is directed through the inlet of the chamber past a capacitance sensor comprising a first, second and third plates. By measuring the capacitance of the grain, the moisture in the grain can be determined.”

Claim(s):

1. “A moisture sensor for an agricultural combine having a clean grain elevator, the moisture sensor comprising: a vertically extending chamber mounted to the clean grain elevator, the chamber having an upper inlet and a lower outlet, and a capacitance sensing means is positioned in the chamber between the outlet and the inlet, wherein the capacitance sensing means senses the capacitance of clean grain in the chamber and provides a capacitance signal that can be related to grain moisture.”
2. “A combine thresher having a continuous grain moisture analyzer.”

APPENDIX B. MASS FLOW YIELD MONITORING UNCERTAINTY ANALYSIS

B.1. Combined Standard Uncertainty for Grain Yield

Impact-based mass flow sensing is the most common method to measure yield for grain harvest. Grain yield can be estimated using the mass flow rate of grain, harvester velocity, grain density, header width, and conversion factors. Key parameters required to compute yield that are measured using sensors include mass flow rate of grain, harvester velocity, and grain density. The standard uncertainty associated with these parameters was evaluated using a zeroth-order analyses to determine the combined standard uncertainty of grain yield.

A zeroth-order uncertainty budget was created for the mass flow sensor (Table B.1). The standard uncertainty associated with a mass flow sensor was determined through experimental trials of metering grain into a combine at constant mass flow rates. Mass flow rates of grain were controlled using flow gates with linear actuators (Risius, 2014). The standard error of five different flow rates was calculated from a 50 measurement sample at steady state flow conditions from six repetitions.

Table B.1: Uncertainty budget for mass flow sensor measurement

Source	Value ($kg\ s^{-1}$)	Probability distribution	Divisor	Standard uncertainty ($kg\ s^{-1}$)	Standard uncertainty ($lb\ s^{-1}$)
Repeatability[a]	0.28	Normal	1	0.28	0.62
Display Resolution[b]	5.0E-03	Rectangular	$\sqrt{3}$	2.9E-03	6.4E-03
Combined sensor standard uncertainty, $\Delta\dot{m}$				0.28	0.62

[a] Largest SE of 50 measurements as found from five constant mass flow rates (5, 10, 15, 25, 30 $kg\ s^{-1}$)
[b] ±0.5 smallest display value = 0.01

The standard uncertainty of the linear regression to predict the mass flow rate of grain was determined by computing the root-mean-square error (RMSE, Equation B.1). The RMSE

can be used to measure the difference between estimates predicted by a model ($\hat{y}$) and the values actually observed (y). The RMSE was calculated and compared with two data sets A and B (Table B.2).

Equation B.1: Root-Mean-Square Error

$$RMSE = \sqrt{\frac{1}{n}\sum_{i=1}^{n}(y_i - \hat{y}_i)^2}$$

Table B.2: RMSE comparison for test stand and harvest conditions

Data set	Environment	Crop	Calibration type	RMSE	
				(kg s^{-1})	(lb s^{-1})
A	Test Stand	Corn	Multi-point	0.26	0.57
B	Harvest	Corn	Multi-point	1.16	2.56

Data set A was measured in a test stand environment where mass flow rate of corn was controlled using actuated doors on a grain wagon with scaled axles. A multi-point calibration was performed at five mass flow rates that ranged from 5 to 30 kg s^{-1} and were nearly equally spaced from one another. Environmental conditions and corn density were controlled throughout testing. Data set B was measured in a field harvest environment on a single machine harvesting corn throughout the 2015 harvest season. A multi-point calibration was performed at the beginning of harvest containing four points ranging from 10 to 25 kg s^{-1}, typical for mass flow rates observed during corn harvest. Data set A has significantly lower RMSE than data set B due to the controlled environment and repetitions performed at the mass flow rates that the sensor was calibrated to. Propagation of uncertainty from the uncertainty budget for mass flow sensor measurement, combined with the RMSE via quadrature yielded the total standard uncertainty for the mass flow sensor ($\dot{m}_t$, Equation B.2)

Equation B.2: Total standard uncertainty for mass flow sensor

$$\Delta \dot{m}_t{}^2 = \Delta \dot{m}^2 + RMSE^2$$

A zeroth-order uncertainty budget was created for the navigation-based velocity sensor (Table B.3) and the grain density measurement (Table B.4). The navigation-based velocity measurements were collected randomly (n = 100) from a field harvest environment traveling at a constant set speed on level terrain. Grain density measurements were collected periodically throughout the 2015 corn harvest season. A total of 127 measurements were recorded.

Table B.3: Uncertainty budget for navigation-based velocity sensor evaluated at 5 kph

Source	Value (kph)	Probability distribution	Divisor	Standard uncertainty (kph)	Standard uncertainty (mph)
Repeatability[a]	8.6E-03	Normal	1	8.6E-03	5.3E-03
Display Resolution[b]	5.0E-09	Rectangular	√3	2.9E-09	1.8E-09
Combined sensor standard uncertainty, $\Delta\vec{v}$				8.6E-03	5.3E-03

[a] SE of 100 measurements at a constant speed setting in harvest conditions
[b] ±0.5 smallest display value = 0.00000001

Table B.4: Uncertainty budget for grain density evaluated during corn harvest 2015

Source	Value (kg m^{-3})	Probability distribution	Divisor	Standard uncertainty (kg hL^{-1})	Standard uncertainty (lb bu^{-1})
Repeatability[a]	2.6	Normal	1	0.25	0.20
Display Resolution[b]	0.05	Rectangular	√3	2.0E-03	2.2E-03
Combined sensor standard uncertainty, $\Delta\rho$				0.25	0.20

[a] SE of 127 measurements taken throughout the 2015 corn harvest season
[b] ±0.5 smallest display value = 0.1

The combined standard uncertainty associated with propagation of grain yield measurement error (U_y) was determined using a linear first-order Taylor series approximation that ignores higher order terms (Equation B.3).

Equation B.3: Grain yield estimation combined standard uncertainty

$$U_y{}^2 = \left(\frac{\partial U_y}{\partial \dot{m}_t}\Delta\dot{m}_t\right)^2 + \left(\frac{\partial U_y}{\partial \vec{v}}\Delta\vec{v}\right)^2 + \left(\frac{\partial U_y}{\partial \rho}\Delta\rho\right)^2$$

Partial derivatives were used to denote that the uncertainty in grain yield is dependent upon the uncertainties of the mass flow sensor, navigation-based velocity sensor, and grain density. When typical corn mass flow rate (15 kg s^{-1}), harvesting speed (5 kph), and grain density (70 kg hL^{-1}) are used, the combined standard uncertainty for grain yield estimation equates to 0.24 MT ha^{-1} (3.8 bu ac^{-1}) when using RMSE from data set A and 0.73 MT ha^{-1} (11.7 bu ac^{-1}) when using RMSE from data set B. Moreover, based on the United States average corn yield for 2015 of 10.6 MT-ha^{-1} (168.4 bu-ac^{-1}), a 2% to 7% relative standard uncertainty in corn grain yield estimation can be expected.

A sensitivity analysis was performed upon each of the input parameters to determine how much grain yield estimation is affected by input values. Input parameters of grain mass flow, harvester speed, and grain density were assigned high and low values and varied independently to observe the impact on model output. The 5th and 95th percentiles were selected from each input parameter distribution (Table B.5). The normal distributions were observed from nearly 2,000 hours of data recorded from the Controller Area Network (CAN) bus on combine harvesters.

Table B.5: Sensitivity of grain yield estimation to input parameter values

		Percentile values			Grain yield sensitivity MT-ha^{-1} (bu-ac^{-1})	
Input parameter	Units	$P_{0.05}$	$P_{0.50}$	$P_{0.95}$	$P_{0.05}$	$P_{0.95}$
Navigation-based velocity, v	kph	2.80	6.43	11.6	5.82 (86.7)	24.1 (358)
Corn mass flow rate, $\dot{m}$	kg/s	5.06	21.2	29.7	2.52 (37.8)	14.7 (218)
Corn grain density, ρ	kg-hL^{-1}	64.8	69.6	74.1	9.85 (146)	11.3 (168)

Grain yield was the most sensitive to variation in navigation-based velocity input values when other input parameters were held at their base values ($P_{0.50}$) due to the placement of the velocity variable in the estimation model. This was of little concern as the combined standard uncertainty for navigation-based velocity ($\Delta\vec{v}$) was negligible compared to other parameters. Grain yield was slightly less sensitive to mass flow rate of corn as an input parameter, while sensitivity to corn grain density was insignificant. Since the total standard uncertainty of grain mass flow rate during harvest conditions was 1.2 kg s^{-1} (2.6 lb s^{-1}), there is potential for estimation error due to the mass flow rate sensor. Increased parameter sensitivity combined with large standard uncertainty creates an increased risk for poor grain yield estimation. Improvements in measurement of grain flow rate presents an opportunity for increased accuracy and performance of grain yield monitoring systems.

B.2. Calibration Impact on Yield Estimation Performance

Yield monitor accuracy is highly dependent upon calibration type and procedure. The number of loads and the distribution of grain mass flow rate can induce error if not properly collected. To study how yield system estimation error is affected by the type of calibration performed, grain was metered by actuating doors from a grain wagon with scaled axles into a combine. Five mass flow rates for dry corn were used to cover a wide range. Mass flow rate set points of 2, 7, 12, 17, and 23 kg s^{-1} were selected from the corn mass flow rate distribution. To better simulate mass flow rates experienced by the sensor during harvest conditions, a variable grain flow rate signal of ±25% was applied to each of the mass flow rate set points (Figure B.1).

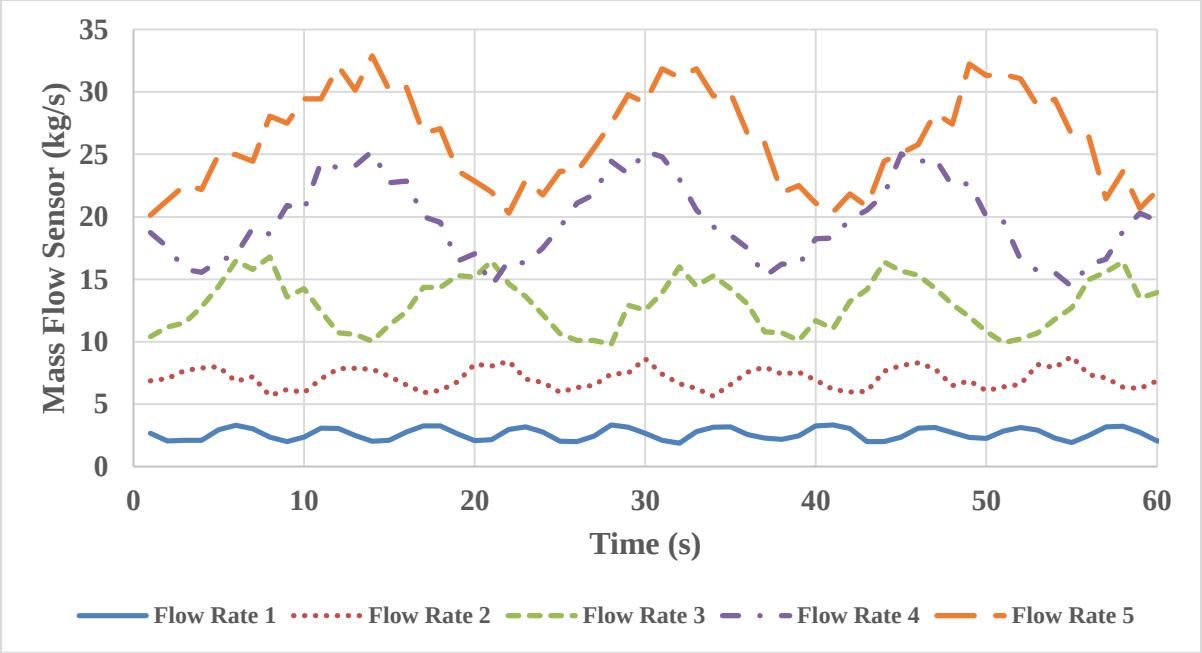

Figure B.1: Impact-based mass flow sensor response to variable corn mass flow rate

A calibration load was collected from each mass flow rate set point to properly build a calibration curve that covered the entire flow distribution. Each calibration load consisted of 2,500 kg of accumulated grain mass. Following the calibration load collection for the impact-based mass flow sensor, the calibration curve was fitted for all possible combinations between one and five calibration points. In total 31 calibration combinations were tested. The regression algorithm updated the yield monitor calibration curve and displayed the yield system estimation error for each calibration load collected. The ground truth load weight for each calibration load was recorded using a grain wagon with scaled axles and used for estimation error computation. Yield system estimation error was recorded for each calibration load corresponding to a mass flow rate set point every time the calibration combination was updated. As the number of calibration points used within the calibration curve regression increases, the overall error and variability of the yield system decreases. The

five mass flow rate set points showed a similar relationship between yield estimation error and the number of calibration points (Figure B.2).

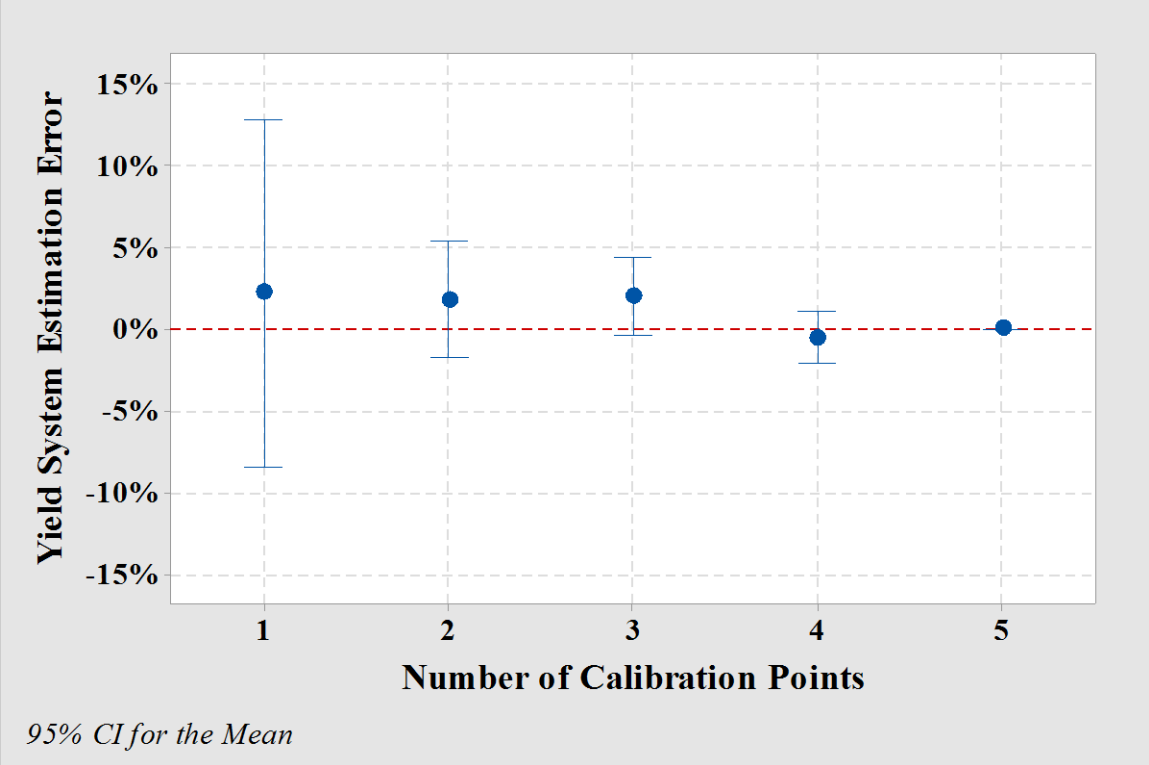

Figure B.2: Calibration type comparison for 12 kg s^{-1} corn mass flow rate set point

Increasing the number of calibration points widens the mass flow rate coverage of a calibration curve. Multi-point calibrations better fit the non-linear signal response of impact-based mass flow sensors and help to eliminate bias error. Proper procedure and conditions must be integrated into yield monitor calibration in order to obtain accuracy. The process to obtain an accurate yield monitor calibration requires time to collect multiple loads that span the range of flow rates for a crop as well as an understanding of how the system performs. A calibration built on diligently collected loads are only accurate as long as the conditions upon which the loads were collected are the same. Opportunity exists for a yield monitor system to maintain accuracy over a wider range of conditions with less intensive calibration.

APPENDIX C. PARTICLE FLOW YIELD MONITORING UNCERTAINTY ANALYSIS

C.1. Combined Standard Uncertainty for Grain Yield

Particle flow yield monitoring was a new method presented for measuring grain yield. Grain yield (Y) can be estimated using the volumetric flow rate of grain ($\dot{V}$), harvester velocity ($\vec{v}$), header width (w), and conversion factors (Equation C.1). Unlike the impact-based mass flow yield monitor, the particle flow yield monitor does not require test weight to measure volume. Key parameters required to compute yield that are measured using sensors include volumetric flow rate of grain and harvester velocity. Volumetric flow rate of grain was a function of pixel displacement rate ($\dot{PD}$), which was measured by comparing grain displacement between image frames as grain flowed through a tube (Equation C.2). The standard uncertainty associated with the two key parameters was evaluated using a zeroth-order analysis to determine the combined standard uncertainty of grain yield.

Equation C.1: Yield estimation for particle flow yield monitor

$$Yield = Y\left(\frac{bu}{ac}\right) = \frac{\dot{V}\left(\frac{bu}{s}\right) * 43{,}560\left(\frac{ft^2}{ac}\right) * 3{,}600\left(\frac{s}{hr}\right)}{\vec{v}\left(\frac{mi}{hr}\right) * h\,(ft) * 5{,}280\left(\frac{ft}{mi}\right)}$$

Equation C.2: Volumetric flow rate estimation from pixel displacement rate

$$\dot{V}\left(\frac{bu}{s}\right) = \frac{\dot{PD}\left(\frac{Pixel\ Lines}{s}\right)}{9.6\left(\frac{Pixel\ Lines}{1\ mm}\right)} * \frac{\pi * (304.8\ mm)^2}{4} * \frac{1\ m^3}{1.0E10\ mm^3} * \frac{28.38\ bu}{1\ m^3}$$

A zeroth-order uncertainty budget was created for the particle flow sensor (Table C.1). The standard uncertainty associated with a particle flow sensor was determined through experimental trials of metering grain into a combine in a test stand environment at constant

flow rates. The standard error of five different flow rates was calculated using 50 measurement samples at steady state flow conditions from six repetitions per flow rate.

Table C.1 Uncertainty budget for pixel displacement rate measurement

Source	Value (kg s^{-1})	Probability distribution	Divisor	Standard uncertainty (pixel lines s^{-1})
Repeatability[a]	19.1	Normal	1	19.1
Display Resolution[b]	5.0E-07	Rectangular	√3	2.9E-07
Combined sensor standard uncertainty, $\Delta\dot{PD}$				19.1

[a] Largest SE of 50 measurements as found from five constant mass flow rates (5, 10, 15, 25, 30 kg s^{-1})
[b] ±0.5 smallest display value = 0.000001

The standard uncertainty of the linear regression between the pixel displacement rate and the ground truth flow rate was determined by computing the root-mean-square error (RMSE). The RMSE was used to measure the error between the estimated pixel displacement rate, and thus volumetric flow rate, and the actual observed flow rate. The linearity was analyzed using two data sets. Data set A represented controlled data from a test stand environment where grain flow rate was controlled using a scaled-axle wagon. The average pixel displacement rate during a test replicate was plotted against the observed flow rate from the grain wagon and the RMSE of the data set was measured. Data set B consisted of uncontrolled data collected during harvest of corn, soybean, and wheat. The three crops differed geographically throughout the Midwestern U.S., moisture content, and test weight. Both data sets produced similar RMSE for the linear regression between pixel displacement rate and flow rate (Table C.2). RMSE contributed more to the total uncertainty.

Table C.2 : RMSE for particle flow test stand and harvest conditions

Data set	Environment	Crop	RMSE (Pixel Lines s^{-1})
A	Test Stand	Corn	155.1
B	Harvest	Corn	167.8

The standard uncertainty of the navigation-based velocity sensor was determined during a previous uncertainty analysis and was relatively insignificant to the combined uncertainty error. The standard uncertainty of the navigation-based velocity was approximately 0.0011 km h^{-1}. Each of the factors contributing to uncertainty for the particle flow yield monitor was combined using a first order Taylor series that ignored higher order terms (Equation C.3).

Equation C.3: Particle flow yield estimation combined standard uncertainty

$$U_y{}^2 = \left(\frac{\partial U_y}{\partial \dot{PF}_t}\Delta \dot{PF}_t\right)^2 + \left(\frac{\partial U_y}{\partial \vec{v}}\Delta \vec{v}\right)^2$$

Under a corn mass flow rate of 15 kg s^{-1}, the average particle flow yield monitor response was 2,150 pixel lines s^{-1}. When pixel displacement rate (2,150 pixel lines s^{-1}) is used with a typical harvesting speed (5 kph), the combined standard uncertainty for grain yield estimation equates to 0.50 MT ha^{-1} (8.3 bu ac^{-1}) when using RMSE from data set A and 0.54 MT ha^{-1} (9.0 bu ac^{-1}) when using RMSE from data set B. The combined standard uncertainty for the particle flow yield monitor was within the impact-based mass flow yield monitor uncertainty range (3.8 to 11.7 bu ac^{-1}) and was much more consistent between the two data sets. This demonstrated the consistency to perform across ranging flow rates and environmental conditions. Based on the United States average corn yield for 2015 of 10.6 MT-ha^{-1} (168.4 bu-ac^{-1}), a 5% relative standard uncertainty in corn grain yield estimation can be expected with the particle flow yield monitor. This uncertainty level is acceptable for a technology development and feasibility project. The majority of the uncertainty can be attributed to the particle flow sensor and could be reduced through future development and research. The particle flow yield monitor shows much promise to overcome the dependencies and inherit error of current yield monitoring technology.